National Library of Canada
Bibliothèque nationale du Canada

Canadian Theses Service
Services des thèses canadiennes

Ottawa, Canada
K1A 0N4

CANADIAN THESES

THÈSES CANADIENNES

NOTICE

The quality of this microfiche is heavily dependent upon the quality of the original thesis submitted for microfilming. Every effort has been made to ensure the highest quality of reproduction possible.

If pages are missing, contact the university which granted the degree.

Some pages may have indistinct print especially if the original pages were typed with a poor typewriter ribbon or if the university sent us an inferior photocopy.

Previously copyrighted materials (journal articles, published tests, etc.) are not filmed.

Reproduction in full or in part of this film is governed by the Canadian Copyright Act, R.S.C. 1970, c. C-30.

AVIS

La qualité de cette microfiche dépend grandement de la qualité de la thèse soumise au microfilmage. Nous avons tout fait pour assurer une qualité supérieure de reproduction.

S'il manque des pages, veuillez communiquer avec l'université qui a conféré le grade.

La qualité d'impression de certaines pages peut laisser à désirer, surtout si les pages originales ont été dactylographiées à l'aide d'un ruban usé ou si l'université nous a fait parvenir une photocopie de qualité inférieure.

Les documents qui font déjà l'objet d'un droit d'auteur (articles de revue, examens publiés, etc.) ne sont pas microfilmés.

La reproduction, même partielle, de ce microfilm est soumise à la Loi canadienne sur le droit d'auteur, SRC 1970, c. C-30.

THIS DISSERTATION
HAS BEEN MICROFILMED
EXACTLY AS RECEIVED

LA THÈSE A ÉTÉ
MICROFILMÉE TELLE QUE
NOUS L'AVONS REÇUE

Canada

NL-339 (r.86/06)

THE UNIVERSITY OF ALBERTA

DESIGN AND CONTROL OF VENTILATION INLETS FOR ANIMAL HOUSING

by

© J.J.LEONARD

A THESIS
SUBMITTED TO THE FACULTY OF GRADUATE STUDIES AND RESEARCH
IN PARTIAL FULFILMENT OF THE REQUIREMENTS FOR THE DEGREE
OF DOCTOR OF PHILOSOPHY

DEPARTMENT OF AGRICULTURAL ENGINEERING

EDMONTON, ALBERTA
SPRING 1986

Permission has been granted to the National Library of Canada to microfilm this thesis and to lend or sell copies of the film.

The author (copyright owner) has reserved other publication rights, and neither the thesis nor extensive extracts from it may be printed or otherwise reproduced without his/her written permission.

L'autorisation a été accordée à la Bibliothèque nationale du Canada de microfilmer cette thèse et de prêter ou de vendre des exemplaires du film.

L'auteur (titulaire du droit d'auteur) se réserve les autres droits de publication; ni la thèse ni de longs extraits de celle-ci ne doivent être imprimés ou autrement reproduits sans son autorisation écrite.

ISBN 0-315-30110-4

THE UNIVERSITY OF ALBERTA

RELEASE FORM

NAME OF AUTHOR J.J.LEONARD

TITLE OF THESIS DESIGN AND CONTROL OF VENTILATION INLETS FOR ANIMAL HOUSING

DEGREE FOR WHICH THESIS WAS PRESENTED DOCTOR OF PHILOSOPHY

YEAR THIS DEGREE GRANTED SPRING 1986

Permission is hereby granted to THE UNIVERSITY OF ALBERTA LIBRARY to reproduce single copies of this thesis and to lend or sell such copies for private, scholarly or scientific research purposes only.

The author reserves other publication rights, and neither the thesis nor extensive extracts from it may be printed or otherwise reproduced without the author's written permission.

(SIGNED) ....

PERMANENT ADDRESS:

1102 11111 87 AVE
EDMONTON
ALBERTA T6G 0X9

DATED 21 APRIL 1986

THE UNIVERSITY OF ALBERTA

FACULTY OF GRADUATE STUDIES AND RESEARCH

The undersigned certify that they have read, and recommend to the Faculty of Graduate Studies and Research, for acceptance, a thesis entitled DESIGN AND CONTROL OF VENTILATION INLETS FOR ANIMAL HOUSING submitted by J.J.LEONARD in partial fulfilment of the requirements for the degree of DOCTOR OF PHILOSOPHY.

J.B. McQuitty
Supervisor

K. W. Domier

Gerald W. Sadler

Mylo A. Hellickson
External Examiner

Date April 3 1986

ABSTRACT

This thesis describes an investigation into the applicability of Archimedes and Momentum numbers as criteria for the control of cold ventilation air jets. Such jets are a feature of the winter ventilation of animal housing throughout the Prairie regions of North America.

A review of the fundamental theories of jet behaviour is presented. The development of current theories pertaining to constrained, non-isothermal jets is traced, the relevance of these theories to the ventilation of animal housing is discussed and the need to obtain further experimental data, using cold inlet air, is identified.

The construction and instrumentation of an experimental facility for this purpose is described. The facility consisted of a room, ventilated with a variable-speed fan and with provision for using a number of air inlet configurations. The presence of animals in the room was simulated with water-filled heating pads. Inlet air was drawn from outside during cold weather and the path of inlet jets was delineated by means of an array of temperature sensors and, photographically, by injecting smoke into the airstream.

Experiments are described in which, for each inlet configuration, jet trajectories were delineated for a variety of airflow rates and with various areas of heating pads exposed. Analysis of the data is based on the definition of a "drop coefficient", which appears to be a useful means of quantifying the tendency of cold jets to drop on entry to a warm environment. The drop coefficient is related linearly to Archimedes number for all inlet configurations with the slope of the relationship depending on the the inlet width and proximity to the ceiling. The effects of varying exposed heated areas on jet trajectories appear to be small but consistent with observations of previous workers. The use of an Archimedes number based on the outlet air temperature, rather than the heated surface temperature, is shown to be valid.

In addition to jet trajectories, the mixing performance of jets also is examined. These analyses were carried out using data on the horizontal and vertical temperature variations within the ventilated room. The data indicate that there is an optimum, rather than merely a minimum, jet velocity required for the promotion of air mixing. The use of a Momentum number, in addition to an Archimedes number, as a criterion for mixing is shown to be redundant. In an attempted analysis of jet entrainment ratios, results are presented that are in complete disagreement with established theory. This disagreement is explained on the basis of assumed heat transfer to the jets from the ceiling.

Archimedes number criteria for control of ventilation jets to provide acceptable trajectories and air mixing are proposed. Analysis of ventilation data from actual barns, together with fan performance data, leads to the conclusion that, under minimum winter ventilation conditions, these criteria cannot be met using conventional ventilation system designs. Alternative designs are proposed and possible strategies for their control are discussed.

ACKNOWLEDGEMENTS

The author wishes to acknowledge the advice, assistance and support of Professor J.B. McQuitty in the completion of this thesis. Acknowlegement also is due to the following people:

- Mr. R. Larson, for his assistance in the construction and calibration of the experimental facility.
- Mr. P. Clark, for providing computer programs and parts of programs that were invaluable in the processing and analysis of data.
- Mr. A. Blecha, for providing the APL regression program that was used in data analysis.

All of the above are in the Department of Agricultural Engineering at the University of Alberta.

Construction of the facility was funded by the Alberta Agricultural Research Council under the Farming for the Future Program of the Alberta Heritage Fund and by the Natural Sciences and Engineering Research Council of Canada.

Table of Contents

Chapter Page

ABSTRACT iv

ACKNOWLEDGEMENTS vii

LIST OF SYMBOLS xv

1. INTRODUCTION 1

1.1 Ventilation in Animal Housing 1

1.2 Dilution and Mixing 3

1.3 Criteria for Ventilation 6

1.4 Airflow Patterns 8

2. THE VENTILATING AIR JET 12

2.1 Isothermal, Submerged Free Jets 12

2.1.1 Jet structure 13

2.1.2 Velocity profiles 17

2.1.3 Divergence of the jet 20

2.1.4 Velocity at the jet axis 21

2.1.5 Entrainment in the jet 24

2.2 Constrained Jets 25

2.2.1 Jets in a confined space 25

2.2.2 Wall jets 28

2.3 Non-isothermal Jets. 29

2.3.1 Temperature profile 29

2.3.2 Concentration profile 32

2.3.3 Jet trajectory 33

2.4 Practical Implications 43

2.5 Aims 45

3. EXPERIMENTAL FACILITY 47

3.1 Requirements 47
3.2 Design 48
    3.2.1 Chamber 48
    3.2.2 Air movement 52
    3.2.3 Animal simulation 55
3.3 Instrumentation 56
    3.3.1 Airflow measurement 59
    3.3.2 Environment and temperatures 61
3.4 Data Collection and Processing 64
    3.4.1 Data collection 64
    3.4.2 Data processing 66
    3.4.3 Photographic data 67
4. METHODOLOGY 69
4.1 Constraints 69
4.2 Experimental Design 70
4.3 Experimental Procedure 72
    4.3.1 Trials 72
    4.3.2 Normal runs 74
    4.3.3 Varying area runs 77
4.4 Data Processing and Reduction 78
5. RESULTS 80
5.1 Jet Trajectories 80
5.2 Varying Heated Areas 89
5.3 Mixing in the Ventilated Space 96
6. DISCUSSION 101
6.1 General Jet Behaviour 101
6.2 Comparison of Inlet Configurations 102

6.3 Equations of Trajectories 104

6.4 Effect of Heated Area 106

6.5 Modification of Archimedes Number 111

6.5.1 Geometrical terms 112

6.5.2 Temperature terms 114

6.6 Mixing in the Ventilated Space 118

6.6.1 Horizontal temperature distribution 118

6.6.2 Vertical temperature distribution 125

6.6.3 Entrainment ratios 130

7. DESIGN IMPLICATIONS 138

7.1 Archimedes Number Criteria for Jets 138

7.2 Mixing Criteria 139

7.3 Inlet Design 140

7.4 Control 150

8. SUMMARY AND CONCLUSIONS 154

8.1 The Drop Coefficient 154

8.2 Criteria for Jet Trajectories 154

8.3 Effect of Heated Area 155

8.4 Modification of Archimedes Number 155

8.5 Criteria for Air Mixing 156

8.6 Heat Transfer from the Ceiling 156

8.7 Design Implications 157

9. RECOMMENDATIONS FOR FURTHER WORK 158

9.1 Modification of Experimental Facilities 158

9.1.1 Thermistor circuits 158

9.1.2 Thermistor placement 158

9.1.3 Air velocity probe array 159

9.1.4 Heating pad water circulation 160

9.2 Topics for Future Investigation 160

9.2.1 Trajectory equations 161

9.2.2 Limits of the Coanda Effect 161

9.2.3 Development of a universal Archimedes number 162

9.2.4 Heat transfer from ceiling 162

9.2.5 Mixing in the ventilated space 163

9.2.6 Development of inlets and control systems 163

10. REFERENCES 165

11. APPENDIX I - CIRCUIT DIAGRAMS 172

12. APPENDIX II - CALIBRATION EQUATIONS 173

13. APPENDIX III - COMPUTER PROGRAMS 175

14. APPENDIX IV - DATA SAMPLES 185

15. APPENDIX V - PHOTOGRAPHY 187

List of Tables

Table Page

4.1 Summary of experimental test series 73

4.2 Tests with varying heated areas 79

5.1 Regression equations for Z against Ar 89

5.2 Regression equations for Z against Ar using pooled data 91

6.1 Regression equations for Z against Ar_d for normal tests only 117

6.2 Regression equations for Z against Ar_d for pooled data 117

6.3 Cubic equations relating COVL and J 124

6.4 Linear equations relating T_0/T_5 and J. 131

7.1 Maximum Ar for $Z<0.25$ and $Z<0.5$ 139

7.2 Opening width required for full-width slots in actual barns under minimum ventilation 142

7.3 Fan test data 144

List of Figures

Figure Page

2.1 Structure of an isothermal, submerged free jet 15

3.1 Overall view of experimental facility 50

3.2 Inlet panels (Dimensions in mm). 53

3.3 Flow-measurement duct (Dimensions in mm). 54

3.4 Plan view of experimental room 57

3.5 Block diagram of instrumentation 58

3.6 Vertical location of thermistors 65

4.1 Typical plots of duct temperature versus time 75

5.1 Sample trajectory plots (Inlet at ceiling). 82

5.2 Sample trajectory plots (Lower inlet position). 82

5.3 Plot of Z versus Ar for ceiling inlets. 86

5.4 Plot of Z versus Ar for lower inlets. 87

5.5 Plot of Z versus Ar using pooled data (full-width, ceiling inlet). 92

5.6 Plot of Z versus Ar using pooled data (full-width, lower inlet). 93

5.7 Plot of Z versus Ar using pooled data (half-width, ceiling inlet). 94

5.8 Plot of Z versus Ar using pooled data (half-width, lower inlet). 95

6.1 Plot of COVL versus J (full-width, ceiling inlet). 119

6.2 Plot of COVL versus J (full-width, lower inlet). 120

6.3 Plot of COVL versus J (half-width, ceiling inlet). 121

Figure Page

6.4 Plot of COVL versus J (half-width, lower inlet). 122

6.5 Plot of COV_5 versus J (full-width, ceiling inlet). 126

6.6 Plot of COV_5 versus J (full-width, lower inlet). 127

6.7 Plot of COV_5 versus J (half-width, ceiling inlet). 128

6.8 Plot of COV_5 versus J (half-width, lower inlet). 129

6.9 Plot of T_0/T_5 versus J (full-width, ceiling inlet). 132

6.10 Plot of T_0/T_5 versus J (full-width, lower inlet). 133

6.11 Plot of T_0/T_5 versus J (half-width, ceiling inlet). 134

6.12 Plot of T_0/T_5 versus J (half-width, lower inlet). 135

7.1 Plot of conditions to satisfy $Ar_d<27$ 145

7.2 Plot of conditions to satisfy $Ar_d<5$ 146

LIST OF SYMBOLS

Symbol	Description	Units
A	cross-sectional area of jet	m^2
A'	effective area of jet orifice	m^2
A_s	cross-sectional area of room	m^2
A_0	initial cross-sectional area of jet	m^2
Ar	Archimedes number	
Arc	corrected Archimedes number (Mullejans)	
Arc'	corrected Archimedes number (Jackman)	
Ar_d	Archimedes number based on exhaust temperature.	
a	orifice turbulence coefficient	
B	room width	m
b	horizontal width of plane jet	m
C	a constant	
C_d	discharge coefficient	
C_p	specific heat at constant pressure	J/kg°K
c	mixing length proportionality constant	
D	distance of orifice from ceiling	m
d	hydraulic diameter of orifice	m
d_0	diameter of circular orifice	m
E	fan characteristic constant	Ns/m^5
F	Froude number	

Fr	Froude number	
G_n	generation rate of contaminant n	m^3/s
g	acceleration due to gravity	m/s^2
H	room height (floor to ceiling)	m
h	vertical thickness of a jet	m
h	vertical dimension of slot orifice	m
h_0	initial thickness of a jet	m
I	fan characteristic constant	Pa
j	jet momentum number	N/m^3
J	dimensionless momentum number	
K	dimensionless velocity decay constant	
k	proportionality constant for centreline velocity of an axially-symmetric jet	m^2/s
k'	proportionality constant for centreline velocity of a plane jet	$m^{3/2}/s$
L	Prandtl mixing length	m
L'	Taylor mixing length	m
l	characteristic length	m
l_d	hydraulic diameter of room	m
M_x	momentum at a section	N
M_0	momentum at orifice	N
M_0'	dimensionless initial momentum	
m	mass flow rate	kg/s
N	jet trajectory constant	
n	number of observations	

p	shape factor for velocity profile	
P	pressure difference	Pa
Q_x	volumetric flow rate at a section	m^3/s
Q_o	volumetric flow rate at orifice	m^3/s
Re	Reynolds number	
Ri	Richardson number	
r	radius of axially-symmetric jet	m
r_o	radius of circular orifice	m
S	lateral mass transfer rate	kg/m^2s
s	shape factor for temperature profile	
t	time	s
T	absolute temperature	°K
T_d	exhaust temperature	°K
T_l	room air temperature	°K
T_m	temperature profile maximum at a section	°K
T_n	temperature at location n	°K
T_o	inlet temperature	°K
T_s	heated surface temperature	°K
T_5	minimum temperature 5m from inlet	°K
U	jet velocity	m/s
U_m	maximum velocity at a section	m/s
U_o	velocity at orifice	m/s
U_t	terminal velocity of a jet	m/s
u	velocity in x-direction	m/s
u'	fluctuating component of u	m/s

$\bar{u}$	time-average of u	m/s
V	mean room air velocity	m/s
v	velocity in y-direction	m/s
v'	fluctuating component of v	m/s
W	lateral heat transfer rate	W/m^2
X	room length	m
x	horizontal distance	m
x'	dimensionless horizontal distance	
x_l	length of laminar flow region	m
y	vertical distance	m
y'	dimensionless vertical distance	
Z	drop coefficient	
α	ratio of buoyancy and momentum forces	
β	coefficient of volumetric expansion	$^{\circ}K^{-1}$
γ	specific gravity	
δ	deviation from mean	
ρ	density	kg/m^3
ρ_o	jet density at orifice	kg/m^3
ρ_l	density of room air	kg/m^3
λ	turbulent Schmidt number	
μ	error-function exponent	
ν	kinematic viscosity	m^2/s
τ	shear stress	N/m^2
χ	contaminant concentration	mole or volume fraction

1. INTRODUCTION

1.1 Ventilation in Animal Housing

One of the principal objectives of housing animals is to provide an environment that is conducive to maximum levels of their production. Although behavioral and emotional considerations should not be discounted, inasmuch as production is diminished by poor health or stress due to physical discomfort, an environment is sought that also will result in the optimum comfort of the housed animal. In addition, the comfort and health of humans working in such buildings must be considered. Furthermore, the environment in an animal building is a complex entity comprised of many factors which, in turn, are influenced by the design of the structure and the management practices adopted within it.

One group of factors that is readily identifiable is that concerned with the air surrounding the animals and includes its temperature, relative humidity, velocity, and concentrations of dust, carbon dioxide (CO_2), ammonia (NH_3), methane (CH_4), hydrogen sulphide (H_2S) and other contaminants. Although the designer of an animal building may influence these by, for example, choice of manure storage and disposal systems, choice of feed, watering and drainage systems and design of pen layout and partitioning, the primary means of controlling these elements of the environment is by ventilation.

The role of ventilation in animal housing, therefore, is to remove air containing the products of animal occupancy and metabolism and to replace this with fresh air (Wathes *et al.* 1983) or cleansed air (Barber, 1981). The products of metabolism to be removed are heat, moisture, CO_2 and CH_4. Depending on the species of animal and the manure handling system, noxious gases such as H_2S and NH_3 also must be removed as must dust, which on its own can predispose animals and man to respiratory problems and can act as a carrier of pathogens (Smith, 1972).

Methods of ventilation for removal of these products can be characterised as either "displacement" or "dilution" systems. Displacement ventilation seeks to purge the airspace with clean air advancing behind a continuous front across the whole ventilated volume. For optimum efficiency, this type of ventilation requires laminar or nearly-laminar airflow which is very difficult to achieve or maintain in an environment containing hot, moving bodies (Randall, 1975). Downward displacement systems using porous ceilings nevertheless have been described for agricultural systems by Pattie and Kagio (1981) and Sainsbury (1980), amongst others. However, the method of ventilation enjoying the most widespread use in confined animal buildings is that of dilution. In such systems the ventilating air generally enters the building as a turbulent jet. The mechanism of dilution is now reviewed briefly.

1.2 Dilution and Mixing

If two stagnant volumes of air containing different amounts of heat, moisture, or contaminant gases are brought together, the concentrations of these quantities in the total volume will tend, eventually, to become uniform throughout the volume. In the case of moisture or gaseous contaminants, this equalization process is by means of molecular diffusion in the direction of concentration or partial pressure gradients. With heat, assuming the volume remains stagnant, conduction would lead eventually to an equalization of temperature throughout the volume. However, if the temperature difference of the two air mixtures results in a difference in density between the two mixtures, then convection currents will be set up giving rise to mixing of all the components in the volume. The mixing caused by natural convection obviously will be augmented by any externally-generated motion of the mixture such as might be expected from air jets caused by ventilation fans. Since dust, in the absence of electrostatic charge or Brownian motion, will not be affected by concentration gradients, mixing due to free or forced convection must be relied on to obtain a uniform concentration in the mixture.

In the animal environment the housed animals themselves are a source of heat and will raise the temperature of the air in their immediate vicinity. This will result in convection currents which, with proper design of inlets and outlets, can be sufficient to provide natural ventilation of their occupied space. If temperature gradients are inadequate for natural ventilation, or higher flow rates are required, ventilation fans are used, but the result is the same: Air with low concentrations of the products of metabolism and occupancy is introduced into the ventilated space where it is mixed with air having a higher concentration of these products. The air space thus contains a diluted mixture which is exhausted continuously. This situation is directly analagous to flow through a stirred tank in chemical process engineering and may be described mathematically in the same way. The process may be represented by the mixing dilution equation:

$$V_s dX_n/dt = (G_n+QX_{ni})-QX_n \qquad 1.1$$

where X_n = concentration of component n at time t (mole or volume fraction),
X_{ni} = concentration of component n in inlet air,
G_n = constant generation rate of component n (m^3/s),
V_s = volume of ventilated space (m^3) and
Q = volumetric flow rate (m^3/s).

The above equation was used as the basis of a model study by Furry and Hazen (1967). These authors used CO_2 as the "contaminant" gas and obtained good agreement between model and prototype results over a range of flow rates. An observed discrepancy between theoretical and experimental values for the plot of $\ln(X_n-X_{ni}/X_0-X_{ni})$ vs (Qt/V), where X_0 = concentration at t=o, most probably was due to incomplete mixing as described by Barber and Ogilvie (1982). The latter authors point out that, especially at very high or low flow rates, incomplete mixing within the airspace is likely to occur and identify three simple models to describe this phenomenon: short circuiting, secondary flow regions and a "tanks-in-series" situation.

Thus, while the simple mixing-dilution model may not apply exactly to practical ventilation systems, discrepancies may be explained in terms of incomplete mixing rather than by the effect of processes, such as diffusion, on the molecular scale. These processes must certainly be going on continuously but their effect is negligible in comparison to the large-scale movements of the air due to free and forced convection. This contention is supported by Mullejans (1966) who states that the turbulent forces caused when air is blown into a closed room, especially if there is a heat source in the room, dominate the molecular transport processes to such an extent that the latter may be ignored.

The dominance of the large-scale air movements on concentrations of gases in animal housing also is confirmed in the results obtained by Brannigan and McQuitty (1971). In this study, heater/gas-diffusion units were located in a room to simulate, at full scale, the conditions in a pen of 20 pigs.

Using a range of ventilation rates, these authors demonstrated the importance of sensible heat production and ventilation rate in the mixing of both NH_3 and CO_2 with air. In addition, the effect of gas density was shown to be of no practical importance in determining the distribution of gases within the air mass.

1.3 Criteria for Ventilation

The simplified model represented by equation 1.1 shows that the concentration of any single contaminant within the air mass or the temperature of the air mass may be controlled by varying the ventilation rate, Q. Two problems now arise:

1. What are the ideal or limiting levels for each of these quantities?
2. What is the flow rate that will give ideal or sub-limiting levels of all quantities simultaneously?

In order to answer the second question, not only must the answer be known to the first, but the generation rates of heat, moisture, dust and contaminant gases must be known also. With these data available, a system of simultaneous equations could be set up and solved for the ventilation rate. Unfortunately, these data are not available for agricultural species (Wathes *et al*. 1983) and so less ideal criteria for determining ventilation rate must be used. In practice, the most common criteria used are the levels of temperature and relative humidity, the former being used under summer conditions and the latter for the low ventilation rates encountered in winter.

Temperature is used with pigs and poultry since it is likely to be the first limiting factor for production as the ventilation rate is lowered in the search for energy efficiency. With ruminants, which can alter their range of thermoneutrality, animal health, rather than energy conservation, should be the prime factor governing ventilation (Webster, 1981). Since adequate data on desirable levels of other contaminants are not available, and since it is measured easily, relative humidity can be used as an indicator of adequate ventilation for ruminants. However, ventilation on the basis of humidity control probably is practised as much to prevent condensation, and maintain the condition of the building, as out of consideration for animal health. The fact that certain, potentially hazardous, micro-organisms are sensitive to relative humidity (Wathes *et al*. 1983) does not appear to have been considered in the selection of ventilation criteria for most systems.

From an environmental control point of view there has been no great incentive, until recently, to use more than one or two criteria for ventilation control. Technology was such that control systems embodying anything more complicated than simple thermostats or humidistats were prohibitively expensive for use in animal housing. The advent of the microcomputer has changed the situation and more complex control strategies using a greater number of criteria are now quite feasible (Leonard and McQuitty, 1986). Thus, not only is it desirable that more data be obtained on the levels of contaminants in animal environments, but these data could be incorporated immediately in ventilation control systems to provide optimum flow rates at all times.

1.4 Airflow Patterns

No matter what flow rate is used, ventilation results in a general movement of air through the building. The velocity of air within the building is highest at the air inlet where the flow generally may be described as a turbulent jet. At the boundary of this jet there is a continuous exchange of momentum with the surrounding air giving rise to entrainment of the surrounding air and a reduction of jet velocity. This, in turn, results in secondary airflows within the room and an airflow pattern is set up within the ventilated space. Ideally, the pattern of secondary airflows will result in complete mixing of the ventilation air. However, as has been mentioned above (Barber and Ogilvie, 1983), incomplete mixing also can result. Full-scale flow visualisation studies by Randall (1975,1980), Randall and Battams (1976) and Boon (1978) have demonstrated that, in addition to the initial velocity of the inlet air, ceiling obstructions, together with the layout of pens and design of partition structures within the building, exert a great influence on the airflow patterns within the building. These airflow patterns are of particular significance in confinement housing when considering airflow at the level of the housed animals.

Comparing the effects of air velocities of 18 m/s and 1.52 m/s over pigs, Bond *et al.* (1965) showed that, if air temperatures were less than 32°C, the higher velocities caused a reduction in daily weight gain and a decrease in feed conversion efficiency. For air temperatures between 35°C and 44°C, higher velocities caused increases in weight gain whereas they had no effect at higher temperatures. As these results indicate, air flow over the animals increases convective and evaporative heat loss. For air temperatures lower than the approximate surface temperature of the animal, excessive air flows cause an elevation of the lower critical temperature (i.e., the lower bound of the thermoneutral range) and the animal must use additional feed energy for increased thermogenesis. At higher temperatures, increased air velocities in the occupied zone cause an elevation of the upper critical temperature while, at excessively high temperatures, there is no potential for evaporative and convective cooling.

More recently, Sällvik and Walberg (1984) have identified an optimum range of chill factors based on pen and animal hygiene, growth, feed conversion and tail-biting behaviour. The chill factors were expressed in W/m² but could be translated into air velocities for a given size of pig in a given ambient temperature. For 50-kg pigs in a 20°C environment, the air velocities corresponding to the optimum chill factor range of 60-80 W/m² were 0.21 to 0.38 m/s.

The elevation of the lower critical temperature of pigs due to air velocity has been incorporated in a mathematical model by Bruce (1981). Randall (1980) used this model in evaluating several combinations of ventilation systems and pen layouts. The results from the above study indicated that reversals of flow direction over the pigs can occur unless careful attention is paid to the direction and speed of air at ventilation inlets. The practical consequence of unstable airflow patterns can be a disruption in the behavior patterns of the housed animal. Thus, one airflow pattern may promote a cool area for dunging and a warmer area for sleeping. If this airflow were reversed, there would be a tendency for dunging to occur in the sleeping area and *vice versa* (Baxter,1984).

Instability of airflow patterns within a building is most likely to occur at low ventilation rates (Randall, 1980) and these generally coincide with the winter air temperatures most conducive to adverse energy losses from the housed animals due to unwanted airflows. Since the initial flow path from the air inlets must be predictable and stable before any rational design of penning and other internal structures is carried out, the designer of ventilation systems requires some means of ensuring this. In practice, this requirement has translated into the adoption of general design rules (e.g., Winchell, 1982; Turnbull and Bird, 1980) aimed at providing air velocities that are sufficient to ensure adequate control and mixing of cold inlet air with warm inside air.

Despite these guidelines, inlet designs are often such that continuous control of inlets in response to changing air flows is impossible, inconvenient or ignored. In addition, under very cold conditions and particularly with old structures, great difficulty is encountered in trying to adjust inlets to control very low air flow rates. There is, therefore, a need to reassess the criteria used in the control of inlets and the design of the inlets themselves. To this end, recent studies have called for a more rational and analytical approach to the problem (Kaul *et al.* 1975; Randall and Battams, 1979; Barber *et al.* 1982). Consequently, the general objective of this project was to study the applicability of the theories propounded by the above authors to ventilation of animal buildings under Canadian winter conditions (i.e., using very low temperature inlet air). The specific aims of this project are detailed in section 2.5.

Before defining the specific aims of the project, however, the theory of ventilating air jets will be reviewed. This, together with reference to recent experimental investigations, will provide the context within which the project was undertaken.

2. THE VENTILATING AIR JET

2.1 Isothermal, Submerged Free Jets

In most modern, forced ventilation systems in animal housing, exhaust fans cause a negative pressure gradient between inside and outside environments. This pressure differential causes a jet of air to be drawn through any ventilation inlet. The form of this jet will depend on the location of the inlet, the temperature difference between the jet and the ambient (i.e., inside) air and the state of motion of the ambient air. If the temperatures of the jet and the ambient air are equal, the jet is said to be isothermal. The jet also is said to be submerged if it discharges into still air. An air mass is considered to be still if velocities within it are less than 0.25 m/s (ASHRAE, 1981) while a free jet is one whose boundaries are unaffected by obstructions or limitations such as walls. From an analytical point of view, the simplest form of jet is one that is isothermal, submerged, free and issuing from a circular outlet.

A jet may be described in terms of angle of divergence, variation of velocity along its axis and the velocity profile at right angles to its axis. Before discussing these, however, mention should be made of the various zones that make up a jet.

2.1.1 Jet structure

Tuve (1953) and, subsequently, ASHRAE (1981) identify four zones within a jet:

Zone 1: Extending approximately four diameters from the outlet face (or vena contracta of an orifice) and in which the maximum velocity of the airstream is unchanged.

Zone 2: Extending to about eight diameters in which the maximum velocity varies inversely as the square root of the distance from the outlet.

Zone 3: The major part of the jet in which turbulence is fully established and which is 25 to 100 diameters in length. In this zone the maximum velocity varies inversely as the distance from the outlet.

Zone 4: The zone in which the jet terminates as the maximum velocity decays, within a few diameters, to magnitudes approaching still air.

Of these zones, Zone 3 is the most important in considerations of air distribution. Tuve (1953) states that measurement and accurate description of the jet in Zones 1 and 2 may be difficult due to rapid transitions, pressure variations and the small distances involved. Nevertheless, Abramovich (1963) gives details of consistent velocity measurements in these regions dating back to 1938.

The latter author, together with Baturin (1972), describes three zones within a jet which are termed the initial, transitional and main regions. These regions correspond approximately to the previously described Zones 1 to 3 except that the extent of these regions differ from those already defined. Abramovich (1963) states that an often-used simplification of a jet is one in which the length of the transitional zone is equal to zero. This approach is adopted by Baturin (1972), who indicates that the length of the initial region, which depends on flow conditions and turbulence at the outlet, varies from approximately two to six diameters.

In addition to differences in dimensions of the zones, the latter two authors describe the structure of the initial region in more detail than do the former two. The jet structure as proposed by Abramovich (1963) is illustrated in Figure 2.1.

Assuming that the velocity field is uniform at the outlet cross-section, the initial region of the jet consists of a linearly converging, constant velocity core surrounded by a diverging mixing layer. If U represents the velocity component parallel to the jet axis, then the outer surface of this boundary layer is defined as being where $U=0$ and the inner surface is defined by the requirement that $U=U_0$, where U_0 is the outlet velocity. Beyond the initial region, the boundary layer continues to expand at the same rate until, at the beginning of the main region, the jet appears to diverge from a single point, P, called the pole of the jet or the apparent source (Nottage *et al.* 1952a).

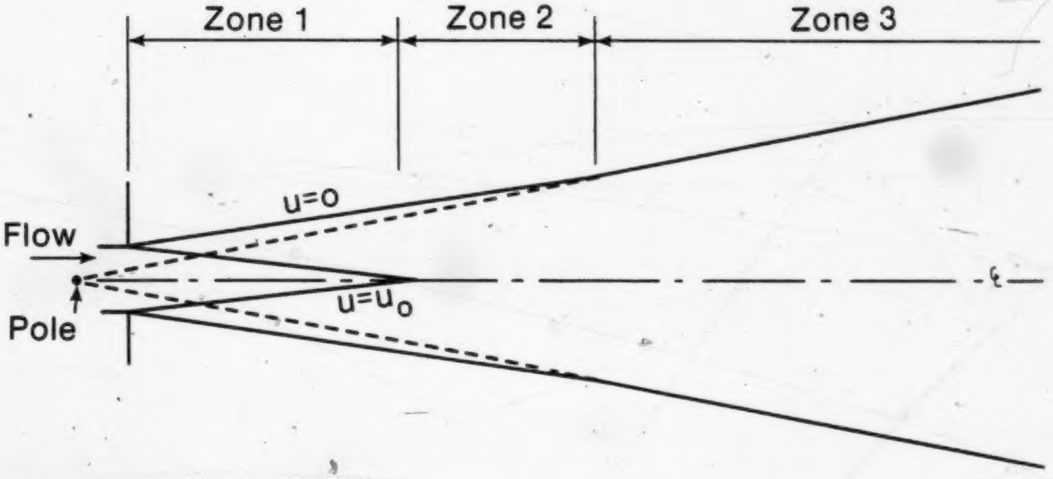

Figure 2.1 Structure of an isothermal,submerged free jet.

Linke (1966) adopted a similar model of jet structure to that of Abramovich (1963) but made use of an orifice Reynolds number to define the length of an initial region of laminar flow, x_l. The orifice Reynolds number was defined as:

$$Re = d.U_o/\nu \qquad 2.1$$

where: d = the hydraulic diameter of the orifice (m)
U_o = the axial velocity at the orifice (m/s), and
ν = kinematic viscosity of the air (m²/s).

Depending on the shape of the orifice and Re, x_l can extend to more than 20 diameters downstream. However, for Re>1500 all jets are completely turbulent from the origin (i.e., x_l=0) although this does not imply that there is not a zone of transition from contained to free flow. Indeed, Abramovich (1963) points out that the structure coefficient, a, that was used to predict core length is independent of Reynolds number over a wide range and is simply a function of velocity profile uniformity at the jet origin. In a discussion that appears to be based on Abramovich's work, Baturin (1972) uses the term turbulence coefficient for a, while Kaul *et al.* (1975) use a similar coefficient, m, which predicts a range of values for the core length (i.e., length of initial region) comparable to those given by Tuve (1953) for the extent of Zone 1. Work by Nottage *et al.* (1952b) also indicates a relationship between outlet turbulence intensity and the distance before the beginning of fully-developed flow. Thus, despite some difference in details, the free, submerged, round, isothermal jet is agreed generally to consist of a main section of fully developed, turbulent flow preceded by a formative section in which a core of uniform, initial velocity is eroded away. Essentially the same situation exists for jets issuing from long, rectangular slots (i.e. for plane jets), nevertheless, the following differences between plane jets and round jets should be noted:

Whereas round jets are axi-symmetric, plane jets are initially symmetric about the axes defined by the vertical and horizontal centre lines of the slot. Slots are characterised by their aspect ratio, which is defined as the ratio of length to width of the opening (ASHRAE, 1981). In Zones 1 and 2, and depending on aspect ratio, the cross-section of a plane free jet will tend to become elliptical or circular and the extent of the various zones of the jet may be predicted in terms of slot width (Baturin, 1972; Kaul *et al.* 1975) or a combination of slot width and aspect ratio (ASHRAE, 1981).

2.1.2 Velocity profiles

The literature abounds with experimental data on the velocity profiles of free jets (Walker, 1977; Rajaratnam, 1976; Baturin, 1972; Abramovich, 1963; Nottage *et al.* 1952a; Koestel *et al.* 1950). In all cases, the velocity profiles within a given region are shown to be similar, regardless of the location of the cross-section at which they are taken, if the profiles are expressed in dimensionless form. In order to obtain a dimensionless plot of velocity parallel to the jet axis against location at right angles to the axis, both velocity and location parameters must be expressed in the form of dimensionless ratios. The dimensionless velocity at some distance, x, along the jet centreline from the outlet, therefore, is defined as U/U_m, and the dimensionless location as y/y_1 where:

U = velocity parallel to the jet axis at some distance, y, from the axis.
U_m = velocity parallel to the jet axis at the axis (i.e. the centreline velocity), and
y_1 = distance from the axis at which the velocity is half of that at the axis.

Abramovich (1963) gives examples of dimensionless velocity profiles in the initial region of both round and plane free jets, while all the other authors mentioned above give details of experimentally-obtained velocity profiles for the fully developed jet. According to Tuve (1953), two theories have been used to develop theoretical velocity profiles for jets. These are the momentum-transfer theory (Prandtl-Tollmein) and the vorticity-transfer theory (Taylor-Goldstein), both of which are described by Abramovich (1963).

The development of the Prandtl-Tollmein theory dates from 1926 and starts with the equation of motion, in the x-direction, for the two-dimensional flow of an incompressible fluid in the boundary layer:

$$\partial u/\partial t+u\partial u/\partial x+v\partial u/\partial y = \nu\partial^2 u/\partial y^2-(1/\rho)\partial p/\partial x \qquad 2.2$$

where: u = velocity in the x direction,
v = velocity in the y direction,
t = time,
ρ = fluid density, and
p = pressure.

Since a free jet has no solid boundaries and, therefore, no laminar sub-layer, the effects of viscosity can be neglected. In addition, free jets are characterised by negligibly small pressure gradients so that both terms on the right hand side of equation 2.2 can be ignored.

Now, all velocities can be represented by a time-average and a fluctuating component. Thus, for example, $u = \bar{u} + u'$ where u' is the fluctuating component and whose time average is zero. Using this, equation 2.2 can be written:

$$u\partial u/\partial x+v\partial u/\partial y +\partial\overline{v'u'}/\partial y = 0 \qquad 2.3$$

where u and v are time-averaged values. Equation 2.3 may be compared with the equation of motion derived from momentum balance:

$$u\partial u/\partial x+v\partial u/\partial y = (1/\rho)\partial\tau_{xy}/\partial y \qquad 2.4$$

where τ_{xy} is the shear stress on a plane perpendicular to that of the axes. Comparison of equations 2.3 and 2.4 yields:

$$\tau_{xy} = -\rho\overline{u'v'} \qquad 2.5$$

Since the product $\rho v'$ represents the fluid mass passing per second through the plane of τ_{xy}, and since u' is the fluctuation of longitudinal velocity, equation 2.5 indicates that the turbulent shearing stress is defined by the lateral transfer of the longitudinal component of momentum. Assuming that transverse velocity fluctuations are proportional to, and of the same order as longitudinal fluctuations, the Prandtl formula for turbulent shearing stress may be written:

$$\tau_{xy} =\pm\rho L^2|\partial u/\partial y|\partial u/\partial y \qquad 2.6$$

where L is the mean free path length for the fluid particles in the stream or the Prandtl "mixing length". Because of the absence of walls, L is assumed to be constant in the transverse direction but, to account for similarity of velocity profiles, is held to vary in proportion to distance along the jet axis, i.e., L=c.x where c is a constant related to jet structure. Thus, substituting into equation 2.4, the Prandtl equation of motion for free turbulence becomes:

$$u\partial u/\partial x+v\partial u/\partial y = \pm 2c^2x^2\partial u/\partial y.\partial^2u/\partial y^2 \qquad 2.7$$

Using this equation, Tollmein obtained solutions for the velocity profiles of both axially symmetric and plane free jets. (The Taylor-Goldstein, vorticity transfer theory results in the same equation of motion and discussion of this theory will be reserved for those sections dealing with temperature and concentration profiles). Although these solutions provide reasonable agreement with experimental data, they are somewhat cumbersome and later workers (Nottage *et al.* 1952a; Tuve, 1953; Walker, 1977) have opted to fit data to the Gaussian error-function curve (i.e., normal probability curve) which has the general form:

$$U/U_m = \exp(-\mu y^2) \qquad 2.8$$

where μ = a constant for a specific profile.

Good agreement with experimental data is obtained with a curve described by:

$$(y/y_1)^2 = 3.3\ln(U_1/U) \qquad 2.9$$

2.1.3 Divergence of the jet

Similarity of the velocity profiles at different sections of the free jet implies similarity of geometric dimensions of the sections. Thus, dimensionless mixing lengths at different sections may be expected to be equal:

$$L_1/h_1 = L_2/h_2 = . . . = \text{constant} \qquad 2.10$$

where h is the width of the jet at any section. Now, since $L = cx$ it follows that:

$$x_1/h_1 = x_2/h_2 = . . . = \text{constant} \qquad 2.11$$

and, in general that:

$$h = \text{constant}.x \qquad 2.12$$

Thus, on the basis of the assumptions associated with the Prandtl mixing length, a free jet is predicted to diverge linearly with distance from its origin. This phenomenon has been observed experimentally by numerous authors (Baturin, 1972; ASHRAE 1981) and the included angle of the jets measured have ranged from 20° to 30°, depending on their initial form and turbulence.

2.1.4 Velocity at the jet axis

Because the pressure in a free jet is virtually constant and equal to the pressure in the surrounding space, the momentum at any cross-section should be the same:

$$\int_0^m U dm = \int_0^A \rho U^2 dA = \text{constant} \qquad 2.13$$

where dm is the mass flowing through an element of the cross-section, dA, per unit time. For an axially symmetric jet whose outer radius at any section is given by r, equation 2.13 can be re-written:

$$2\pi\rho\int_0^r U^2 y.dy = \text{constant}$$

and thus:

$$2\pi\rho U_m^2 x^2 \int_0^{r/x} (U/U_m)^2 y/x.dy/x = \text{constant} \qquad 2.14$$

As a result of the similarity of jet profiles, the term U/U_m is a function only of the dimensionless coordinate y/x. Thus, the integral is a constant and the result is :

$$U_m = k/x \qquad 2.15$$

where k is a constant.

In other words, the centre-line velocity of an axially symmetric jet varies inversely as the distance from the pole of the jet.

For a plane jet, whose vertical thickness at any section is given by h, equation 2.13 may be rewritten:

$$\rho U_m^2 x \int_0^{h/2x} (U/U_m)^2 dy/x = \text{constant} \qquad 2.16$$

which results in:

$$U_m = k'/\sqrt{x} \qquad 2.17$$

where k' = a constant.

Thus, the centreline velocity of a plane free jet varies inversely as the square root of distance from the pole.

In both equations 2.15 and 2.17, the axial velocity can be expressed in dimensionless form as U_m/U_0 and this can be evaluated theoretically. Tollmein's solution of the Prandtl momentum-transfer equation results in the expression for an axially symmetric jet:

$$U_m/U_0 = 0.96 r_0/ax \qquad 2.18$$

where r_0 is the radius of the initial cross-section of the jet and a is a coefficient related to jet structure. Values for a, given by Abramovich (1963), range from 0.066 to 0.076. Tollmein's expression for a plane jet is:

$$U_m/U_0 = 1.7(ax/h_0)^{1/2} \qquad 2.19$$

where h_0 is the initial width of the jet and a is in the range 0.09 to 0.12.

Walker (1977) shows that expressions for dimensionless axial velocity can be obtained by substituting the normal distribution function (equation 2.9) into an equation for the momentum at a cross-section. For an axially symmetric jet, this results in the expression:

$$U_m/U_o = K\surd A_o/x \qquad 2.20$$

where K is termed the decay constant and has a value of 7.60. A_o is the area of the initial cross-section of the jet. Expressing equation 2.20 in terms of r_o gives:

$$U_m/U_o = 13.47 r_o/x \qquad 2.21$$

which is in the middle of the range given by Abramovich (1963)-for the Tollmein solution:

$$12.63(r_o/x) < U_m/U_o < 14.55(r_o/x)$$

Similarly, for a plane jet, the expression derived by Walker (1977) is:

$$U_m/U_o = K\surd(h/x) \qquad 2.22$$

where K here has the value of 2.76 and h is the outlet slot width. Expressing equation 2.19 in similar terms results in a range of values for U_m/U_o:

$$2.45\surd(h/x) < U_m/U_o < 2.83\surd(h/x)$$

Thus, the use of the normal distribution to describe the velocity profile seems to be well justified in that it gives similar results to the more theoretically-rigorous approach of Tollmein, yet is more easy to apply.

A concept associated with axial velocity is that of throw. The throw of a jet is defined (ASHRAE, 1981) as the distance an airstream travels after leaving an outlet before the maximum stream velocity is reduced to a specified terminal velocity, U_t. The actual value of U_t that is used varies with applications. ASHRAE (1981) recommends use of U_t=0.5m/s for ceiling slot diffusers and U_t=0.25 m/s for all other outlets.

2.1.5 Entrainment in the jet

As has been described in section 2.1.2, a free jet expands by means of transferring momentum (or vorticity) to the surrounding air. This means that surrounding air is entrained into the jet to become part of it. This is an important concept in ventilation systems based on the mixing/dilution principle and it is useful to have a quantitative measure of entrainment. This is provided by the ratio of volumetric flow through any jet cross-section (Q_x) to that through the initial cross-section (Q_0). Thus, entrainment ratio = Q_x/Q_0. (ASHRAE, 1981)

The mass flow, m, through any section of an axially symmetric jet can be expressed, using polar coordinates, as:

$$m = 2\pi\rho\int_0^\infty rU dr \qquad 2.23$$

from which the momentum at that section follows:

$$M_x = mU = 2\pi\rho\int_0^\infty rU^2 dr \qquad 2.24$$

Substituting the expression for the velocity profile (equation 2.8) in equation 2.24 and integrating gives:

$$M_x = \pi\rho U_m^2/2\mu \qquad 2.25$$

Now, at the initial cross-section:

$$M_0 = \rho A_0 U_0^2 \qquad 2.26$$

Thus, assuming conservation of momentum:

$$U_m/U_0 = (2\mu A_0/\pi)^{1/2}. \qquad 2.27$$

Also, the volume flow through any section is given by:

$$Q_x = 2\pi\int_0^\infty rU dr \qquad 2.28$$

while that through the initial section of the jet is:

$$Q_0 = A_0 U_0 \qquad 2.29$$

If equation 2.8 is substituted into equation 2.28 prior to integration, division by equation 2.29 and combination with equation 2.27 yields the following expression for entrainment ratio:

$$Q_x/Q_o = 2U_o/U_m \qquad 2.30$$

Similarly, for a plane jet:

$$Q_x/Q_o = \sqrt{2}(U_o/U_m) \qquad 2.31$$

Corresponding ratios given by Baturin (1972) are $2.18(U_o/U_m)$ and $(2.07)^{0.5}(U_o/U_m)$ respectively.

2.2 Constrained Jets

Whereas a free jet, by definition, is one that flows into an infinite volume of fluid, most air jets in practical ventilation systems flow into confined volumes and often impinge on a surface such as a wall or ceiling. The general effect of these boundaries is to inhibit the free entrainment of air by the jet, thereby altering its characteristics from that of a free jet. The most general form of constrained jet is one that simply discharges into a finite volume. A wall jet is a special case of this type and is a jet that discharges along a boundary of the finite volume. Both the general and special cases will be discussed separately. Isothermal conditions are assumed throughout.

2.2.1 Jets in a confined space

Linke (1966) and Baturin (1972) have both described results of model studies on air jets discharged into rooms.

These results appear to agree with plots of jet boundaries in full-scale rooms obtained by Nottage *et al.* (1952a). In all cases the jet, issuing from an orifice that is small in comparison to the area of the wall in which it is located, starts to develop as a free jet. The jets shown by Linke (1966) and Nottage *et al.* (1952a) both show initial linear divergence at similar angles (20° to 23°) regardless of initial velocity. In both cases, however, significant reverse flows are shown outside the jet and the velocity profiles become increasingly different from that of a free jet with increasing velocity, especially at larger distances from the origin. The results of Nottage *et al.* show a tendency of jets to stop diverging in the most restricted direction while continuing to diverge in the less restricted direction. Due to the presence of reverse flows outside the jet boundary, the jet never actually reaches a wall or limiting surface.

The above general behavior of jets in confined spaces also is described in ASHRAE (1981) where a need for more engineering data on these jets is expressed.

Baturin (1972) cites unpublished results, again from model studies, obtained by Sadovskaya and also by Rosenberg in the Soviet Union. These investigations indicated that, until the jet cross-section has expanded to occupy 20-25 percent of the cross-sectional area of the confining space, it behaves as a free jet. However, beyond this point, conservation of momentum no longer applies and the rate of divergence of the jet is retarded. A second "critical cross-section" occurs when the jet has expanded to occupy 40 to 42 percent of the cross-section of the space. At this point the momentum of the jet drops sharply and the jet begins to die rapidly. Increasing the initial turbulence of the jet causes more rapid divergence and, hence, the critical sections occur closer to the jet origin.

The influence of room dimensions on the throw of a confined jet was such that, in a model of circular cross-section, the axial velocity decayed practically to zero within three to four diameters of the model. This behavior was confirmed by Linke (1966) and Kaul *et al.* (1975) who have observed that, regardless of the location of the jet, there exists a maximum jet length of about three room heights.

The results reported by Baturin (1972) indicate that the area of the room cross-section has more influence on the jet than does the shape of the cross-section. A useful generalizing parameter appears to be the dimensionless length $\sqrt{A_s}/d_o$ where A_s is the cross-sectional area of the room and d_o is the initial diameter of the jet. Graphs of axial velocity (U_x/U_o) against a dimensionless distance parameter, $x' = ax/\sqrt{A_i}$, indicate that the throw is greater and the velocity decreases more slowly for smaller values of $\sqrt{A_s}/d_o$.

2.2.2 Wall jets

If a jet is discharged along a plane surface, or if an edge of the jet orifice coincides with such a surface, a wall jet results. To all intents and purposes, these behave as if they were one half of an axial or plane jet issuing from an orifice of twice the width or diameter respectively. Virtually no entrainment occurs along the wall, where there is a very thin boundary layer, while normal entrainment occurs at the unrestricted boundaries of the jet resulting in a velocity distribution similar to that for half a free jet (Baturin, 1972). Experimental verification of this behavior is given by Tuve (1953) who shows velocity profiles of wall jets closely approximating one-half of a normal distribution with the maximum velocity adjacent to the wall. Similar results are shown for a low-speed non-isothermal wall jet by Albright and Scott (1974).

If the jet orifice is located a small distance away from the wall, the jet still will tend to adhere to the surface and spread over it. As the jet entrains air on the side nearest the wall, entrainment becomes limited and a region of low pressure results. This tends to attract the jet in the direction of the wall, to which it eventually becomes attached. This phenomenon generally is referred to as the Coanda effect. Baturin (1972) states that jets directed at a surface at angles of less than 40° to 45° will remain attached to the surface. The same author cites unpublished results of scale model studies carried out by

Sadovskaya which indicate that isothermal jets discharging parallel to a ceiling will attach to it if they are located at greater than 0.65 of the ceiling height.

2.3 Non-isothermal Jets.

If the temperature of a jet is different from that of the surrounding air into which the jet discharges, the jet is said to be non-isothermal. If a jet were non-isothermal, it cannot be fully described simply in terms of velocities within the jet. A full description of a non-isothermal jet requires, firstly, a description of the temperature profile of the jet and, secondly, since temperature differences give rise to buoyancy effects, a description of the path of the jet.

2.3.1 Temperature profile

Neglecting the effects of molecular thermal conductivity and the transformation of work due to viscous forces into heat, heat transfer in a turbulent flow is a result of the mixing of layers of fluid with different temperatures. Thus, heat transfer within a jet may be described in terms of velocities and temperature using equations analagous to those in section 2.1.2.

The equation of the thermal boundary layer of a turbulent jet can be written (Abramovich, 1963):

$$u\partial T/\partial x+v\partial T/\partial y+\partial\overline{v'T'}/\partial y=0 \qquad 2.32$$

where u, v and T are time-averaged values, T being absolute temperature. Equation 2.32 may be compared to the steady-state, heat balance equation:

$$u\partial T/\partial x+v\partial T/\partial y = (\partial W/\partial y)/(C_p g\rho) \qquad 2.33$$

where: C_p = specific heat at constant pressure,
g = acceleration due to gravity,
ρ = mass density, and
W = lateral heat transfer/unit time/unit area.

Such a comparison results in an expression of the law of heat transmission for turbulent mixing:

$$W = -C_p g\rho\overline{v'T'} \qquad 2.34$$

This equation is directly analagous to equation 2.5 and application of the concept of the Prandtl mixing length results in:

$$W = \pm C_p\gamma L^2|\partial u/\partial y|\partial T/\partial y \qquad 2.35$$

where γ = specific gravity of the fluid.

Substitution of equation 2.35 in equation 2.33 leads to the Prandtl equation for the thermal boundary layer of a non-isothermal plane jet:

$$u\partial T/\partial x+v\partial T/\partial y = \pm c^2x^2\partial/\partial y.(\partial u/\partial y.\partial T/\partial y) \qquad 2.36$$

Since the air into which the jet discharges has a finite temperature, T_1, the absolute temperature in equation 2.36 may be replaced conveniently with a temperature difference:

$$\Delta T = T-T_1 \qquad 2.37$$

On the basis of equation 2.36, the Prandtl-Tollmein theory predicts that the velocity and temperature fields of a submerged jet must be similar. That is, at any cross-section:

$$U/U_0 = \Delta T/\Delta T_0 \qquad 2.38$$

In practice, the temperature profile has been shown by

Nottage *et al*. (1952b), Wilson *et al*. (1970), Albright and Scott (1974), and others to be wider than the velocity profile. The fact that experimental results have failed to confirm the prediction of equation 2.38 has led to the use of the Taylor-Goldstein theory to predict temperature profiles.

Whereas Prandtl's theory depends on the lateral transfer of longitudinal momentum and the assumption that the fluctuating component of this remains constant over the mixing length, Taylor's theory depends on the conservation of vorticity or conservation of moment of momentum. The result of the application of Taylor's theory is that, although equations 2.32 to 2.34 are still valid, a different mixing length must be used. The relationship of the Taylor mixing length L' to L is given by:

$$L' = L\sqrt{2} \qquad 2.39$$

and, consequently, the thermal boundary layer equation becomes:

$$u\partial T/\partial x+v\partial T/\partial x = 2c^2x^2\partial/\partial y.(\partial u/\partial y.\partial T/\partial y) \qquad 2.40$$

Solution of equation 2.40 leads to the result that, at any point in the flow, the dimensionless temperature difference is equal to the square root of the dimensionless velocity, i.e.,:

$$\Delta T/\Delta T_m = \sqrt{(U/U_m)} \qquad 2.41$$

This is in contrast to equation 2.38 and is in closer agreement with experimental results. Nevertheless, as Hinze (1959) points out, both the Prandtl and Taylor theories are purely phenomenological, cannot be correct in all details, but continue to be useful in the solution of engineering problems.

Applying the conservation of heat content of the jet and using equations 2.18 and 2.19, expressions for temperature decrease along the jet axis may be derived. For a round jet, the dimensionless temperature decrease is given by:

$$\Delta T_m/\Delta T_o = 0.7r_o/ax \qquad 2.42$$

and, for a plane jet, the equivalent expression is:

$$\Delta T_m/\Delta T_o = 1.04(ax/h_o)^{-1/2} \qquad 2.43$$

The divergence of the temperature profile, like that of the velocity profile, is linear along the jet axis and the actual angle of divergence is a function of turbulence at the jet orifice (Wilson *et al*. 1970). In experiments carried out by Black *et al*. (1970), the entrainment ratio was shown to be greater for a cold jet than for an isothermal or warm jet. This was explained by the buoyancy of warm air underneath the jet causing increased turbulence at the jet boundary. In such a situation, the angle of divergence of the jet would be increased.

2.3.2 Concentration profile

This section is included here because of the similarity between temperature and concentration profiles. If a jet contains an admixture at a different concentration to that of the air into which it discharges, the process of turbulent mixing will modify the concentration profile within the jet. In ventilating jets, this process is of significance in the dilution and subsequent removal of contaminants.

Just as the temperature profile depends on the transfer of heat from the jet to the surrounding fluid, so does the concentration profile depend on the turbulent diffusion of admixture from the jet to the surrounding fluid. The two processes are exactly analagous and the dimensionless concentration and temperature profiles are the same. As with heat transfer, diffusion at the molecular level is neglected and the diffusion process is represented by:

$$S = 2\gamma c^2 x^2 . \partial U/\partial y . \partial X/\partial y \qquad 2.44$$

where S = mass of admixture transferred laterally per unit area per unit time, and
X = admixture concentration.

As with the temperature profile, the concentration profiles are similar and obey the law:

$$\Delta X/\Delta X_m = \Delta T/\Delta T_m = (U/U_m)^{1/2} \qquad 2.45$$

from which follows the result that the variation of concentration along the jet axis is the same as the variation of temperature as expressed in equations 2.42 and 2.43.

2.3.3 Jet trajectory

Whereas the axis of an isothermal jet discharging horizontally into a stagnant environment will be a straight line, the axis of a non-isothermal jet will be curved due to the effect of buoyancy or gravity. The axis of a warm jet will curve upwards and that of a cold jet will curve downwards. The curve described by the axis is called the jet trajectory and is of importance in ventilation design as well as in other fields such as submarine disposal of effluent and the dispersal of smoke plumes.

Jet trajectories are described normally in terms of dimensionless distance parameters based on some characteristic dimension of the jet orifice. Thus, Nottage et al. (1952b) represented the trajectory of a round cold jet by:

$$y/d_0 = N(x/d_0)^2 \qquad 2.46$$

where: d_0 = orifice diameter,
y/d_0 = drop of the jet,
x/d_0 = throw of the jet, and
N = an empirical constant.

This equation was derived from a somewhat simplified analysis of the forces on the jet and N, therefore, may be considered to be a function of the "momentum impulse force" and the buoyant force acting on the jet. Although not giving an explicit equation for the jet trajectory, Farquharson (1952) shows previously derived curves describing trajectories for different values of a constant, α. The value of the constant, which represents the ratio of gravitational force (due to density differences) to velocity pressure in the jet, is given by:

$$\alpha = \sqrt{A'g\Delta T_0}/(U_0^2 T_1) \qquad 2.47$$

where: A' = effective area of jet inlet,
U_0 = velocity of air at the vena contracta,
ΔT_0 = temperature difference at the inlet, and

T_1 = absolute temperature of the room air.

This ratio of momentum to buoyant forces appears in the above, and various modified forms throughout the literature. Depending on the precise application and definition of the terms in equation 2.46, the ratio is referred to variously as a buoyancy number, an Archimedes number (Ar) or a Richardson number (Ri). The ratio is closely related to the Froude number (Fr) used in hydraulics and, in fact, $\alpha = 1/Fr^2$.

Koestel (1955) derived a differential equation for the jet trajectory on the basis of an analysis of momentum and buoyancy forces. His simplified solution to this equation depended on the assumption that the trajectory slope (dy/dx) was "not too great" and is expressed by:

$$y/d_0 = (\Delta T_0 \beta g d_0 / v_0^2)[(p/s+1)/6K](x/d_0)^3 \qquad 2.48$$

where: ΔT_0 = temperature difference at the jet orifice,
β = coefficient of expansion ($=1/T_1$),
p = shape factor for the velocity profile,
s = shape factor for the temperature profile and,
K = proportionality constant for velocity decay (See Equation 2.20).

This equation correlated well with experimental results but subsequent correlations with experimental data have indicated the need to reduce the cubic exponent on the throw term. Examples of such correlations are given by Frean and Billington (1955) and Baturin (1972). The former authors give equations derived from their own experiments with warm jets:

$$y/\sqrt{A'} = 0.20\alpha(x/\sqrt{A'})^{2.44} \qquad 2.49$$

and from additional data on both warm and cold jets:

$$y/\sqrt{A'} = 0.238\alpha(x/\sqrt{A'})^{2.5} \qquad 2.50$$

In both equations A' and α are as defined previously. Baturin (1972) gives equations derived from data on heated and chilled jets of round and planar configurations. For horizontal round jets:

$$y/r_0 = 0.02Ar(T_0/T_i)^{1/2}(x/r_0)^3 \qquad 2.51$$

where r_0 = the radius of the jet orifice,
T_0 = jet temperature at the orifice, and
Ar = Archimedes number where the characteristic length is given by r_0.

Similarly, for plane jets:

$$y/b_0 = 0.57Ar(T_0/T_i)^{1/2}(x/h_0)^{2.5} \qquad 2.52$$

where h_0 = the width of the orifice slot, and
$h_0/2$ = the characteristic length in Ar.

The $\sqrt{(T_0/T_i)}$ terms in equations 2.51 and 2.52 appear to be analagous to the shape factor terms in Koestel's equation (2.48). Similar equations are given by Kaul *et al.* (1975).

The problem of turbulent jet trajectories is not confined, of course, to ventilation. Abraham (1963) and Fan and Brooks (1969), for example, obtained numerical solutions to the problem as found in the discharge of buoyant effluent into water. The former author showed that the jet trajectory depends on a Froude number and gave plots of trajectories for various values of this number which he defined as:

$$F = U_0^2\rho_0/(\rho_i-\rho_0)gB \qquad 2.53$$

where: B = width of a slot opening
ρ_i = density of the ambient fluid, and
ρ_0 = density of the jet at the orifice.

Fan and Brooks (1969) calculated trajectories for various values of a dimensionless initial momentum, M_0', which was itself a function of a densimetric Froude number Fr. Thus:

$$\begin{aligned} Fr &= U_0\sqrt{\rho_i}/[(\rho_i-\rho_o)gB]^{1/2} \\ &= (\lambda/k)^{1/2}M_0'^{3/2} \qquad 2.54 \end{aligned}$$

where: λ = the turbulent Schmidt number and
k = the entrainment constant for the jet.

Cederwall (1971) found the above theoretical work to be in good agreement with results of experiments. The theory of Fan and Brooks gave marginally superior agreement than that of the earlier work of Abraham for a buoyant slot jet discharging into a homogeneous, stagnant environment. The hydraulic Froude numbers given in equations 2.53 and 2.54 differ from the force ratios given earlier in that actual fluid densities are used. When turbulent jets occur in ventilating air, the fluid is assumed to act as a perfect gas and temperatures, therefore, can be substituted for densities. This has the practical advantage that air temperatures are easier to measure than air densities.

Any significant deviation from perfect gas behavior could be expected to arise from the effect of humidity on air density. Randall and Battams (1977), however, have shown experimentally that even the high humidities associated with pig housing do not lead to significant errors from the use of the perfect gas assumption.

The preceding discussion on trajectories has dealt, at least implicitly, with jets that are essentially free. The inference may be drawn from section 2.2 that walls, ceilings and confining spaces will have some effects on the trajectory of non-isothermal jets. Also, a further, complicating factor arises from the possibility that any or all of these confining surfaces may be at temperatures that are different from either the ambient air or the jet itself.

Perhaps the simplest situation of this nature is that of a non-isothermal jet discharging along an insulated ceiling. In the case of a cold jet, the Coanda effect simply acts to counter the buoyancy forces and delays the drop of the jet. Baturin (1972) reports experimental work indicating that, if the jet orifice is within 4 orifice widths of the ceiling, a cold jet will cling to the ceiling.

The more general case of non-isothermal jets discharging into rooms with heated surfaces has been addressed by Mullejans (1966) who developed both flow and heat transfer equations and conducted a series of confirmatory experiments in small rooms, the walls, floor and ceilings of which could be heated. In these experiments the jet trajectory was shown to depend on an Archimedes number although the trajectory was different from that of a free jet. The differences were due to recirculation within the room and the setting up of standing vortices outside the jet.

The Archimedes number initially proposed by Mullejans (1966) was of the form:

$$Ar = g\beta\Delta T_0 l_d / V^2 \qquad 2.55$$

where $\beta = 2/(T_s + T_0)$
$l_d = 2BH/(B+H)$
$V = Q/BH$, and
T_s = absolute temperature of the heated surface.

The dimension l_d was chosen arbitrarily to represent the hydraulic diameter of a room with width, B, and height, H. V was termed the fictitious mean air velocity and was based on the total air supply rate, Q.

Noting that the value of Ar for which jets remained horizontal depended on the inlet slot size, a further modification was introduced by multiplying Ar by a dimensionless slot area. The "corrected" Archimedes number was thus:

$$Arc = Ar(bh/l_d^2) \qquad 2.56$$

where: b = slot width, and
h = slot height.

Jets with Arc < 40 remained horizontal and hit the far wall of the test room, whereas those with Arc > 40 fell initially and then dissipated before reaching the opposite wall.

The above general results notwithstanding, Mullejans also noted that flow patterns for full-width jets differed from those of jets whose width was less than that of the room. Although, as might be expected, the Coanda effect was more pronounced with full-width jets, plane jets tended to sink more readily (i.e., at lower values of Arc) than non-plane jets. When jets did attach to a ceiling, a hysteresis effect was observed in that, once attached, a jet would remain horizontal as Arc was increased far beyond the value at which an initially "free" jet would attach to the ceiling.

In addition to the effects of inlet parameters on jet trajectories, Mullejans (1966) investigated the effect of heated surface area. By covering portions of the heated surfaces with foil, he decreased the heat exchange between the surface and the air and observed a decrease in the sinking of inlet jets. Although no quantitative data were reported, presumably the reduction in radiant and convective heat exchange resulted in a reduction in the air temperature outside the jet thereby reducing buoyancy effects.

Following the example of Van Gunst *et al*. (1967), Jackman (1970) replaced the inlet area (bh) in Mullejans' corrected Archimedes number by an effective area, A', obtained by multiplying bh by an orifice coefficient. For bluff-edged orifices, this coefficient has the value of 0.6. Also, a further correction was applied to allow for attachment of a jet to the ceiling. The correction applied was to multiply Arc by (2D/b).(h/b), where D is the distance of the upper edge of the jet orifice from the ceiling. This correction was restricted to cases where b is less than half the room width and, in addition, D is less than half of b.

Bearing in mind these restrictions, Jackman's corrected Archimedes number, therefore, may be expressed as:

$$Arc' = Ar.2A'Dh/(l_d b)^2 \qquad 2.57$$

Using this corrected Archimedes number, Jackman proposed a design procedure for air conditioning inlets in which the inlet aspect ratio (b/h) could be derived from a jet trajectory equation expressed by:

$$y/\sqrt{A'} = .04Arc'x^3/BH(B+H) \qquad 2.58$$

Randall and Battams (1977, 1979) applied Jackman's corrected Archimedes number to the problem of animal building ventilation. Using a full-width inlet at the ceiling of a simulated pig barn, these authors sought to determine values of Arc' for which inlet jets would remain horizontal on entry to the building. The effect of animals was simulated with rubber bags filled with heated water which provided a heated floor area. The pattern of heating these "simulated pigs" could be varied to investigate the effect of the area and location of the heated surface.

Although continuous trajectories could have been obtained photographically, these were not quantified. Instead jets were characterised as being stable horizontal, stable falling or unstable. In general, jets fell on entry for Arc' > 71 and remained horizontal for Arc' < 30. If the heated surface, which occupied 1/3 or 2/3 of the floor area, was within the first 2/3 of the room length, the jet would remain horizontal for Arc' < 44. These values agree well with those of Mullejans (1966) and Jackman (1970).

Just as Fan and Brooks (1969) used initial momentum to characterise the trajectories of effluent jets, several researchers have used the concept of initial momentum in analysing ventilating air jets. Jackman (1970) used what was termed "initial momentum flow" to relate jet momentum to throw and to determine a mean room air velocity. The initial momentum flow was defined as:

$$M_0 = \rho_0 Q_0 U_0 \quad (N)$$
$$= \rho_0 A' U_0^2 \quad (N) \qquad 2.59$$
$$= \rho_0 (U_x x/K)^2 \quad (N)$$

where K is the velocity decay constant which Jackman took to have a value of 5.8.

Kaul *et al.* (1975) gave a similar definition of jet momentum for a full-width slot inlet but used actual, rather than effective area. Thus:

$$M_0 = \rho_0 U_0^2 Bh \quad (N) \qquad 2.60$$

In order to arrive at some parameter to describe mixing within a room, these authors divided the initial momentum by the room volume to give a "momentum number":

$$j = \rho_0 U_0^2 h/XH \quad (N/m^3) \qquad 2.61$$

Experiments by these authors showed that, for X/H ratios ranging from 1 to 6, a value of $j > 10^{-2}$ N/m³ was required to develop three-dimensional eddies and, therefore, adequate mixing and air exchange within the room.

Barber (1981) has suggested that the "momentum number" of equation 2.61 could be divided by $\rho_0 g$ in order to obtain a dimensionless momentum number:

$$J = U_0^2 h/gXH \qquad 2.62$$

The momentum number used by Kaul *et al.* (1975) can be generalised to include slots of less than room width by replacing Bh in equation 2.60 with the slot area, A. If this is carried through to equation 2.61 and, in addition, the inlet area is expressed in terms of effective area, A', the following expression for j results:

$$j = \rho_0 Q_0^2 / C_d BXHA' \quad (N/m^3) \qquad 2.63$$

Now, the corrected Archimedes number from equation 2.57 may be expressed as:

$$Arc' = \rho_0 g(T_s - T_0)(B+H)A'BH / C_d(T_s + T_0)Q_0^2 \qquad 2.64$$

and comparison of equations 2.62 and 2.63 results in the following relationship between j and Arc':

$$j = \rho_0 g(T_s - T_0)(B+H) / C_d(T_s + T_0)Arc'X \qquad 2.65$$

Since ρ_0 is inversely proportional to absolute temperature, and since g, B, H, and X are constants for a given room, equation 2.65 may be simplified to the form:

$$j = C(T_s - T_0) / T_0(T_s + T_0)Arc' \qquad 2.66$$

where C is a constant. If the dimensionless J is used, the relationship becomes:

$$J = C(T_s - T_0) / (T_s + T_0)Arc' \qquad 2.67$$

The value of C in equation 2.67 will, of course, be different to that in equation 2.66.

2.4 Practical Implications

From the point of view of animal housing design, the preceding discussion of the behavior of non-isothermal jets has a number of important implications. For instance, the shape of the building and the location of inlets must be governed, at least in part, by the limited throw of a confined jet. Also, the layout of pens within a building, together with the location and type of heaters used, should take into account possible effects on jet trajectory.

There are also important implications regarding the design of the inlets themselves. Barber *et al.* (1982) have suggested that inlets should be capable of providing jets that simultaneously satisfy the Archimedes number criterion of Randall and Battams (Arc' <30) and the momentum number criterion of Kaul *et al.*($j>10^{-2}$) The satisfaction of the Archimedes number criterion would ensure a satisfactory trajectory of the jet, thereby preventing exposure of animals to draughts, whereas satisfaction of the momentum criterion would ensure adequate mixing of inlet and room air. On this basis, the continuous slot inlets that conventionally are used in Canadian animal barns were shown to be inappropriate for Prairie winter conditions. Barber *et al.* (1982) suggest the use of preheating or recirculation systems to modify the density of the incoming air in order to overcome this deficiency.

A further area where implications exist is in the control of variable inlets. Conventional inlet control systems are based on the sensing of pressure drop across the inlet (i.e., they are based on flow velocity). If the above criteria were to be adopted, inlet control systems would have to incorporate temperature and inlet geometry sensors. Also, they would need to be adjustable to accommodate various room dimensions. Although these requirements are well within the capabilities of modern microprocessor-based controllers, they do serve to highlight a disadvantage of the Archimedes number as used by Randall and Battams (1979):

it has evolved into a somewhat cumbersome entity.

The above is but one reason mitigating against the wholesale adoption of the previously-discussed theory and applying it to Western Canadian conditions. Although there was no clear theoretical reason to doubt the universality of the Archimedes number approach to prediction of jet trajectories, the precise numbers arrived at by Randall and Battams (1979), for instance, required verification at large values of ΔT_0. The inlet temperature differences used by these and other researchers have been in the order of 20°K whereas, under Prairie winter conditions, ΔT_0 could be as high as 40°K or even 60°K. In addition, criteria were required for slots that do not extend the full room width and that are located some distance from the ceiling. The above authors did not investigate these cases and, in view of the observations of Mullejans (1966) and Jackman (1970), this constituted a gap in current knowledge. The aim of this project was to provide such data.

2.5 Aims

The aims of this project were:

1. To verify that the results of previous researchers apply to animal housing at low outside air temperatures.
2. To investigate, under the above conditions, the trajectories of jets that do not extend the full room width and that are not adjacent to the ceiling.
3. To develop design criteria for ventilation inlets in

Prairie animal housing and to examine their practical application.

4. To establish whether a parameter that is less cumbersome than Arc' or j could be used effectively in ventilation control systems.

For convenience and clarity, in the remainder of this report, unless specifically stated to the contrary, the term Ar may be taken as equivalent to Arc'. In other words Ar will indicate the corrected Archimedes number as used by Randall and Battams (1979).

3. EXPERIMENTAL FACILITY

3.1 Requirements

In order to investigate the behaviour of cold ventilating air jets, a facility was required that would allow both quantitative and qualitative experimental work. The alternatives of full-scale or model studies were examined.

The use of scale models to study non-isothermal jets is quite feasible but may require distorted modelling techniques (Dybwad *et al*. 1974) and may not give kinematic as well as dynamic similarity between the model and the prototype (Timmons, 1980). Therefore, the decision was made to construct a full-scale facilty. Practicality precluded the use of a whole barn for this purpose, however, so a compromise was made to use a space large enough to observe full-scale airflows in the region of a ventilation inlet. Provision was required to test various inlet types and configurations while some means of moving air through the inlet was required that would provide sufficient flow and that would be varied continuously over the range of flows used. A means of measuring flow rates to within at least 0.025 m^3/s over the range of flow also was desired, as was some means of determining the path of inlet air jets.

Since it was desirable that the facility should reflect the agricultural application of the study, and since animal housing was the specific application under consideration, some means of accounting for the effects of animals in the ventilated space was required. However, apart from managerial constraints, the use of actual animals in the facility was precluded by the fact that their surface temperatures could vary and would be difficult to record directly. Therefore, some system was required that would simulate, in a controlled fashion, the presence of animals in the ventilated room.

Another desirable feature was the ability to refrigerate the inlet air and thus reduce dependence on seasonal cold weather periods to provide suitable experimental conditions.

3.2 Design

3.2.1 Chamber

Considerations of cost dictated that the test chamber be constructed within an existing buildng. Furthermore, in order to provide refrigerated inlet air, the most convenient site for the test chamber was in a controlled-environment building at the University of Alberta's Agricultural Engineering Farm at the Ellerslie Research Station, Alberta. The use of this facility allowed inlet air to be cooled by 15-20°C relative to outside air with a minimum temperature of about 0°C. This was not cold enough to simulate true winter conditions, but it allowed preliminary testing and calibration work to proceed during the summer.

Location of the test chamber within an existing building was the main factor in determining its dimensions. The major inside dimensions are indicated on the overall view of the chamber shown in Figure 3.1. The length of the room was limited by the need to provide sufficient space in the proximity of the inlet to allow unimpeded flow. The clear distance between the inlet wall and that of the surrounding building is 1.3 m. At one end of this space, a large door (0.9 m x 2.0 m) was located that could be opened in cold weather to allow inflow of cold outside air. Outside air also could enter freely through a vent in the exterior wall in the space above the chamber and, if the cooling and heating coils were disabled, could be introduced through the air conditioning duct in the enclosing room.

The height of the chamber was dictated by the location of this air-conditioning duct. To avoid undue limitation of width, the chamber was constructed to fit underneath the duct resulting in a ceiling height of 1.9 m. The ceiling was extended outwards over the inlet wall by a distance of 450 mm to simulate the effect of the eaves of an actual building.

To allow observation of flow patterns, a clear space was required along one side of the chamber. This space also was used to house all instrumentation and control equipment and was 1.2 m wide, resulting in an inside width for the chamber of 5.4 m. The construction of the chamber was of a timber frame with plywood cladding. The floor, walls and

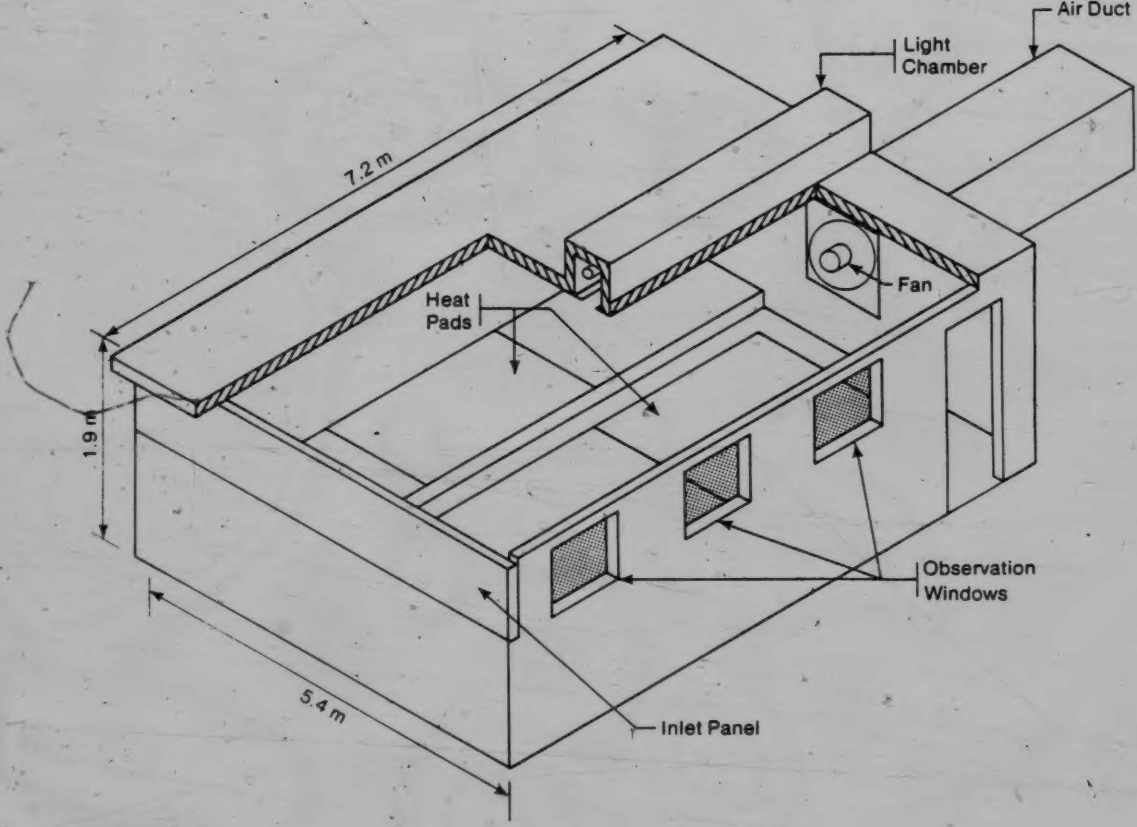
Air Duct
Light Chamber
7.2 m
Fan
Heat Pads
1.9 m
Observation Windows
5.4 m
Inlet Panel

Figure 3.1 Overall view of experimental facility

ceiling were all insulated with glass fiber insulation having a thermal resistance (i.e., RSI value) of 2.1 $m^2 {}^\circ C/W$, with all joints on the inside surface being sealed with caulking compound to ensure that air entering the chamber would come only through the inlet. Care was taken also to provide a good seal around the door. Three observation windows were provided along one wall of the chamber. These were made of clear, acrylic plastic sheet mounted flush with the inside wall. Removable, insulated panels were made to fit into the window frames when observations were not in progress.

To provide a narrow band of light for flow visualization and to avoid flow disturbances caused by ceiling obstructions such as light fittings, a light chamber was constructed above the ceiling at the centreline of the ventilated room. This was insulated in the same way as the rest of the ceiling and contained a single row of flourescent tubes backed by an aluminum-foil reflector. The bottom of the light chamber embodied a 100 mm-wide strip of clear, acrylic plastic mounted flush with the ceiling, through which light passed into the ventilated room.

To allow various inlet configurations to be tested, only the bottom part of the inlet wall was built as a permanent part of the structure. The top part of the wall was completed by inserting panels, of similar construction to the wall, that contained the desired inlet configuration. Two types of inlet were constructed for testing. These were a continuous full-width slot and a central slot of half the room width (Figure 3.2). Both inlets had approximately the same area (1.5 m²) and could be located adjacent to the ceiling and at heights of approximately 0.3 m and 0.6 m below the ceiling. All joints around the removable panels were sealed with duct tape.

3.2.2 Air movement

Air was drawn through the chamber by means of a variable-speed exhaust fan. The fan was sized to give approximately the same capacity per unit inlet length as would be found in a typical swine finishing barn (Turnbull and Bird, 1980). A conventional axial-flow ventilation fan (Model 562-2, Ziehl-Abegg Co., Kuenzelsau, W. Germany) was chosen with a diameter of 562 mm and seven constant-pitch blades. The fan was mounted on the shaft of an 800-W, single-phase AC motor and had a nominal, free-delivery output of 3 m³/s at 1050 RPM. Speed control was achieved with a commercial regulation unit (Avon Electronics, Special Engineering Developments Ltd., Totton, Hants., England). Since the ceiling height was somewhat lower than in an actual barn, and to facilitate installation in the existing structure, the fan was mounted low in the wall opposite the inlet; the height of the fan centreline above the floor was 725 mm. The above considerations notwithstanding, the precise location of the fan in the outlet wall would not have a significant effect on the overall pattern of air

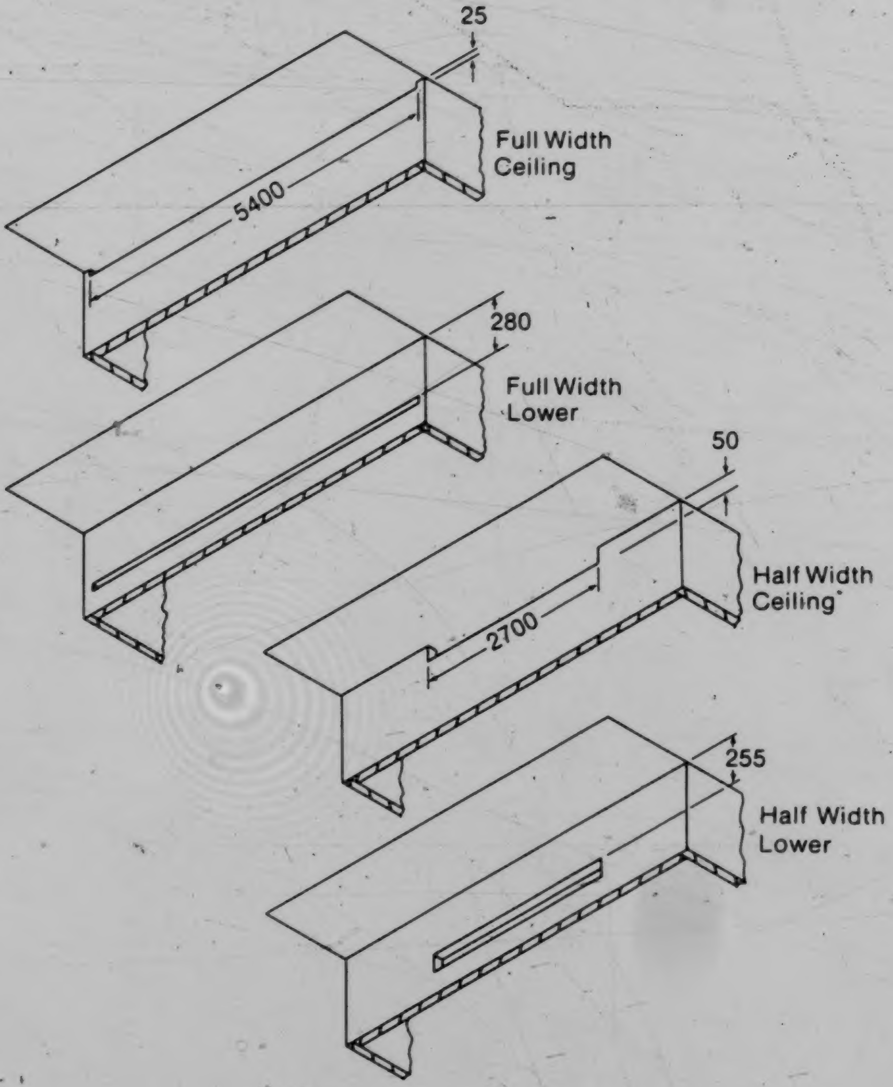
25
5400
Full Width
Ceiling
280
Full Width
Lower
50
2700
Half Width
Ceiling
255
Half Width
Lower

Figure 3.2 Inlet panels (Dimensions in mm).

movement within the chamber.

To measure airflow from the fan, a flow measurement duct was constructed downstream of the fan in accordance with the principles set out by Jorgensen (1983) which are practically identical to those set out in established standards (AMCA, 1974). The duct, which is illustrated in Figure 3.3, was 6.1 m in length, square in section and constructed of galvanized steel with 50-mm thick sheets of polystyrene insulation on the inside. The inside cross-section was 508 mm square, while the insulation tapered outwards at the fan end to accommodate the fan diameter. A flow straightener was included in the duct.

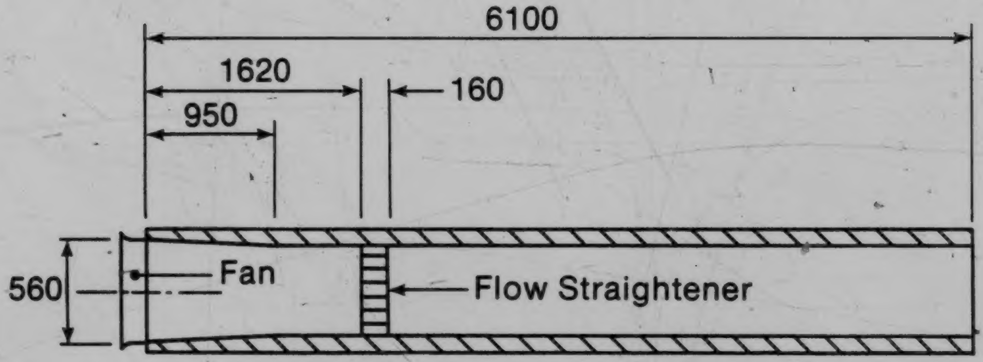

Figure 3.3 Flow-measurement duct (Dimensions in mm).

3.2.3 Animal simulation

The complete simulation of the effects of housed animals on the room environment would require the provision of sources of heat, moisture and contaminant gases such as CO_2 and NH_3. In the investigation of airflow patterns, the prime requirement is to take account of those factors that affect air density and, of the above, heat sources are the predominant factor. Randall and Battams (1979) investigated the effect of relative humidity on air densities and concluded that these were negligible compared with those of air temperature. This could be deduced also from examination of a psychrometric chart showing the variation of specific volume with temperature and absolute humidity. Similar inferences can be made reasonably with regard to the effects of contaminant gases.

On this basis, the presence of animals in the chamber was simulated only by means of heat sources. After considering a design of "artificial pigs" similar to that of Brannigan and McQuitty (1971) together with other heat sources, the method offering least cost per unit area appeared to be the use of fluid heating pads. These are known more generally as waterbed mattresses. Six of these pads were installed, each one being equipped with two thermostatically-controlled heater units. Each heater unit was rated at 360 W so that the possible total heat output from all pads combined was equivalent to that from forty-eight, 54-kg pigs (Turnbull and Bird, 1980) which would occupy approximately the same floor area (22 m^2).

Apart from cost, the heating pads had the advantage that reasonably uniform temperatures could be maintained over large areas. The thermostats were set to provide surface temperatures of approximately 30°C which corresponds to the surface temperature of finishing pigs (Esmay, 1978). The high thermal mass of the pads ensured that variations in their mean temperatures with time were small and slow although heat exchange with the room caused the surface temperatures to vary. If the pads are to be used in future studies, consideration should be given to the use of a pump to circulate water through the pads in order to improve temperature uniformity and reduce the rate of surface temperature variation. The pads were arranged in two rows along the length of the room. Narrow aisles, as shown in Figure 3.4 , were left to provide access to the fan, inlets and thermostat controls.

3.3 Instrumentation

Instrumentation of the facility was aimed at measuring air flows through the room, the paths of cold air jets as they entered the room, and relevant temperatures and environmental parameters. A block diagram of the instrumentation is shown in Figure 3.5, while diagrams for individual circuits are given in Appendix I.

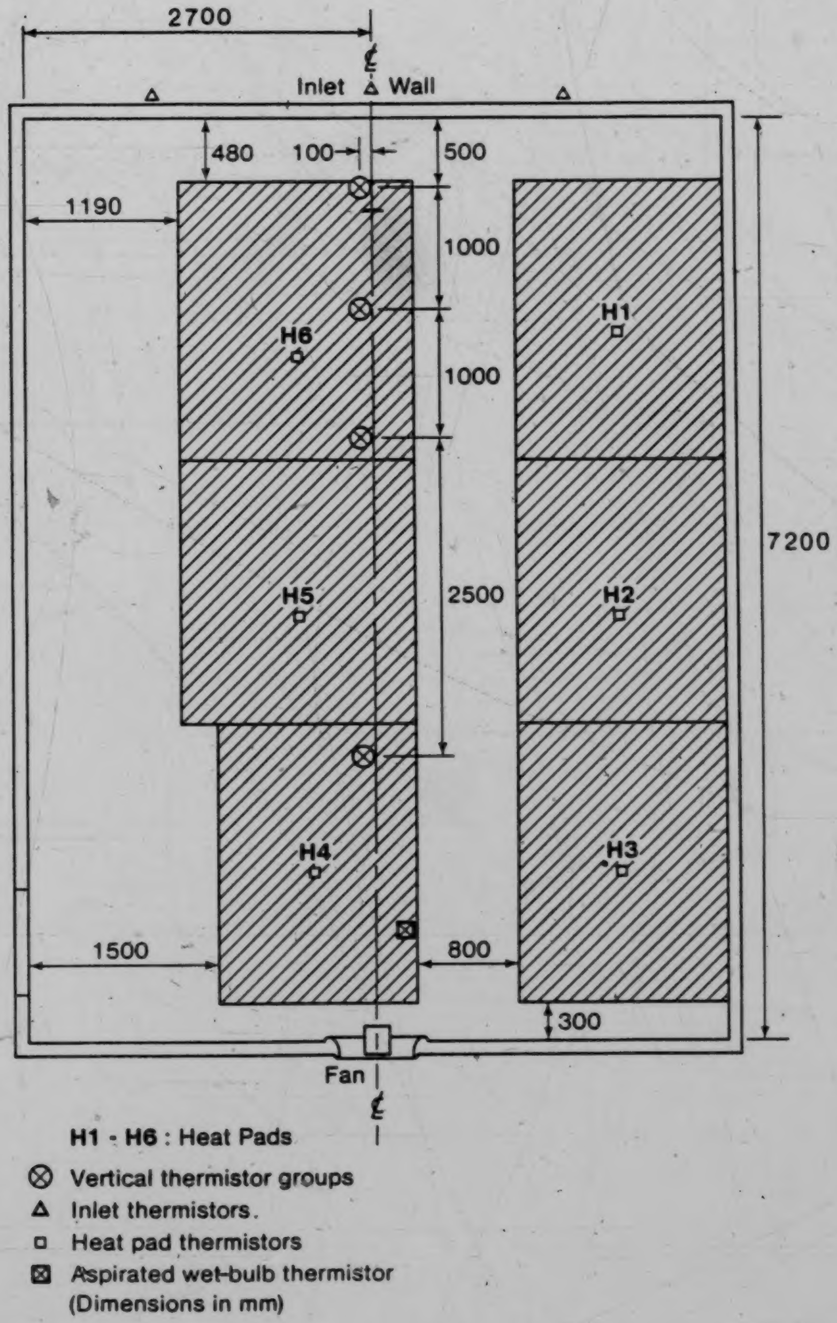
2700
℄
Inlet
Wall
480
100
500
1190
1000
1000
2500
7200
H1
H2
H3
H4
H5
H6
1500
800
300
Fan
℄
H1 - H6 : Heat Pads
⊗ Vertical thermistor groups
△ Inlet thermistors.
□ Heat pad thermistors
⊠ Aspirated wet-bulb thermistor
(Dimensions in mm)

Figure 3.4 Plan view of experimental room

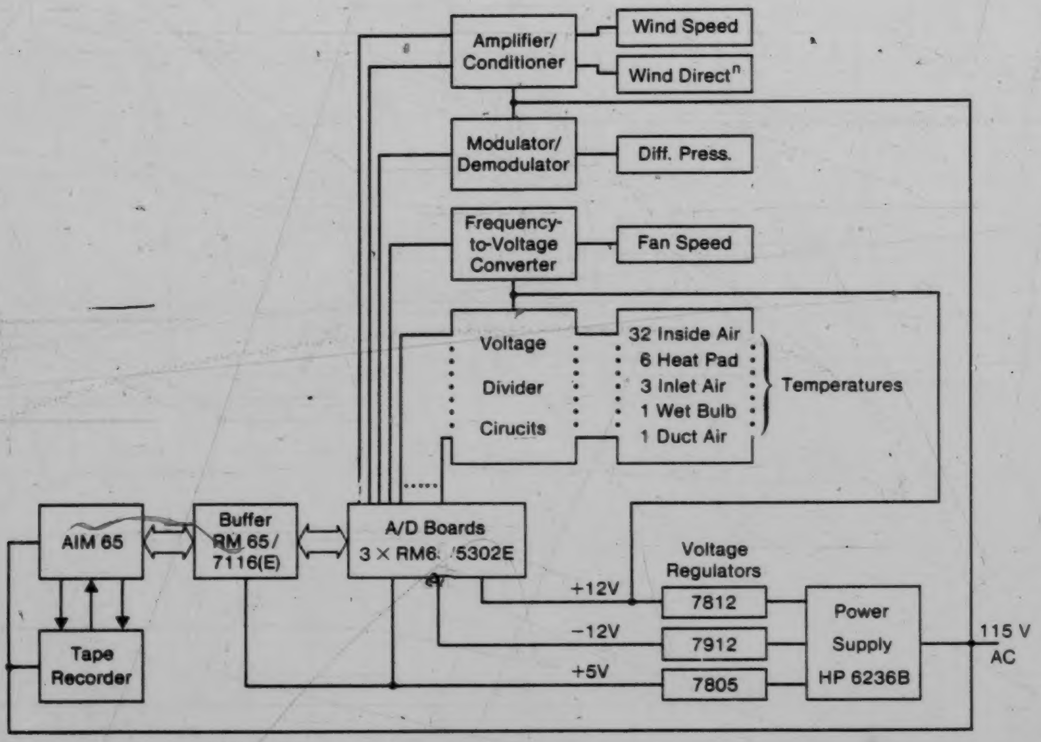
Amplifier/ Conditioner
Wind Speed
Wind Direct^n
Modulator/ Demodulator
Diff. Press.
Frequency-to-Voltage Converter
Fan Speed
Voltage Divider Cirucits
32 Inside Air
6 Heat Pad
3 Inlet Air
1 Wet Bulb
1 Duct Air
Temperatures
AIM 65
Buffer RM 65/ 7116(E)
A/D Boards 3 × RM6 /5302E
Tape Recorder
Voltage Regulators
+12V
7812
−12V
7912
+5V
7805
Power Supply HP 6236B
115 V AC

Figure 3.5 Block diagram of instrumentation

3.3.1 Airflow measurement

By application of the fan laws (Jorgensen, 1983), flow rates may be determined, after suitable calibration, from the fan speed or the pressure differential across the fan. Fan speed was measured using a Hall-effect switch that was activated by two magnets glued to the fan hub. The pulses from this switch were fed to a frequency-to-voltage conversion circuit (Appendix I) that provided a dc voltage output proportional to fan speed. The circuit was calibrated in the laboratory using a signal generator and this calibration was checked *in situ* using a strobo-tachometer (Model 30-K, Pioneer Electric and Research Corp., Forest Park, Ill.). The calibration was linear and the output was 7V at 1100 RPM.

Differential pressure was measured using a variable reluctance, differential pressure transducer (Model DP45, Validyne Engineering Corp, Northridge, CA.) in conjunction with a modulator-demodulator unit (CD12 Universal Transducer Indicator, Validyne Engineering Corp.) that provided a dc voltage output proportional to differential pressure. The pressure measurement system was calibrated using a micro-manometer (Microtector 1430, Dwyer Instruments Inc., Michigan City, IN.) and gave a linear output of 0.33V/mm H_2O.

Flow rates were measured at the end of the fan duct using two methods. The first method used sulphur hexaflouride (SF_6) as a tracer gas in a duct-dilution technique which has been described elsewhere by Leonard *et al.*(1984a). The injection rate of SF_6 at the fan was measured with a soap film meter similar to that described by Ower and Pankhurst (1977). The SF_6 concentration at the end of the duct was measured with an electron-capture detector/chromatograph (AI Industrial, Cambridge, England) which was calibrated against a certified gas mixture with an SF_6 concentration of 0.33±0.015 ppm and zeroed using ambient air.

The second flow-measurement technique involved the use of a heated thermistor anemometer (Model TA3000, Airflow Developments Ltd., High Wycombe, England). This was calibrated using a standard flow nozzle and a differential pressure tranducer that, in turn, was calibrated with an inclined manometer. This calibration facility was set up in the Department of Mechanical Engineering, University of Alberta. To determine air flow through the duct, flow velocity was measured on a 25-point grid across the duct. These velocities were averaged and the resulting mean was multiplied by the duct area to give the flow rate. Under calm conditions, and using appropriate care, the two methods described above gave results within 5% of each other. Some of this difference was undoubtedly due to incomplete and non-uniform mixing of the tracer gas with the duct air, especially at low flow rates. For this reason and because of the relative convenience of use, the thermistor anemometer was used alone for most of the fan calibration work and also, during experimental runs, to check flow rates.

Using the above flow measurement techniques, the fan output was calibrated against speed and pressure differential for each inlet configuration. A computer program, written in APL and developed previously in the Department of Agricultural Engineering, was used to fit calibration equations to the data. These are shown, together with values of r^2, in Appendix II. The equations used are not neccessarily those giving the best fit (highest r^2) to the data, but were selected on the basis of established fan performance theory. Thus, delivery should be a linear function of fan speed and a quadratic function of pressure difference across the fan. In spite of this limitation the lowest value of r^2 for any of the equations selected was 0.97.

All flow rate calibration equations were based on the standard air temperature of 20°C. Subsequent calculations of flow rates using these equations were corrected for temperature but not for atmospheric pressure. The latter correction was deemed unnecessary since the effect of changes in atmospheric pressure on air density is relatively small in comparison to that of temperature changes.

3.3.2 Environment and temperatures

Since excessive wind could have an effect on the pressure/flow calibration, especially at low flow rates, wind speed and direction were monitored using a cup anemometer and wind vane (Models 1005 and 1001, Sierra Instruments, Redlands, CA). Both of these provided a dc voltage output. Other environmental parameters monitored were the dry-bulb temperatures of inlet and room air, the wet-bulb temperature of the room air, and the surface temperatures of the heat pads (Figure 3.4).

All temperatures were measured with curve-matched thermistors (UUB31J1, Fenwal Electronics Inc., Framigham, Mass.). These were attached to the ends of 15.2-m speaker-wire leads, protected with heat-shrink tubing,and connected in simple voltage-divider circuits (Appendix I). The voltage outputs from these circuits were converted to temperature values using an equation, supplied by the manufacturer, that related thermistor resistance to absolute temperature (Appendix III).

Although the use of voltage-divider circuits had the advantage of simplicity, they proved far from ideal in practice. In order to obtain reasonable resolution, a supply voltage of 12V was used for these circuits. This resulted in excessive current through the thermistors which, in turn, caused "self-heating" and neccessitated the application of extensive calibration procedures. The use of constant-current circuits is recommended strongly for any future use of this facility.

The thermistors were calibrated *in situ* against a digital temperature indicator (Omega 450 ATH thermistor thermometer, Omega Engineering Inc., Stamford, CT.) which, in turn was calibrated in a fluid bath against a resistance temperature detector with a rated accuracy of ±0.06°C (Fluke 2180A RTD Digital Thermometer, John Fluke Mfg. Co. Inc., Everett, WA.) in the Department of Mechanical Engineering, University of Alberta (Appendix II). The time constant of the thermistors as they were used was approximately 45s, while that of the temperature indicator was approximately 80s. This discrepancy of time constants meant that reliable calibration data could be obtained only under conditions of static or slowly-varying temperature.

For the air temperature thermistors, a correction equation was developed initially on the basis of a limited number of calibration points. This assumed that the error in temperature measurement was proportional to the power dissipated by the thermistors or, in other words, to I^2R heating. The equation was applied to give corrected values of thermistor resistance and, in fact, accounted for a substantial portion of the error. However, additional calibration points indicated the need for a further, linear correction. This was calculated using all available data and was applied to the indicated temperatures. The overall result was that the corrected temperatures were within 0.2°C of those indicated by the calibration standard over the range -28°C to +16°C.

The heat dissipation characteristics of the thermistors attached to the heating pads were, of course, different to those suspended in air. Consequently, a separate calibration was carried out for these sensors and the correction equation so developed was applied directly to the indicated temperatures.

Not only were thermistors used to measure temperatures *per se* ,but they were used also to determine the path of the cold air jets. Four groups of eight thermistors were suspended from the ceiling in vertical lines at different distances from the inlet. The location of these groups is indicated in Figure 3.4 while the vertical spacing of the thermistors in each group is shown in Figure 3.6. The vertical spacing was varied depending on the inlet configuration under investigation in an effort to obtain the maximum amount of information on the jet trajectory in each case. In retrospect, however, more useful data could have been obtained had the spacings been kept uniform throughout all the tests.

3.4 Data Collection and Processing

3.4.1 Data collection

Data collection and recording were based on an AIM 65 microcomputer (Rockwell International, Anaheim, Ca.). The main features of the system are shown in Figure 3.5. The analog signals from the various transducers described previously were converted to digital form using three analog-to-digital (A/D) circuit boards (RM65/5302E,Rockwell International, Anaheim, Ca.) with each board handling 16

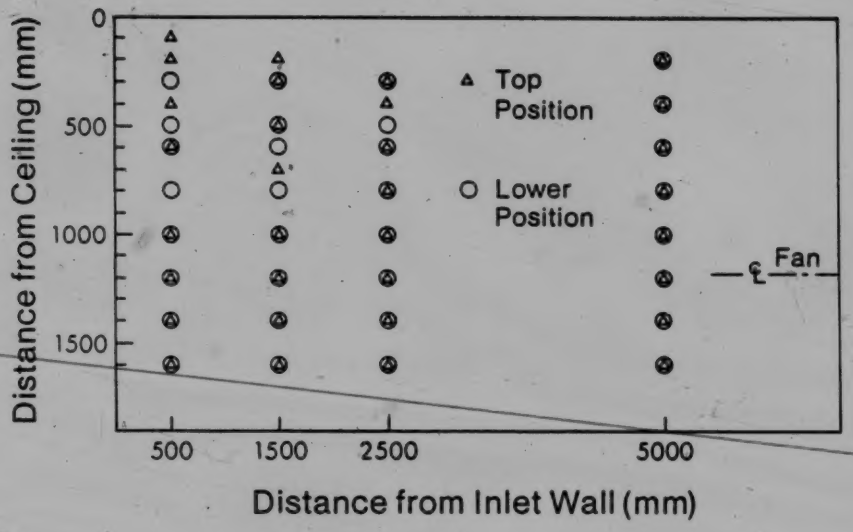

Figure 3.6 Vertical location of thermistors.

single-ended analog signals. The A/D boards were memory-mapped into the computer, by means of dip switches on each board, so that each channel could be addressed as a memory location. Potentiometers were provided on each A/D board for adjustment of offset and gain and these were used in calibration of the boards. This was carried out over the range 0-10V using a variable output, bench power supply (HP 6215A, Hewlett-Packard Co.,Palo Alto, CA.) and a digital multimeter (Fluke 8060A, John Fluke Mfg. Co. Inc., Everett, WA.).

The software that controlled data aquisition is listed, in Appendix III. Essentially this consisted of a main program, written in BASIC, that called a number of subroutines, some of which were written in assembly language. Assembly language was used in the interests of speed and memory limitations for subroutines that provided a real-time clock, read data channels into buffer storage and transferred data to magnetic tape. These routines were loaded into memory by the main program at the start of each run. The main program allowed an operator to specify the interval between data scans (30s to 24h) and the resolution of the A/D conversion (8 bit or 12 bit). The operator also could obtain a display or print-out of data to check on system function.

Data were recorded on magnetic tape as voltages in a hexadecimal ASCII format. These data then were read into memory of a Rockwell AIM 65/40 computer before being transferred by a serial, RS-232 link to an IBM-PC computer where they were stored on diskette. This somewhat circuitous path was taken in order to handle the recording format used by the Rockwell computers. Listings of the AIM 65/40 input and output routines, which are both in assembler language, may be found in Appendix III. As a backup to diskette storage, data were down-loaded subsequently to disk storage on the University of Alberta's mainframe computer in the Department of Computing Services.

3.4.2 Data processing

The raw data were processed on an IBM-PC computer using the BASIC program listed in Appendix III. This program served the following functions:

1. Stripped tape-format and checksum data from the recorded data and converted the remaining ASCII data to decimal form.
2. Converted the raw voltage data to useful engineering units using appropriate calibration and correction equations.
3. Calculated, for each set of data, airflow rates and Archimedes numbers based on both fan speed and pressure differential.
4. Recorded the converted and calculated data in a diskette file.

As with the raw data, the converted data files also were stored on the mainframe computer. Examples of raw and converted data are shown in Appendix IV with annotations indicating the allocation of channels to the various sensors.

3.4.3 Photographic data

In addition to the record of temperature profiles in the chamber, a photographic record of inlet jet trajectories was desired and the use of both bubbles and smoke to delineate the jet were considered. Preliminary trials were carried out with a bubble generator that used helium to adjust the buoyancy of soap bubbles. However, this approach was abandoned due to the difficulties perceived in maintaining neutral buoyancy of bubbles in a highly non-isothermal jet. To generate a suitable smoke, hot oil, smoke bombs and chemical smoke generators such as those described by Nottage *et al.*(1952c), Baturin (1972) and Pattie and Milne (1966), were considered. After some trial and error, a technique utilizing titanium tetrachloride ($TiCl_4$) was adopted. A small diaphragm pump was used to bubble air firstly through water and then through a solution of $TiCl_4$. The resulting titanium oxide formed a dense white smoke which was introduced to the inlet at the location of the light chamber. To prevent the water freezing, the apparatus had to be housed in the instrumentation room which could have caused some warming of the smoke above the inlet air temperature. However, since the air for the smoke generator was drawn from outside, passed through only about 1m of tubing inside the instrumentation room, and then passed through approximately 4m of tubing exposed to outside temperature before being released at the inlet, the inlet air and smoke would have been very nearly isothermal.

Although both smoke concentration and temperature profiles within a jet are likely to be wider than the velocity profile (Abramovich, 1963), photographs of the smoke path were considered to provide a good indication of the jet centreline and its overall behavior. Details of the photographic equipment and procedures used are given in Appendix V together with sample photographs of each type of inlet over a range of flow rates.

4. METHODOLOGY

4.1 Constraints

The nature and scope of the experimental procedures followed in this project were governed by a number of constraints. The most significant of these was the requirement for low air temperatures. For the purposes of this work, low air temperature was defined as being below -10°C and, in general, data were gathered only when the outside air temperature was below this value. Exceptions to this occurred at the end of the winter in order to complete the experiment. In these two cases the air temperature was approximately -8°C.

Another climate-related constraint was the need for low wind velocities in order to obtain controlled low airflows using the variable-speed fan. At low fan speeds, wind velocities in excess of 4 m/s tended to cause pressure differences between inside and outside the room that dominated the effect of the fan. Although the room airflow had been calibrated against pressure differential, wind-induced pressures fluctuated excessively and the calibration of airflow against fan speed was invalid under these conditions.

Since the experimental work was to be completed in one winter, the above constraints limited the number of days which would be available for data collection. This, together with the fact that available manpower was limited to one person, governed the number of inlet configurations that could be tested. Although each of the inlets that had been constructed could be located in any of three positions on the inlet wall, a decision was made to investigate the inlets in two positions only. Thus, the full-width and half-width designs were tested in locations adjacent to the ceiling and approximately 300mm below the ceiling of the room. For convenience, these configurations were identified according to the following code:

FT = Full width, ceiling position
FL = Full width, lower position
HT = Half width, ceiling position
HL = Half width, lower position

4.2 Experimental Design

Since the number of replications of a given test would be limited by the constraints detailed above, and owing to the difficulty of quantifying jet characteristics such as trajectory, a rigorous statistical experimental design was considered to be impractical.

The primary objective of the whole study was to verify the experimental results of previous researchers who had used warmer inlet air. Consequently, for a given inlet configuration, data were required, firstly, that would demonstrate the relationship of an Archimedes number to the jet trajectory and, secondly, that would demonstrate the effect of varying the heated surface area on the jet trajectory.

Thus, for a given configuration two types of test run were required. The first, or normal, test was to observe the jet trajectory for different values of Ar. Since there was no control over inlet temperature, and since geometric variables were constant for a given inlet, this was achieved by varying the airflow rate (i.e., the fan speed). For these tests, a constant, maximum heated area was used.

For the second, or heated area, test, the fan speed was held constant and the area of exposed heated area within the room was varied. This was achieved by selectively covering the heat pads with "blankets" made of fibreglass insulation (RSI=2.1) contained in envelopes made of polythene sheet. The pads were covered or uncovered in pairs according to their location along the length of the room. Thus, the two pads nearest the inlet wall were treated as a pair as were the two in the middle and the two closest to the fan.

In order to minimise the confounding of results with time- or weather-dependent variables, no two series of tests of the same type were performed on the same inlet configuration on the same day. This requirement, taken with the previously mentioned constraints, resulted in an estimate that the maximum number of test series that could be expected to be performed with a given inlet configuration would be three. These were apportioned so that at least two normal series and one heated area series were carried out on each configuration. The rationale behind this apportionment was that the data on the effect of Ar on jet trajectory were of primary importance and needed verification by at least one replication. Further Ar data were obtained by using results from the heated area runs when all the heat pads were uncovered.

Using N1, N2 and H to identify the test type, all test series could be identified by combining these codes with the inlet configuration codes given in section 4.1. Thus, the first normal series using the half width inlet located adjacent to the ceiling is designated by the code HTN1.

Although complete randomisation of the order in which tests were carried out would have been desirable, this was hampered by the physical difficulty of changing inlets and sealing them in cold weather. Consequently, all tests on a given configuration were done in sequence before the configuration was changed. Table 4.1 summarises the tests carried out and shows the order of testing together with relevant prevailing weather conditions.

4.3 Experimental Procedure

4.3.1 Trials

Prior to actual data-gathering, trial runs were carried out to develop experimental techniques, to check instrumentation and to get some idea of the response characteristics of the room. In view of the limited number of data-gathering runs, this was necessary to prevent the

TABLE 4.1: SUMMARY OF EXPERIMENTAL TEST SERIES.

DATE	CODE	TEMP(°C)	WIND(m/s)
23 DEC 84	FTN1	-26	2
26 DEC 84	FTN2	-22	1
09 JAN 85	FTN3	-15	1
31 DEC 84	FTH	-16	4
09 JAN 85	FLN1	-13	1
30 JAN 85	FLN2	-26	1
01 FEB 85	FLH	-25	0
01 FEB 85	HTN1	-21	1
03 FEB 85	HTN2	-20	2
06 FEB 85	HTH	-17	1
06 FEB 85	HTN3	-16	1
03 MAR 85	HLN1	- 8	0
04 MAR 85	HLN2	-10	3
04 MAR 85	HLH	- 8	3

experimental results becoming skewed by a learning process during the course of the actual test program.

The first trials were carried out using inlet air that was nearly isothermal with that in the room. The major purpose of these trials was to test the operation of the smoke generating unit and to develop suitable photographic techniques for recording jet trajectories. These trials also were used to test the operation of instrumentation and recording systems.

Before data-gathering commenced, a single trial series was carried out using low temperature (-20°C) inlet air. This trial was necessary to check the operation of all systems under actual test conditions and to determine an approximate value for the room time constant. Knowledge of speed of the response of the room to a change in airflow rate was required since the system was required to be at, or very close to equilibrium when trajectories were recorded. The response of the room was determined by measuring the air temperature downstream of the fan in the exhaust duct at two-minute intervals. This experiment indicated that, at low flow rates, equilibrium could be considered to have been reached within 12 minutes from a change of flow rate. This equilibration time would have been less for higher flow rates. Typical plots of duct temperature against time are shown in Figure 4.1.

4.3.2 Normal runs

As can be seen from the curves in Figure 4.1, the heat transfer from the heat pads to the room air generally was insufficient to maintain the initial room temperature, higher airflow rates resulting in increased cooling. From the point of view of validating the jet trajectory criteria of Randall and Battams(1979), this was not important since room air temperature does not contribute to Ar. However, as the room became cooler, so did the temperature of the heat pads' surfaces, resulting in a decreased Ar. Since observation of jet behavior at high values of Ar was desirable, unnecessary cooling of the room was avoided by using low airflow rates at the beginning of a test series and increasing the airflow rate with each test in the series.

Also, consideration of other Archimedes or Froude numbers, such as those used by Cederwall (1971), Fan and

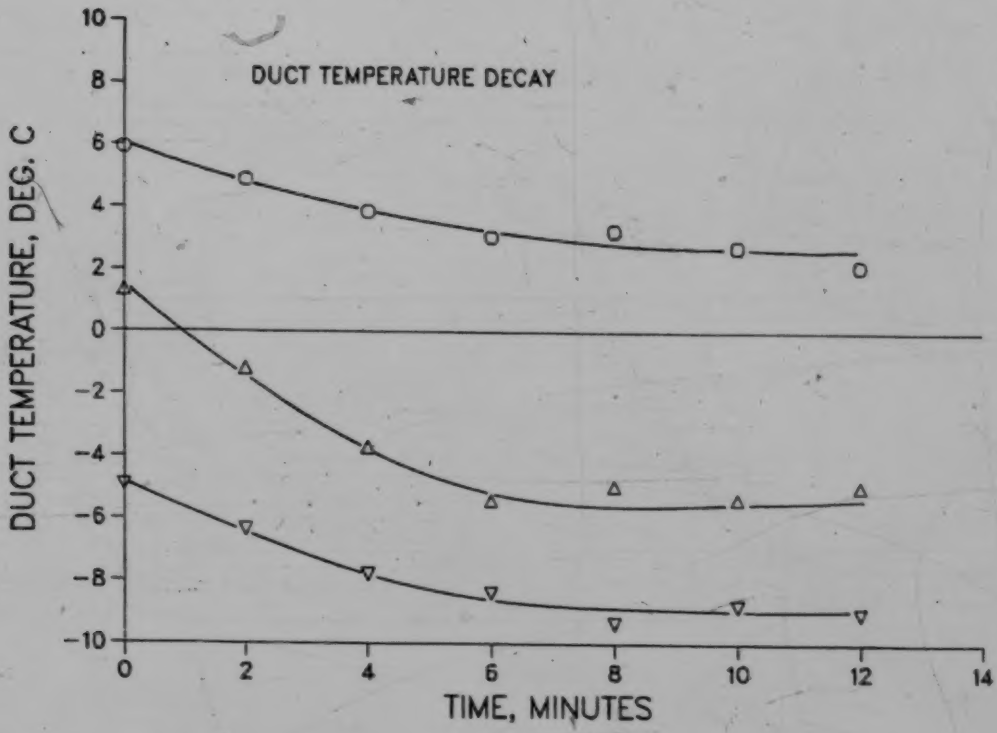

Figure 4.1 Typical plots of duct temperature versus time.

Brooks (1969) and Koestel (1955) suggested that room air temperature should be a factor in predicting the path of a jet based on a buoyancy ratio. Thus, to obtain high, room temperature-based Archimedes numbers,the initial use of high flow rates would have been counter-productive.

The general format of a normal test series was to uncover all the heat pads and to open the inlet and fan duct outlet before setting the fan to run at a slow speed. The data recording system was started and was set to scan all sensors every two minutes. At least 12 minutes were allowed to elapse so that the room could equilibrate. At the end of this period, the smoke generator was started and the inlet jet was photographed at a time approximately coincident with a data scan to enable subsequent correlation of photographic and temperature data. The time at which photographs were taken was noted and, as a further check, sketches were made of the apparent jet trajectories using the thermistor strings as reference points.

Data recorded throughout a test series were checked later against manual readings of temperatures, fan speed and pressure differential. The zero of the differential pressure indicator was checked prior to each series. In addition, approximate checks on airflow rate were carried out using the hot-thermistor anemometer.

Due to low outside air temperatures and manpower limitations, it was not possible to record anemometer readings from a full 25-point profile of the duct as described in the calibration procedure. However, the anemometer probe was scanned across the duct section in order to obtain an estimate of mean air velocity for subsequent comparison with fan speed and pressure data. During the course of the experiments, the anemometer periodically was used elsewhere in the measurement of ventilation flows from actual animal barns. This resulted in intermittent calibration problems due to dust fouling the probe but, when properly calibrated, these approximate anemometer readings gave flow rates that were in close agreement with those calculated from pressure and fan speed data.

Between series FLN1 and FLN2, a cup from the wind anemometer blew off in a storm and could not be replaced. Consequently, wind speed data were obtained by telephone from the Edmonton International Airport, which is sufficiently close to the experimental facility (10km) to provide an acceptably accurate indication as to whether local conditions were calm enough for tests to proceed. In fact, subjective judgment and the degree to which pressure differential was fluctuating also seemed to provide a reliable indication.

Throughout a normal test series, the experimental room remained sealed apart from the air inlet and fan.

4.3.3 Varying area runs

The procedure used for those series of tests in which the area of exposed heated surface was varied was similar to that used in the normal runs with two major exceptions. Firstly, the fan speed setting was not altered during the series and, secondly, the room did not remain sealed during a test series but was entered in order to uncover or cover heat pads.

The speed at which the fan was run was selected on the basis of data from previous, normal runs. The object was to select a speed at which the inlet jet had an intermediate trajectory so that any effect of heated area on the trajectory would be most apparent.

The order in which heating pads were covered/uncovered varied from series to series. Although not randomized, this variation was employed to show up any tendency of the jet trajectory to depend on the manner in which the heated area was changed. The order in which heating pads were exposed is shown in Table 4.2. As can be seen from this table, two series were carried out with the full width inlet at the lower position (FLH(1) and FLH(2)). The reason for this was that the airflow rate for FLH(1) was considered to be slightly low so an additional test, FLH(2) was run immediately afterwards using a higher fan speed.

In all cases, when pads were covered the surface temperature sensor was relocated on top of the insulating cover. After any change in the exposed area, time was allowed for the room to equilibrate before obtaining photographs of the jet as described in section 4.3.2. Again, this equilibration period was used to obtain "manual" readings of pressure differential, fan speed and flow rate for checking purposes.

4.4 Data Processing and Reduction

The raw data from a test series were processed on the same day as described in section 3.4.2. This allowed correlation with field notes and showed up any faults or discrepancies within the system before the next run was commenced. This feedback proved useful in confirming the suitability of the fan speeds used, in refining the

TABLE 4.2: TESTS WITH VARYING HEATED AREAS.

CODE	PADS UNCOVERED			
FTH	ALL	IN+MID	IN	FAN
FLH(1)	NIL	FAN	FAN+MID	ALL
FLH(2)	ALL	FAN+MID	FAN	NIL
HTH	NIL	IN	IN+MID	ALL
HLH	NIL	FAN	FAN+MID	ALL
ORDER	1	2	3	4

calibration of temperature sensors, in indicating the need for recalibration of the hot-thermistor anemometer and in checking that equilibration times were sufficient.

After the final experimental test, the computer program used to convert raw to meaningful data was modified to incorporate all calibration corrections and all the raw data were reprocessed. At this point those data corresponding to the photographic record of trajectories were extracted and these were used for subsequent manipulation and analysis.

5. RESULTS

5.1 Jet Trajectories

The data that were of interest in determining the jet trajectories were the temperatures indicated by the array of thermistors in the ventilated room. To reduce these to a similar basis, they were expressed as dimensionless temperature differences according to the following equation:

$$\Delta T_n = (T_n - T_0)/(T_d - T_0) \qquad 5.1$$

where: ΔT_n = dimensionless temperature difference at location n.
T_n = temperature at location n (°K),
T_0 = temperature at the inlet (°K), and
T_d = temperature downstream of the fan (°K).

Because of air mixing within the exhaust duct, T_d was used as a reference temperature since it could be considered as more representative of exhaust temperature than any of the other temperatures measured. Results obtained by Glennon *et al.* (1984) indicate that substantial temperature differences may occur between even the top and bottom of inlets to exhaust fans.

For each vertical group of thermistors, the minimum temperature difference was identified and taken to indicate the sensor closest to the jet centreline. Where two sensors in a string indicated the same minimum temperature difference, the centreline of the jet was assumed to pass mid-way between the sensors. Having identified the location of the jet centreline at each vertical string of sensors, an approximate plot of the total jet trajectory could be obtained. Examples of such plots are shown in Figures 5.1 and 5.2. The temperature-based plots shown in these figures should not be interpreted as portraying the actual jet trajectories since the sensors, particularly those in the upper part of the room, may not have been located near the actual jet centreline. Similarly, the sharp changes in direction portrayed in these plots are due to, and coincide with, the location of the temperature sensors. Nevertheless, the plots do indicate whether a jet fell on entry or remained in the upper part of the airspace. This was confirmed by the photographic record and sketches of the photographically-derived trajectories are shown for comparison.

For each "trajectory" plot, a corrected Archimedes number, Ar, was calculated using equation 2.56 which may be written explicitly in the following form:

$$Ar = g(T_s - T_0)C_d bh(B+H)BH/(T_s + T_0)Q^2 \qquad 5.2$$

Where: g= acceleration due to gravity (m/s^2),
T_s= temperature of heated surface (°K),
T_0= temperature of inlet air (°K),
C_d= orifice discharge coefficient,
b= width of inlet slot (m),
h= height of inlet slot (m),
B= width of room (m),
H= height of room (m) and
Q= flow rate (m^3/s).

The temperature of the heated surface, T_s, was calculated as the mean of the surface temperatures of the six heat pads. The orifice coefficient, C_d, was taken to have a value of 0.6 for all inlets. This value is the same

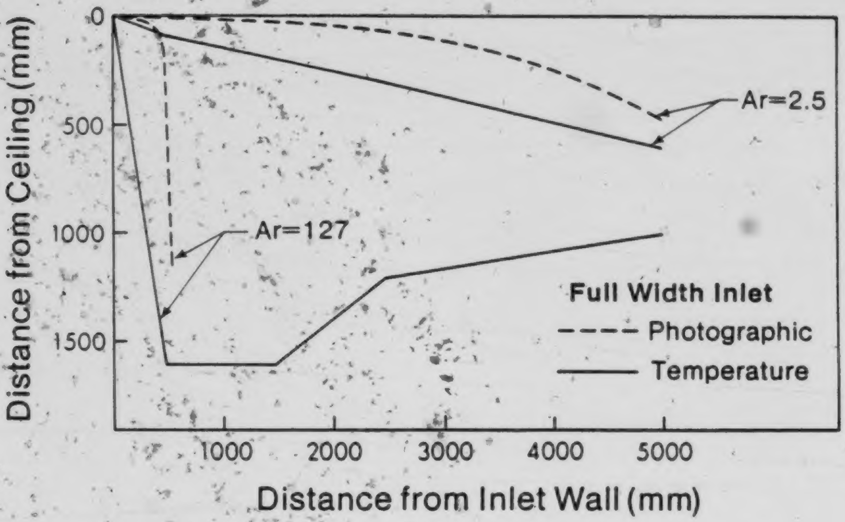

Figure 5.1 Sample trajectory plots (Inlet at ceiling).

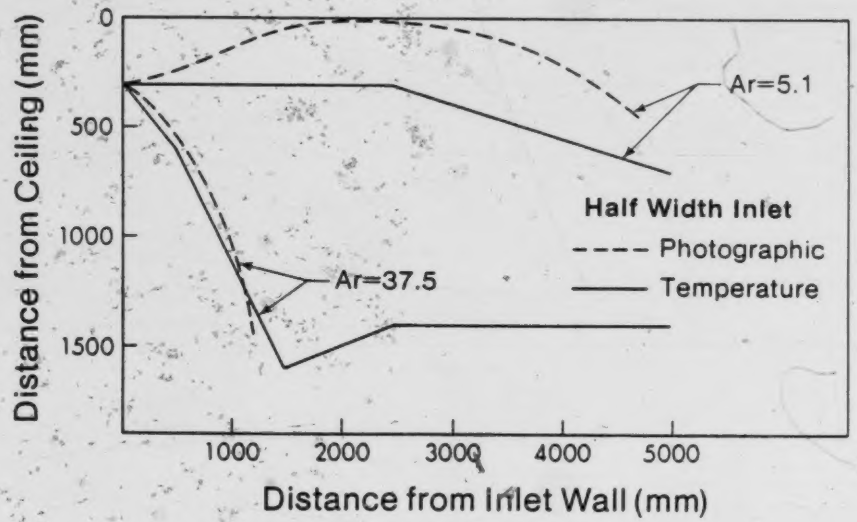

Figure 5.2 Sample trajectory plots (Lower inlet position).

as that used by Jackman (1970) and Randall and Battams (1979). Since, in some instances, the calibration of flow rate against pressure differential may have been affected by wind at low fan speeds, the flow rates used in the calculation of Ar were based on the fan speed calibration.

Although Randall and Battams (1979) reported that jets having values of Ar between 30 and 71 exhibited inconsistent behaviour, sometimes falling on entry and sometimes remaining horizontal, such behaviour was not observed in these tests. Rather, the jet trajectories seemed to display a general and continuous tendency to remain horizontal as Ar was decreased. These continuous "families" of trajectories are analogous to those obtained by Fan and Brooks (1969) in their numerical solution of the trajectories of warm, submarine effluent plumes.

Having, thus, a continuum of trajectories, the classification used by Randall and Battams (1979) (dropping, horizontal or unstable) was deemed to be inadequate, especially in assessing the effects of inlet widths and position. Therefore, a more precise descriptive measure was sought. A general equation describing jet trajectories would provide such a measure and, on the basis of work concerned with free jets (Frean and Billington, 1955; Koestel, 1955), this equation could be expected to be of the general form:

$$y' = Ar.f(x') \qquad 5.3$$

where y' = dimensionless vertical distance and,
x' = dimensionless horizontal distance.

Sufficient data were not available from this study to determine the precise form of $f(x')$ in equation 5.3 (Section 6.3). However, a single number describing the tendency of the jet to drop also would be useful in establishing design criteria, in the comparison of inlet performance and in the more rigorous, statistical design of future experiments in this area. Ideally, this number would be dimensionless and applicable to any type of room/inlet geometry.

In order to provide such a number, the concept of a drop coefficient is postulated. This coefficient may be thought of, perhaps, as a dimensionless average slope of the jet trajectory. The coefficient is independent of other variables, such as room geometry and air temperatures, and is defined as follows:

If the location of the jet centreline can be defined at n points in the room, each having coordinates relative to the jet orifice of (x,y), then the drop coefficient, Z, may be defined as:

$$Z = \Sigma(y_i/x_i)/n \qquad 5.4$$

Equation 5.4 indicates that the larger the value of Z, the more rapidly the jet drops after entry into the ventilated space. Z is more sensitive to the initial part of the trajectory because division by the horizontal distances from the orifice (x_i) effectively gives more weight to the early part of the jet. In this region, temperature differences were greatest and dissipation was minimal, allowing the best possible delineation of the trajectory.

Using equation 5.4, values of Z were calculated for each test. Because of the uncertainty of the true location of the jet centreline in the upper part of the airspace, an approximation was made whereby, if the minimum dimensionless temperature difference were indicated by the top sensor in a group, then the drop of the jet(i.e., y) was said to be zero at that horizontal distance from the inlet (i.e., x).

To facilitate comparison of different inlets, the values of Z were plotted, for each inlet configuration, against Ar. Examination of general equations for the trajectories of both heated and chilled free jets (Frean and Billington, 1955; Koestel, 1955) indicates that, for these jets, Z would be related linearly to Ar. Assuming that equation 5.3 is applicable, the same could be expected for the jets of this study and the plots of the data, together with the best-fit straight lines obtained by least squares linear regression, are shown in Figures 5.3 and 5.4. The equations to these curves are shown in Table 5.1, together with the equation fitted to all the data regardless of inlet type or position. The values of R^2 for these regressions vary from 0.78 to 0.95 and, although higher values of R^2 were obtained for quadratic and cubic functions, there seems little justification for using these, instead of linear functions, as the basis for comparing inlet performance. Furthermore, the error implied by the R^2 values does not appear to be unreasonable.

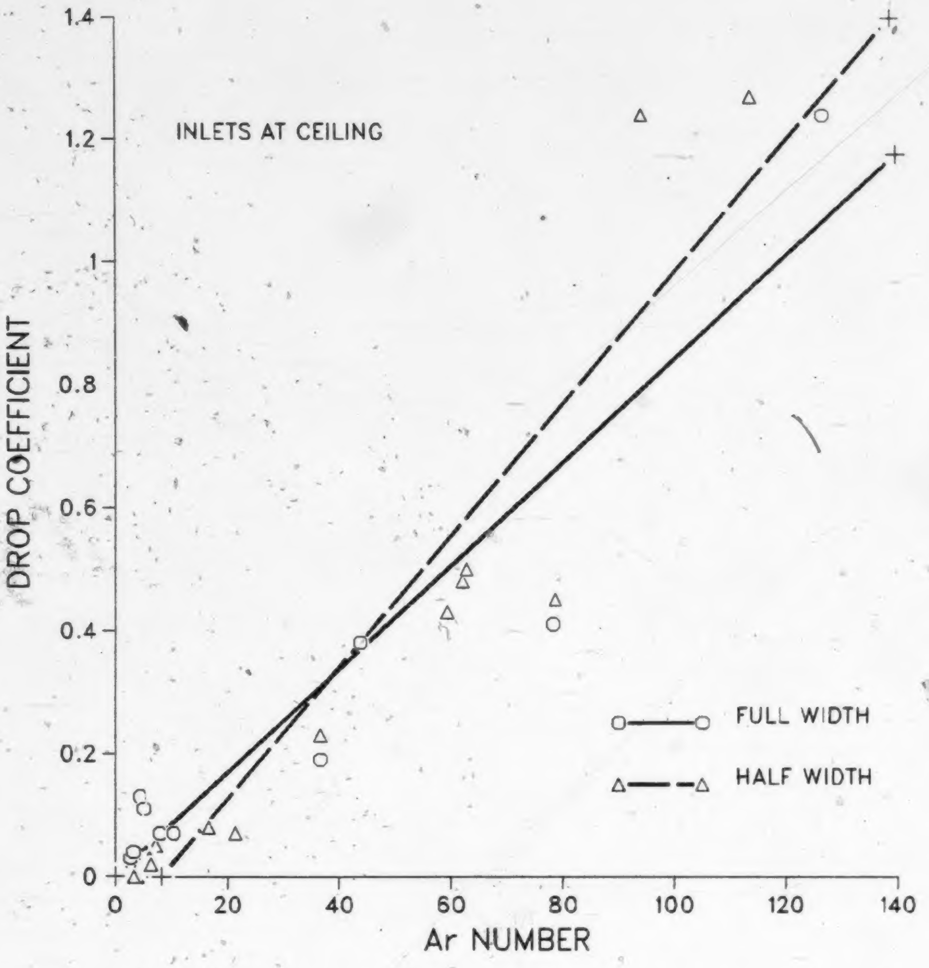

Figure 5.3 Plot of Z versus Ar for ceiling inlets.

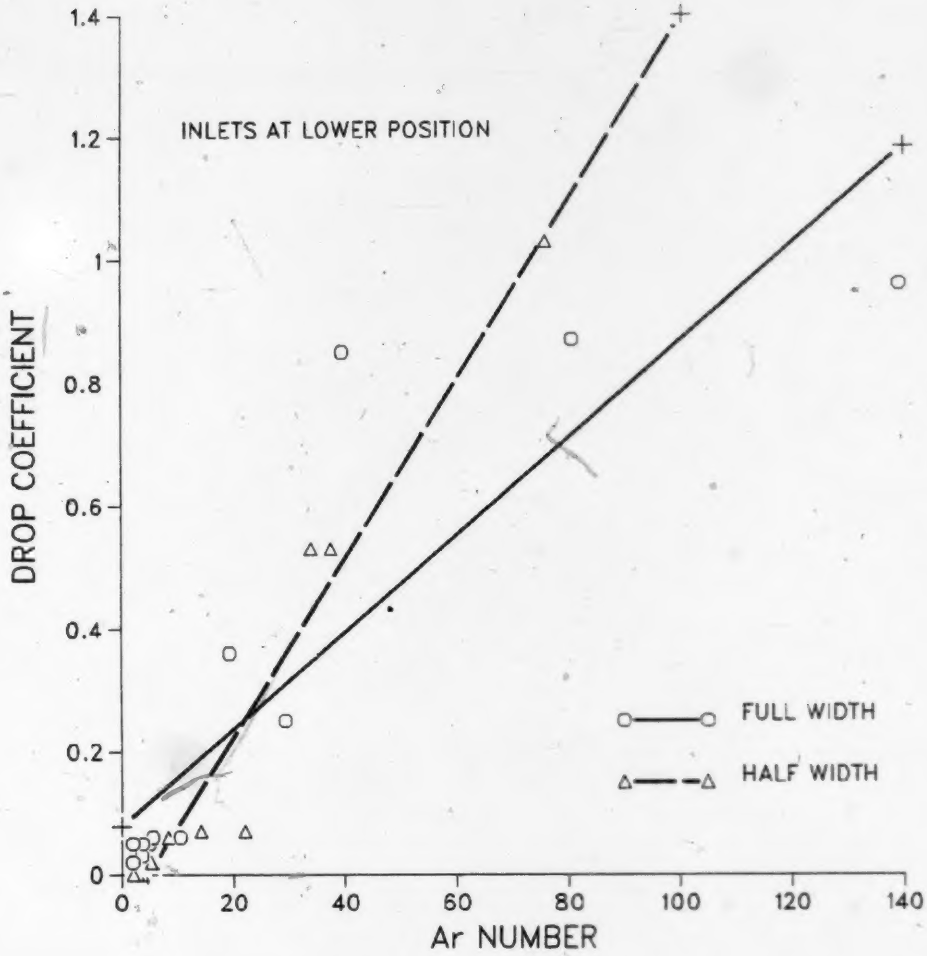

Figure 5.4 Plot of Z versus Ar for lower inlets.

To identify those points contributing most to this error, 95% confidence bands were superimposed on the regression plots shown in Figures 5.3 and 5.4. Points that were outside the confidence bands were identified and the data from the tests that they represented were re-examined. In some cases, this procedure showed up simple errors in calculation of Z or incorrect identification of jet trajectories due to ambiguities in the temperature data. In these instances, the data were corrected as required and replotted. The remaining points outside the confidence bands all corresponded to tests with high values of Ar or, in other words, low velocities.

With low velocity jets, measurements of both Ar and Z were subject to greater error than with high velocity jets. As can be seen from Figures 5.1 and 5.2, "trajectories" of jets with high values of Ar appear to rise after falling initially. In fact, the plotting of trajectories of these low energy jets so far into the airspace may be misleading since they dissipate quite rapidly. Although the smoke tracer injected with these jets was observed to rise due to convection off the warm pad surfaces, the true location of the jet centreline beyond the second line of sensors cannot be fixed with certainty. This uncertainty would have resulted in some error in the calculation of Z although, because of the dominant effect of the early part of the jet, the error would be small.

TABLE 5.1: REGRESSION EQUATIONS FOR Z AGAINST Ar.

INLET CONFIGURATION	EQUATION	R^2	DATA PAIRS
FT	Z=0.0084Ar - 0.0013	0.90	10
FL	Z=0.0079Ar + 0.0782	0.78	12
HT	Z=0.0107Ar - 0.0878	0.89	15
HL	Z=0.0146Ar - 0.0692	0.95	11
ALL DATA	Z=0.0094Ar - 0.0015	0.83	48

More significant errors would probably be due to uncertainties associated with flow measurement. These were due to the fact that the calibration of both fan speed and pressure differential against flow rate were inherently less accurate at low flows. A further consideration is that any effects of wind would have been of greatest significance at low flow rates. Taken together, these factors could reasonably account for the unexplained error of the regression analyses.

5.2 Varying Heated Areas

The data from the varying heated area tests were processed in a similar fashion to those from the normal tests as described in the preceding section. That is, dimensionless temperature differences were calculated using equation 5.1, the minimum temperature difference for each line of sensors was identified and a jet trajectory was delineated for that test. An Archimedes number was calculated for each test trajectory using equation 5.2 but the method for determining the temperature of the heated surface, T_s, differed from that used for the normal test data.

Although readings were recorded from all the heat pad temperature sensors, only those from uncovered pads were used in the calculation of T_s. The sensors for the covered pads, being located on top of the insulating "blankets", generally indicated temperatures that were within a few degrees of the outlet air temperature and the air temperatures in the lower part of the airspace. Since these temperatures were generally 10°C to 20°C higher than the inlet air temperatures, the covered heat pads were, no doubt, contributing to the buoyancy effects on the incoming jets and the Archimedes numbers calculated using only the exposed pad temperatures would, therefore, be too high. Nevertheless, in the absence of a rigourous definition of what constitutes a heated surface, and to maintain comparability with the experiments of Randall and Battams (1979), the above approach was used as a starting point in the analysis of the data.

To determine if varying of the exposed heated area had any effect on the jet trajectories, the data were plotted in the Z-Ar plane and use was made of the regression analysis described in the preceding section. Since the fan speed setting was held constant for each test series and, for most inlets, only one series of this type was run, data from each series were grouped around a single Archimedes number. Without a range of Archimedes numbers in the varying-area data, a comparison of normal and varying-area regression lines would be meaningless; therefore, a more simple approach was adopted.

The varying-area data for each inlet and location were pooled with the data from the normal test series and linear regression equations were obtained together with 95% confidence bands. These were plotted together with the varying-area data points. Any gross deviation of jet behaviour from that observed in the normal tests would be evident from a marked change in the slope of the regression line, reduction of the value of R^2 of the regression, or the varying area points consistently being outside the confidence bands.

The equations to the regression lines for the pooled data are shown, together with R^2 values, in Table 5.2 and the plots of the regression lines, confidence bands and data points are shown in Figures 5.5 to 5.8.

TABLE 5.2: REGRESSION EQUATIONS FOR Z AGAINST Ar USING POOLED DATA.

INLET CONFIGURATION	EQUATION	R^2	DATA PAIRS
FT	$Z=0.0084Ar - 0.0488$	0.85	14
FL	$Z=0.0082Ar + 0.120$	0.58	20
HT	$Z=0.0108Ar - 0.1165$	0.87	19
HL	$Z=0.0145Ar - 0.0684$	0.95	15
ALL DATA	$Z=0.0093Ar - 0.0012$	0.72	68

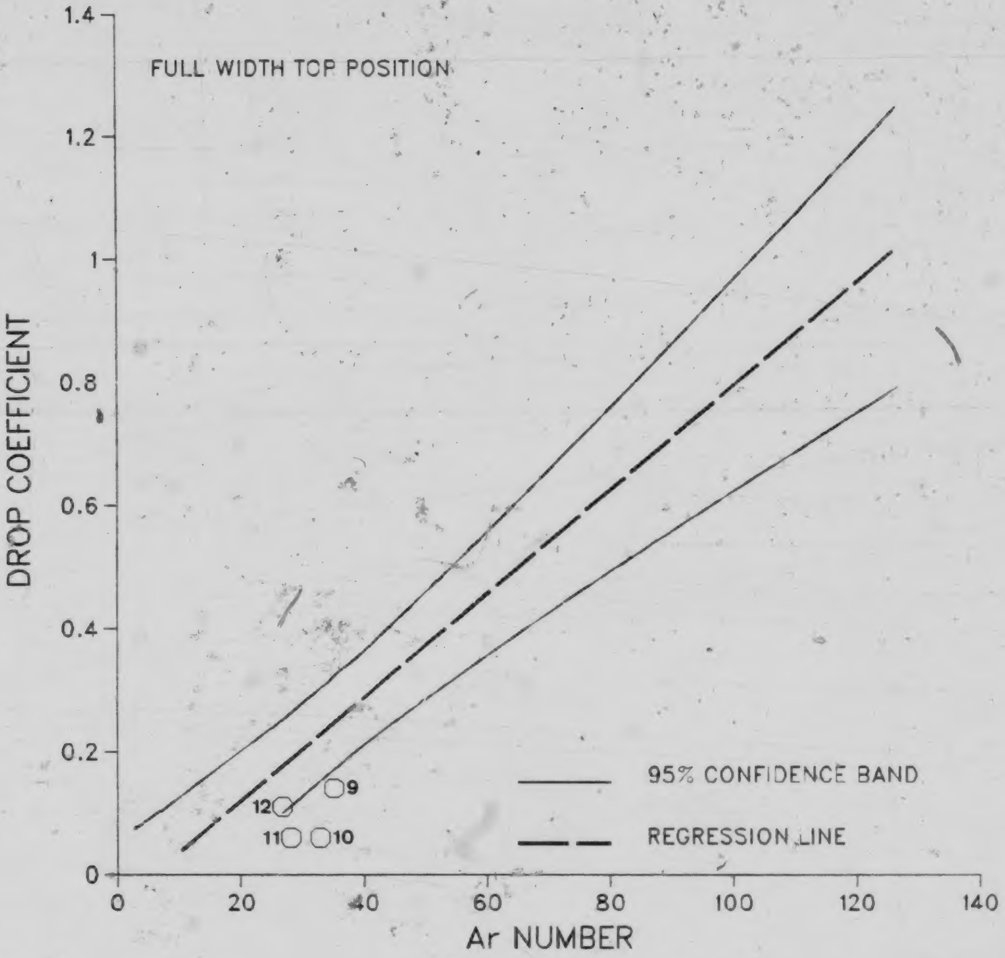

Figure 5.5 Plot of Z versus Ar using pooled data (full-width, ceiling inlet).

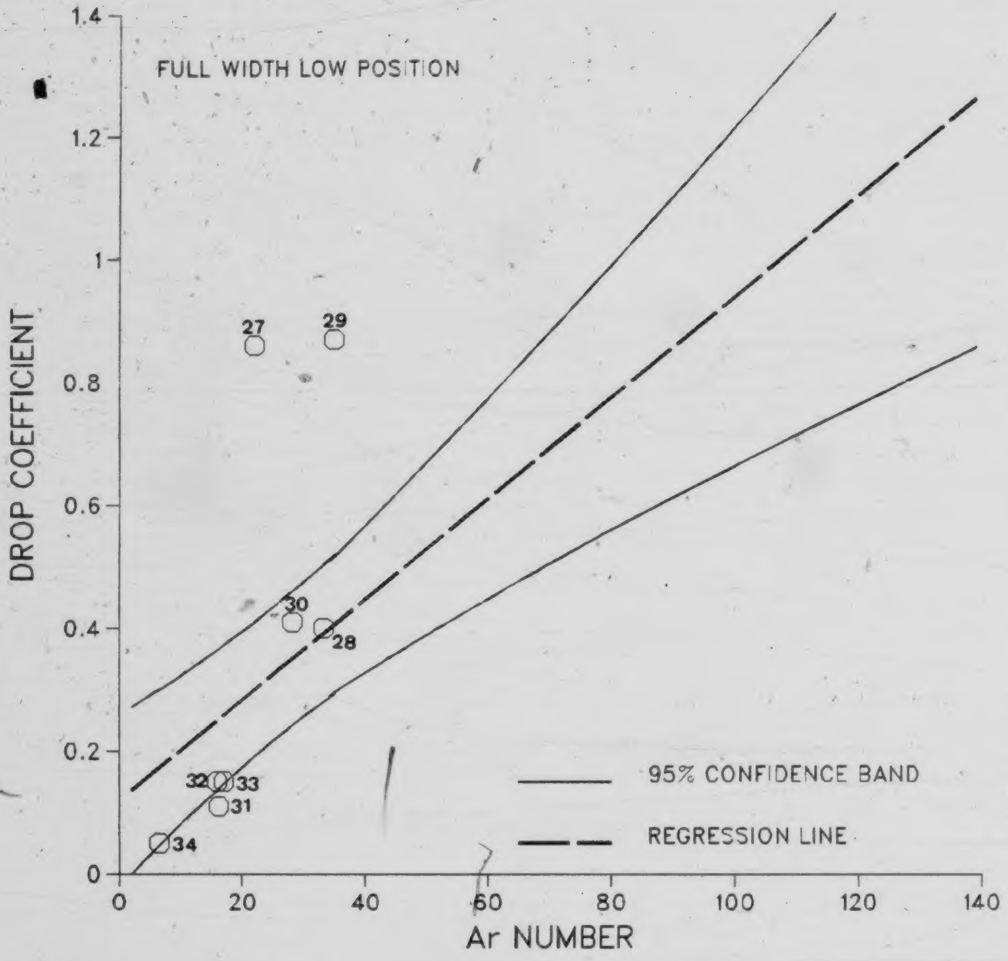

Figure 5.6 Plot of Z versus Ar using pooled data (full-width, lower inlet).

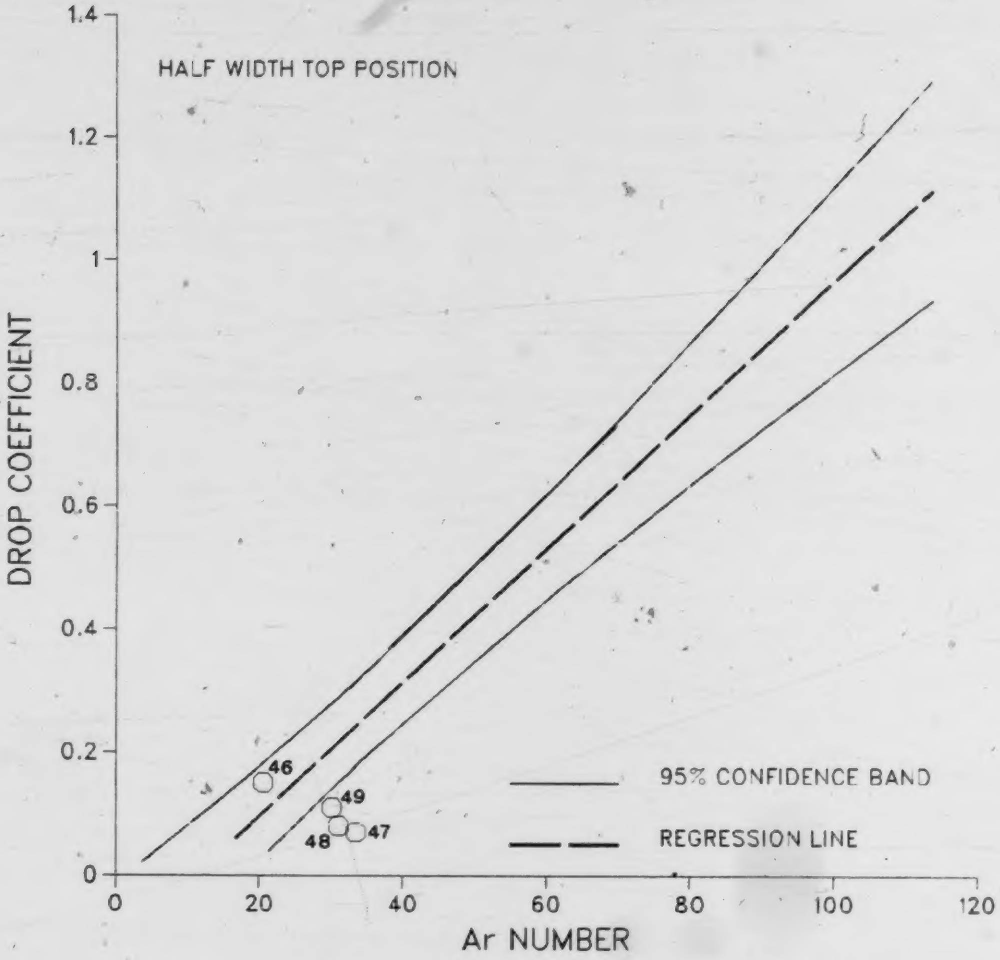

Figure 5.7 Plot of Z versus Ar using pooled data (half-width, ceiling inlet).

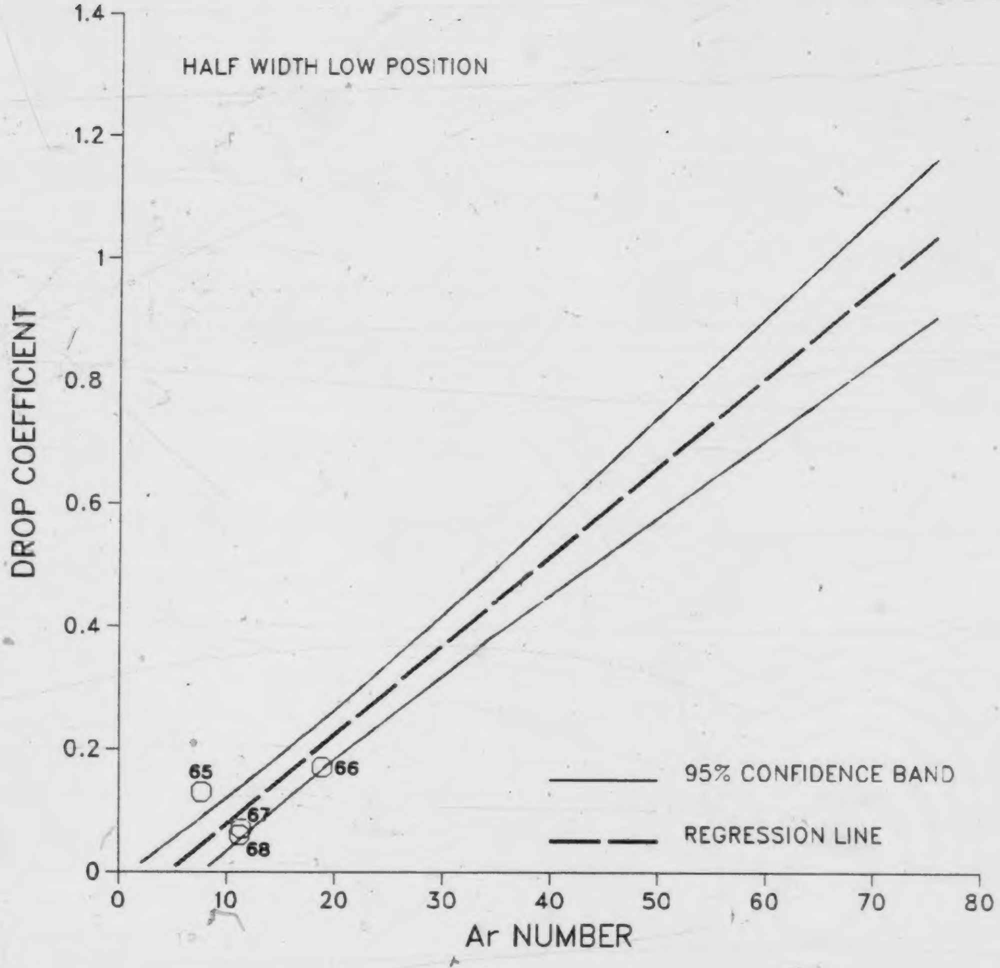

Figure 5.8 Plot of Z versus Ar using pooled data (half-width, lower inlet).

5.3 Mixing in the Ventilated Space

Although these experiments were not set up to investigate air mixing in a ventilated space, the temperature data that were collected can be used to make some inferences on this topic. Although the picture is complicated by the presence of heating pads, the cold air may be thought of as a thermal tracer and the degree of mixing, therefore, can be related to temperature distributions and uniformity in both horizontal and vertical planes within the ventilated space.

As with the trajectory analyses described above, all temperature data were normalised by expressing them in terms of dimensionless temperature difference. A measure of the variation among these normalised temperatures then was required. The measure used was that of a coefficient of variation which may be expressed as:

$$COV = \sqrt{[\Sigma\delta_i^2/(n-1)]}/\bar{x} \qquad 5.5$$

where: COV = coefficient of variation among n points, and
δ_i = deviation from the mean, $\bar{x}$, of the ith point.

For each test the value of COV was calculated for each vertical group of sensors and also for the lower part of the airspace represented by the bottom four sensors of each vertical group. The location of these lower sensors was constant regardless of inlet height and they, therefore, provided a good basis for comparison of the mixing characteristics of the various inlets. The coefficient of variation of these lower sensors was denoted by COVL.

One of the factors governing the mixing performance of a jet is the rate at which it entrains surrounding air. An obvious measure of this is the entrainment ratio defined in section 2.1.4 and, ideally, calculation of entrainment ratios for each inlet configuration would give some indication of relative effectiveness in promoting air mixing. Furthermore, as can be seen from equations 2.29 and 2.30, the entrainment ratio depends on the type of jet and, therefore, could be expected to vary with inlet type and location. However, the expressions for entrainment ratio embodied in these equations are specifically for free isothermal jets and are given in terms of flow rates and velocities at sections of the jet. Since neither of these were measured directly in these experiments, an indirect indicator of entrainment ratio was required.

Bearing in mind the similarity of velocity and temperature decay along the jet centreline, and noting the form of equations 2.29 and 2.30, one such indicator could be the ratio of inlet temperature to centreline temperature which, when expressed non-dimensionally, takes the form $\Delta T_0/\Delta T_m$ where the temperature differences are as defined in equation 5.1. In order to be useful as a basis for the comparison of different jets, this ratio must be evaluated at a consistent location. In these experiments, because of the arrangement of the temperature sensors, the most suitable location appeared to be at the group of sensors furthest (5m) from the inlet wall. Thus, taking the centreline temperature difference, ΔT_m, to be the lowest from any of the eight sensors, the ratio $\Delta T_0/\Delta T_m$ was calculated for all normal tests.

The use of the downstream duct temperature to calculate the dimensionless temperature differences above led to some inconsistencies in the sign of the ratio $\Delta T_0/\Delta T_m$. This was due to the fact that ΔT_m at the measuring location was generally small and, therefore, very susceptible to any temperature measurement errors. To overcome these effects, absolute temperatures were used instead of temperature differences. Thus, the final ratio used in comparing the entrainment performance of jets was simply T_0/T_m. For convenience T_m at 5m from the inlet wall was denoted by T_5 and, in general, lower values of T_0/T_5 would indicate higher entrainment and mixing by the jet.

Another measure of entrainment is the variation of temperature across the jet at some distance from the orifice. As the jet entrains air from the surroundings, the temperature profile flattens out until, finally, the jet is indistinguishable from the room air. In this case, the evaluation of temperatures at right angles to the jet centreline was not possible, but the vertical variation of temperature at the last group of sensors (5m from the inlet) could give an indication of entrainment, especially for higher velocity jets (i.e., jets with low Archimedes numbers). This variation was represented by the coefficient of variation of temperatures indicated by these sensors,

COV_s, where for the reasons indicated above, absolute temperatures rather than temperature differences were used. Values of COV_s were not used for those cases where the inlet jet had dispersed within 5m of the inlet wall.

As well as an evaluation of the mixing and entrainment performance of the jets, an index of this performance was required for possible use as a design criterion. Since Barber *et al.* (1982), on the basis of work by Kaul *et al.* (1975), have proposed the use of a momentum number, J, as a mixing criterion, this was calculated for each test using equation 2.61. The Archimedes number, Ar, was also considered as a mixing criterion.

The momentum number of Kaul *et al.* (1975) was derived specifically for full-width inlets by dividing initial momentum by room volume. Extending this concept to part-width inlets and making the number dimensionless after Barber *et al.* (1982) results in the following expression for J:

$$J = Q^2/gBHXA' \qquad 5.6$$

Furthermore, comparison of equations 5.6 and 5.2 leads to the following relationship between J and Ar:

$$Ar = (B+H)(T_i-T_0)/[JC_dX(T_i+T_0)] \qquad 5.7$$

For a given ventilated space, B, H, X and C_d are constant and the temperature ratio term is likely to remain fairly constant over a range of T_0. Thus, for the experimental room concerned, by letting $T_s - T_o = 40\,^\circ K$ and $T_s + T_o = 540\,^\circ K$, the relationship between J and Ar could be approximated by:

$$Ar = 0.124J^{-1} \qquad 5.8$$

In fact, when a regression analysis was carried out on all the data from normal tests, the experimentally determined relationship was:

$$Ar = 0.125J^{-1.0075} \qquad (R^2=0.98) \qquad 5.9$$

Because of the above relationship, the plotting of the mixing indicators COVL, COV_5 and T_o/T_m against both Ar and J was considered to be unneccessary. However, for illustrative purposes and convenience of scaling, all three indicators were plotted against J. These plots are shown in Figures 6.1 to 6.12.

6. DISCUSSION

6.1 General Jet Behaviour

From the temperature data, the photographic record and observations recorded during the tests, a number of general comments can be made on the behaviour of the cold jets studied. These concern the penetration of the jets into the room and the attachment of jets to the ceiling.

The work of Linke (1966) and Kaul *et al.* (1975) mentioned in section 2.1 suggests that, in these experiments, no jet should have penetrated further than 5.7m into the room (three times the ceiling height). In fact, high speed jets, or those with low values of Ar, were identified readily by temperature at a distance of 5m into the room and, in some instances the jet was identifiable with the smoke tracer, albeit in a dispersed form, for the full length of the room (7.2 m). Since the penetration, or throw, of jets has implications in the location of inlets and the maximum width of buildings, further investigations should be carried out to check the penetration distances that can be expected from ventilation jets.

With the exception of the slowest jets (high Ar), all jets tended to adhere to the ceiling of the room. This, of course, counteracted the tendency of the jets to drop and was to be expected for the jets discharging adjacent to the ceiling. However, the attraction to the ceiling of the lower jets was not so predictable.

Baturin (1972) has reported experiments indicating that cold jets would cling to a ceiling if the jet orifice was within a distance of 4h of the ceiling, h being the vertical width of the orifice. In the present experiments , using the lower inlet location,,the orifices were approximately 6h and 12h from the ceiling for the half- and full-width slots respectively. An additional experiment was carried out with the full-width slot located approximately 600mm (24h) below the ceiling and, at this location, the jet would not attach to the ceiling at any velocity. Because attachment to the ceiling counteracts the dropping of the jet, and because of the relevance of this effect to inlet design and location, more work is required to determine the limiting distance of the orifice below the ceiling beyond which jets will not attach.

6.2 Comparison of Inlet Configurations

The graphs shown in Figures 5.3 and 5.4, together with the equations shown in Table 5.1, illustrate the usefulness of the drop coefficient ,Z, to describe the severity of jet drop. In general, the greater the slope of the regression line, the greater the tendency of the jet to drop. Thus, it is of interest to note that the slopes of the regression lines appear to depend on the inlet type and location.

Examination of the equations in Table 5.1 indicates that the tendency of full-width jets to drop was very similar for both locations of the jet and was less than that of the half-width jets. In contrast, the half-width jet from the lower inlet location showed a greater tendency to drop than that from the ceiling location. These results can be explained qualitatively in terms of air entrainment and the Coanda effect.

In the case of a full-width jet discharging along the ceiling, entrainment of room air can occur only on the underside of the jet. The tendency to entrain air from the boundary layer adjacent to the ceiling "pulls" the jet towards the ceiling while the walls limit entrainment at the sides of the jet. Except for a small portion of the jet close to the orifice, the situation is identical for a full-width jet discharging at a small distance from the ceiling. Nevertheless, the slope of the regression line for the full width jet in the lower position could be expected to be, if anything, greater than that for the upper position. The fact that the results do not indicate this is not considered to be significant, bearing in mind the closeness of the slopes and the lower regression coefficient of the equation for the lower position inlet.

In contrast to full-width jets, half-width jets are able to entrain air along their sides and, in addition, the area of limited entrainment at the ceiling is smaller. The net result is a reduction in the attraction of the jet to the ceiling. As a half-width jet is moved away from the ceiling, entrainment at the top of the jet increases until, at some distance from the ceiling, entrainment occurs all around the jet and it remains unattached along its entire length. The smaller the degree of attachment to the ceiling, the greater the effect of the gravitational forces tending to make the jet drop.

6.3 Equations of Trajectories

The desirability of obtaining general equations for jet trajectories has been mentioned in section 5.1 and equations for free jets are described in section 2.3.3. In the present case, the jet trajectories were influenced by the confining boundaries of the room and, therefore, would not be expected to conform to free-jet equations. Nevertheless, because of their simplicity, there might be a temptation to use free jet equations to provide approximations to constrained jet trajectories. This possibility was investigated.

The linear relationships between Ar and Z for the various inlets indicated that the trajectory equations were themselves linear in Ar in the same way as those proposed for free jets by Frean and Billington (1955) and Koestel (1955). These equations (2.47 and 2.49) are both of the general form:

$$y/l = C\alpha(x/l)^k \qquad 6.1$$

where l is a characteristic length, C and k are constants and α is an Archimedes number. In the form used by Frean and Billington, l is taken to be the square root of the effective orifice area and α is directly proportional to the

Ar used in these experiments as expressed in equation 5.2

By substituting equation 6.1 in the expression for Z (equation 5.3), substituting the result in one of the regression equations relating Z and Ar and substituting appropriate values from measured data into equation 6.1, two further equations were set up with C and k as the unknowns. An attempt was made to solve these equations by numerical iteration. This procedure resulted in values of k and C that were unrealistically large and small, respectively, and the approach was abandoned on the assumption that the data did not fit equation 6.1.

As an alternative approach, the value of C=0.238 used by Frean and Billington (1955) was assumed to be valid and a value of k was determined that gave the value of Z predicted by the regression equation for a given inlet and value of Ar. Using these values of C and k, trajectories were plotted using equation 6.1 and compared with the experimentally-obtained temperature and photographic trajectories.

Except for the case of the half-width inlet in the lower position for high values of Ar, the calculated trajectories did not provide a good approximation to the observed trajectories. This result was not unexpected since the attraction of jets to the ceiling caused gross deviations from free jet behaviour while those jets from the low, half-width inlet at high values of Ar were the closest to being free. The rational development of trajectory equations that take into account the effects of walls and ceilings is beyond the scope of this thesis and was not pursued further.

6.4 Effect of Heated Area

Comparison of Tables 5.1 and 5.2 gives an indication of the effect of pooling varying heated area data with those from normal test series. Examining the regression equations themselves shows that, although the additional data caused some minor changes in intercept values, the slopes of the equations essentially remained the same. This is not surprising in view of the limited amount and range of data added in each case. Larger differences are apparent, however, if the values of R^2 are compared.

Except for the case of the low half-width inlet, the R^2 values were all decreased by the addition of varying heated area data. In the two top position cases, this decrease was not large but was greater in the case of the low full-width inlets, decreasing from 0.78 to 0.58. Reference to the plots of the regression lines and confidence bands shown in Figures 5.5 to 5.8 is useful in explaining the decreased R^2 values.

With the full-width inlet adjacent to the ceiling (Figure 5.5), three of the four varying area points lie below the 95% confidence bands. While this might seem significant, the trend between divergence of points from the regression line and area of exposed heated area is the reverse of that expected. Although the relationship of points 10, 11 and 12 is consistent with the observations of Randall and Battams (1979) on the effect of the location of the heated area within the room, the relationship of points 9, 10 and 11 runs counter to the expectation that, as exposed heated area is increased, points would lie closer to the regression line. In this case point 10, representing two pairs of exposed pads, would be expected to lie closer to the line than point 11, where only one pair of pads was exposed.

This apparent contradiction, however, should be viewed taking into account possible errors in measurement of Ar. The data concerned are all within a small range of Ar and have values of Ar that are high enough to suspect some errors in flow measurement. These errors could be large enough to cause the anomaly described above.

Possibly of more importance is the general observation, based on the relationship of all the additional points to the regression line, that a reduction in heated area appears to cause a decrease in drop coefficient. This is in agreement with the results of Mullejans (1966).

The results for the full-width inlet in the lower position (Figure 5.6) have a wider spread, although a smaller proportion of the additional data points lie outside the confidence bands. The most prominent points outside the confidence bands are points 27 and 29. Together with points 28 and 30, these represent test series FLH(1) and their large deviation from the regression line can be explained in terms of the range of Ar used in this series, together with the order in which heat pads were uncovered.

As can be seen from Table 4.2, this test series began with all the heat pads covered. This implies that convective mixing of air within the room was minimised. Also, the moderately high values of Ar used in this series implies that the jets did not have sufficient energy to cause major air mixing by themselves. Thus, the cold inlet air did not mix with the upper part of the airspace which remained relatively warm and stagnant. The incoming air dropped rapidly and the lack of mixing implies that insufficient time was allowed for the room to equilibrate before taking readings.

On this basis, point 28 might be expected to have a higher value of Z and, in fact, the value of Z used is a result of the way in which the jet dropped for this test. The temperature data from the test indicate that the jet fell rapidly at the location of the first line of sensors. Because the second-from-top sensor indicated a marginally lower temperature, the jet centreline was taken to be located at that point thereby giving rise to an artificially low drop coefficient.

Since the heat pads were exposed in sequence from the fan wall, the effects of increasing exposure on jet trajectory would not be expected to be rapid. Nevertheless, by the time the test represented by point 30 was run, sufficient area had been exposed to promote convective mixing and re-establish shorter equilibation times. The second group of points for this inlet (31-34), which were obtained at lower values of Ar, lie much closer to the regression line but are all below the line.

Figure 5.8 shows the data pertaining to the half width inlet in the same location. Here, three of the four additional points lie outside the 95% confidence bands. Again, there is enough uncertainty associated with air flow measurement, at the values of Ar used, to discourage the drawing of any detailed conclusions regarding the relationship of the points to each other. Nevertheless, in this case points 47, 48 and 49 show the expected progression towards the regression line as increasing area is exposed. The data for point 46 were obtained with all pads covered and, because Ar is based on a mean "floor temperature" in this case, is not strictly comparable with the other points. Again, apart from point 46, tests with reduced exposed heated area gave points below the regression line.

Like the data from series FLH(2), those from series HLH (Figure 5.7) were obtained at lower values of Ar than for the other varying heated area series. With both of these series only one point lies outside the 95% confidence bands suggesting that higher energy jets are affected less by a decrease in heated floor area. Although these data lie relatively close to the respective regression lines, the tendency of the points to be below the lines is still observable.

Whilst the results that have been presented above are somewhat limited, they do allow the drawing of some general conclusions regarding the effects that varying the heated surface area in a room can have on the behaviour of cold ventilating jets. Firstly, variation in the heated area does have an effect on the tendency of cold jets to sink. This effect appears as a tendency of the jets to drop less with a decrease in heated area or, in other words, as isothermal conditions are approached. This is in agreement with the results of others, such as Mullejans (1966).

Secondly, the effects on jet trajectory are not dramatic but are more noticeable with low velocity (high Ar) jets than with those having higher velocities.

Finally, there is some evidence to support the observations of Randall and Battams (1979), detailed in section 2.3.3, suggesting that the location of the heated area is significant. The closer the heated surface to the inlet, the greater was the effect on the jet.

Because the effects noted above appear to be small, the correction of Ar to allow for changes in exposed heated area and the position of these areas in relation to the inlet is probably not justified. However, if similar experiments were carried out over a wider range of values of Ar, a basis for such correction could be determined.

Assuming that the heated area effects remain small over the entire range of Ar, another point of contention is the rationale for calculating Ar on the basis of heated surface temperature. The question arises as to when a surface should be considered to be heated. Should any surface above the inlet air temperature be considered as a heated surface or, in the case of animal housing, should the housed animals be treated as the heated surface? If the latter is the case, how should space heaters, such as black-iron hot-water pipes be treated? No doubt suitable answers could be found to these questions on the basis of localised convective heat transfer and momentum relationships, but at the expense of further complicating the calculation of Ar. If heated area effects are small, a better approach may be to remove the heated surface temperature from the calculation altogether.

6.5 Modification of Archimedes Number

Although the Archimedes number, Ar, calculated using equation 5.2, correlates closely with the drop coefficient, Z, and is a useful parameter in describing jet behaviour, some aspects of it bear reappraisal. Equation 5.2 is the end point in an evolution that started with the Archimedes number proposed by Mullejans (1966) that is given in equation 2.54. During the process of evolution, a number of terms have been introduced into the equation (Section 2.3.3) on arbitrary or empirical grounds that could, perhaps, be simplified or changed to provide a more universal description of jet behaviour. These terms may be divided into those dealing with room geometry and those dealing with thermal characteristics.

6.5.1 Geometrical terms

The fact that the slopes of the Z vs Ar regression lines in Table 5.1 show marked differences between inlet configurations indicates that there is scope for redefining the geometrical terms embodied in the Archimedes number expression given in Equation 5.2. Ideally, the relationship of Z to Ar would be independent of inlet or room geometry which clearly was not the case in these experiments. Considering only the regression line slopes from Table 5.1, an independent Archimedes number would need to be multiplied by factors to take account of reduction in inlet width and lowering of the inlet from the ceiling.

Comparison of the slopes derived from the two ceiling inlets indicates that halving of the inlet width in this case indicates that a width factor is required of approximately 11/8 or, still more approximately, 1.5. A similar analysis of the two half-width inlets indicates that an inlet position factor of 15/11 or, approximately, 1.5 is required. This analysis applies, of course, to a specific case and is included to indicate orders of magnitude rather than a general rule. Further experimental work would be required to formulate the latter, but the order-of-magnitude analysis does throw some doubt on the inlet location factor recommended by Jackman (1970).

As detailed in section 2.3.3, Jackman suggested multiplying the corrected Archimedes number by $2Dh/b^2$, where D is the distance of the top edge of the inlet below the ceiling. The correction was restricted to cases where $b<B/2$ and $D<b/2$ and, consequently, was not applied to the calculation of Ar in equation 5.2 since, for the half-width inlets, $b=B/2$. However, for geometries that are similar to those used in these experiments, the effect of applying this factor would be to decrease, rather than increase, Ar as the results suggest is required.

Although the preceding discussion implies the need for additional factors to be included in the Archimedes number formula, this would result in increased and undesirable complication. In fact, there is a distinct possibility that the same effect could be achieved by re-examining the geometric terms already present in the expression for Ar. These terms are the hydraulic diameter of the room, the dimensionless area of the inlet slot and the fictitious room air velocity, all of which are described in section 2.3.3.

Mullejans (1966) appears to have adopted the hydraulic diameter of the room as a characteristic dimension on arbitrary grounds. In the absence of any clear indications to the contrary, there is no good reason why the hydraulic diameter should not be satisfactory as a characteristic dimension, but its subsequent inclusion in the dimensionless inlet area (Equation 2.55) is open to question. Baturin (1972) has reported results indicating that a useful parameter in describing the throw of round jets was $\sqrt{A_r}/d_0$. For plane jets discharging into rooms with rectangular sections, this ratio could be expressed as BH/bh which is the inverse of a dimensionless inlet area that might be preferable to the $bh(B+H)^2/(2BH)^2$ used by Mullejans. In a similar vein, there seems to be no clear reason as to why the "fictitious room velocity", V, in equation 2.54 is calculated as Q/BH rather than Q/bh.

Further confusion arises when several inlet slots are spaced along the length of the inlet wall. Randall and Battams (1979) have addressed the case of numerous, closely-spaced slots but, when slots are widely spaced so that the individual jets do not coalesce rapidly, there seems to be little justification for using a hydraulic diameter based on the total room width, B.

Data from the experiments reported here are insufficient to resolve any of the above points. A further, comprehensive series of experiments would be required to determine suitable dimensionless geometric quantities to account for inlet width and position. The above discussion is included to illustrate the potential usefulness of such experiments.

6.5.2 Temperature terms

Whereas there are insufficient data from these experiments to draw useful conclusions about the geometric terms in the Archimedes number, the same is not true of temperature-related data. In the discussion on the effects of varying heated area (section 6.4), the neccessity of calculating Ar on the basis of a heated surface temperature was questioned and, on that basis, an alternative was sought.

The two terms involving the heated surface temperature in the Archimedes number are the reference temperature difference, (T_s-T_0), and the coefficient of thermal expansion, $\beta = 2/(T_0+T_s)$. Taking the last term first, β, which should be the reciprocal of the room air temperature, is approximated as the simple arithmetic mean of inlet and heated surface temperatures. Since the actual room air temperature is difficult to determine, unless a multipoint average is taken, β would be represented just as validly by the reciprocal of the outlet temperature $1/T_d$. Bearing in mind that the temperatures here are absolute, the difference in the coefficients calculated using the different approaches will, in any case, be small.

Similarly, in the calculation of the reference temperature difference, (T_s-T_0), T_s may be replaced by T_d. Although (T_s-T_0) represents the maximum air temperature difference possible, (T_d-T_0) is, perhaps, a better indicator of the actual buoyancy force acting on the jet since T_d is closer than T_s to the actual room air temperature.

The validity of using T_d to approximate the actual room temperature was confirmed by analysis of mean ambient and exhaust temperatures obtained during the monitoring of commercial laying and pullet rearing facilities (Feddes *et al.* 1984; Glennon *et al.* 1984). Average values from fourteen sets of data obtained in five barns gave an overall mean difference between T_d and the room air temperature of 0.6°C (range: +2.8°C to -2.2°C). In all cases, the reported room air temperatures were multi-point averages obtained from a number of sensors located throughout the ventilated space.

On the basis of this reasoning, the Archimedes number was re-calculated for all the tests carried out using the following expression:

$$Ar_d = g(T_d-T_0)C_d bh(B+H)BH/2T_d Q^2 \qquad 6.2$$

The relationship of Ar_d to Ar is given by the regression equation obtained from all test data:

$$Ar_d = 0.55Ar-0.85 \quad (R^2=0.99) \qquad 6.3$$

and the relationship of Ar_d to Z is shown in the regression equations of Tables 6.1 and 6.2. Table 6.1 is based on data from normal test runs only and is directly comparable to Table 5.1, while Table 6.2 is based on the data from varying heated area tests pooled with those from normal tests and, therefore, is directly comparable to Table 5.2. As might be expected from equation 6.2, the equations in Tables 6.1 and 6.2 bear essentially the same relationship to each other as those of Tables 5.1 and 5.2. If anything, the values of R^2 are improved by using Ar_d instead of Ar and the slopes of the Ar_d equations, especially those in Table

TABLE 6.1: REGRESSION EQUATIONS FOR Z AGAINST Ar_d FOR NORMAL TESTS ONLY.

INLET CONFIGURATION	EQUATION	R^2	DATA PAIRS
FT	$Z=0.0154Ar_d+0.0142$	0.89	10
FL	$Z=0.0157Ar_d+0.0845$	0.92	12
HT	$Z=0.0184Ar_d-0.0656$	0.78	15
HL	$Z=0.0261Ar_d-0.0387$	0.96	11
ALL DATA	$Z=0.0171Ar_d+0.0117$	0.85	48

TABLE 6.2: REGRESSION EQUATIONS FOR Z AGAINST Ar_d FOR POOLED DATA.

INLET CONFIGURATION	EQUATION	R^2	DATA PAIRS
FT	$Z=0.0157Ar_d-0.0189$	0.87	14
FL	$Z=0.0169Ar_d+0.1144$	0.91	20
HT	$Z=0.0187Ar_d-0.0945$	0.63	19
HL	$Z=0.0263Ar_d-0.0441$	0.96	15
ALL DATA	$Z=0.0174Ar_d+0.0112$	0.76	68

6.2, fall more definitely into the expected sequence than those in Tables 5.1 or 5.2. This means that the slope of equations describing jets from the full-width, ceiling inlet would be expected to be the lowest, since these jets would tend to drop the least, followed by the full-width inlet in the lower position, the half-width ceiling inlet and the half-width, lower inlet. In addition, comparison of Tables 6.1 and 6.2 shows that addition of the varying heated area data had less effect, as measured by R^2 values, with the Ar_d equations than with the conventional equations of Tables 5.1 and 5.2.

The preceding discussion indicates that, for this experimental situation, an Archimedes number based on outlet temperature would be just as useful as one based on the temperature of the heated surface. There seems to be no reason why this should not extend to other situations since, except for extreme cases of short-circuiting (Barber and Ogilvie, 1982), the outlet temperature will be related closely to the room air temperature and, indeed, to the heat exchange from warm surfaces within the room. Also, as mentioned in section 6.4, the outlet temperature is easier to measure and removes ambiguities that could arise from multiple heated areas at different temperatures and locations.

6.6 Mixing in the Ventilated Space

6.6.1 Horizontal temperature distribution

As outlined in section 5.3, the three indicators of mixing in the airspace were based on observed temperature variations. The most comprehensive of the three indicators was the coefficient of variation of all the temperatures observed in the lower part of the airspace, COVL. This is plotted, for each inlet configuration, against the dimensionless momentum number, J, in Figures 6.1 to 6.4.

The curves that are superimposed on the data points in the above figures are the best-fit cubic functions obtained by least squares regression. The equations to these curves

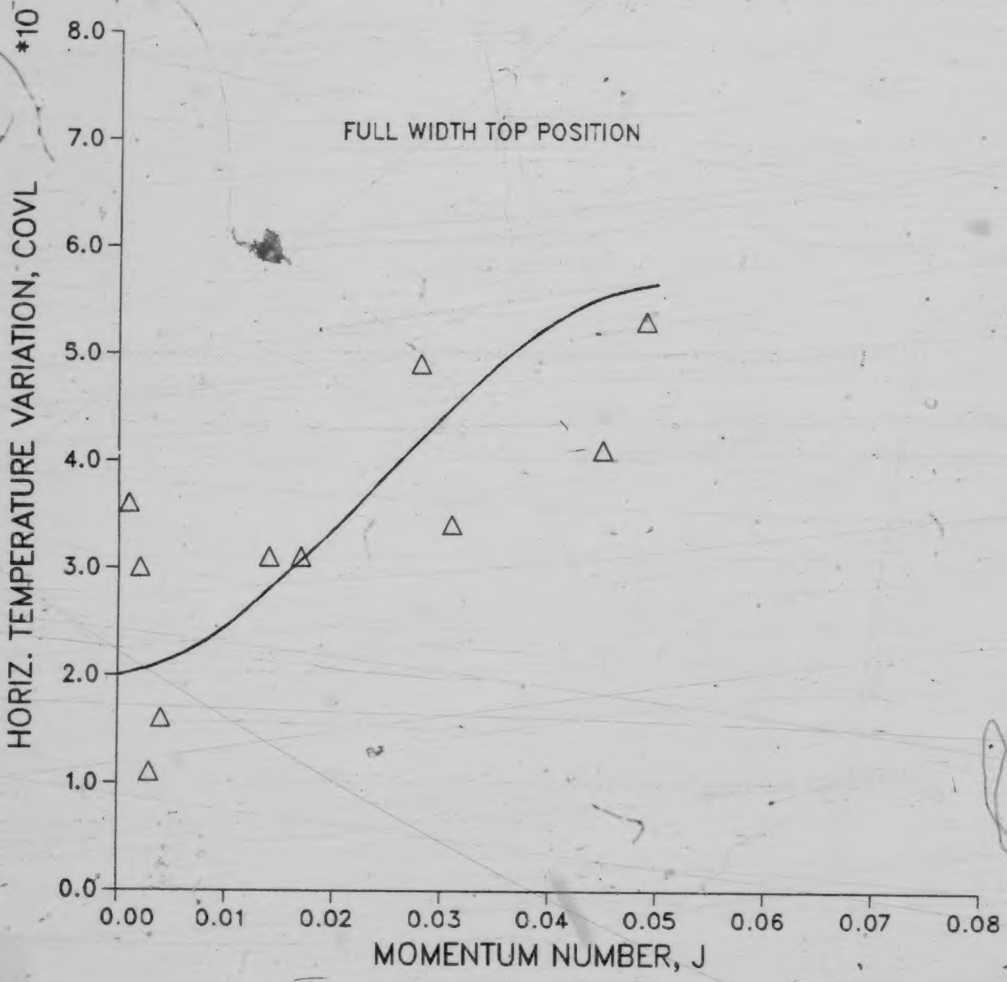

Figure 6.1 Plot of COVL versus J (full-width, ceiling inlet).

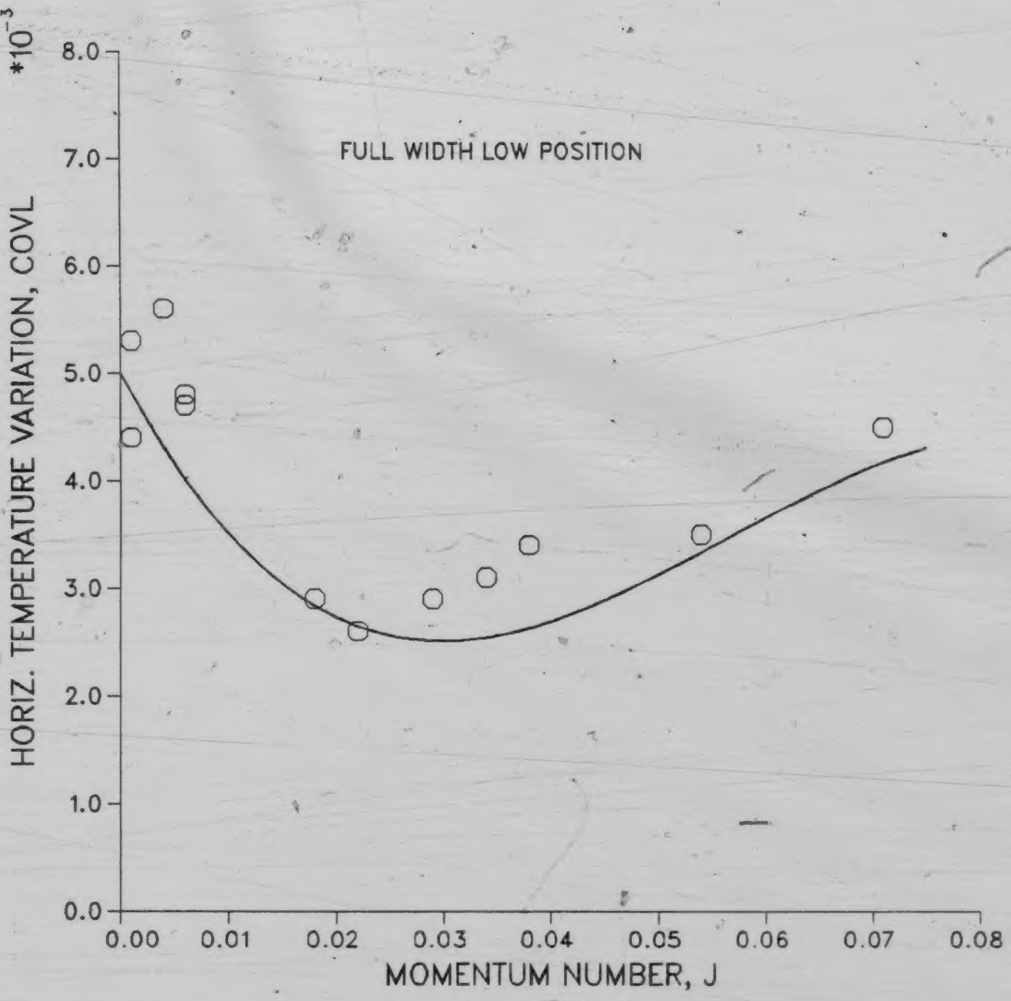

Figure 6.2 Plot of COVL versus J (full-width, lower inlet).

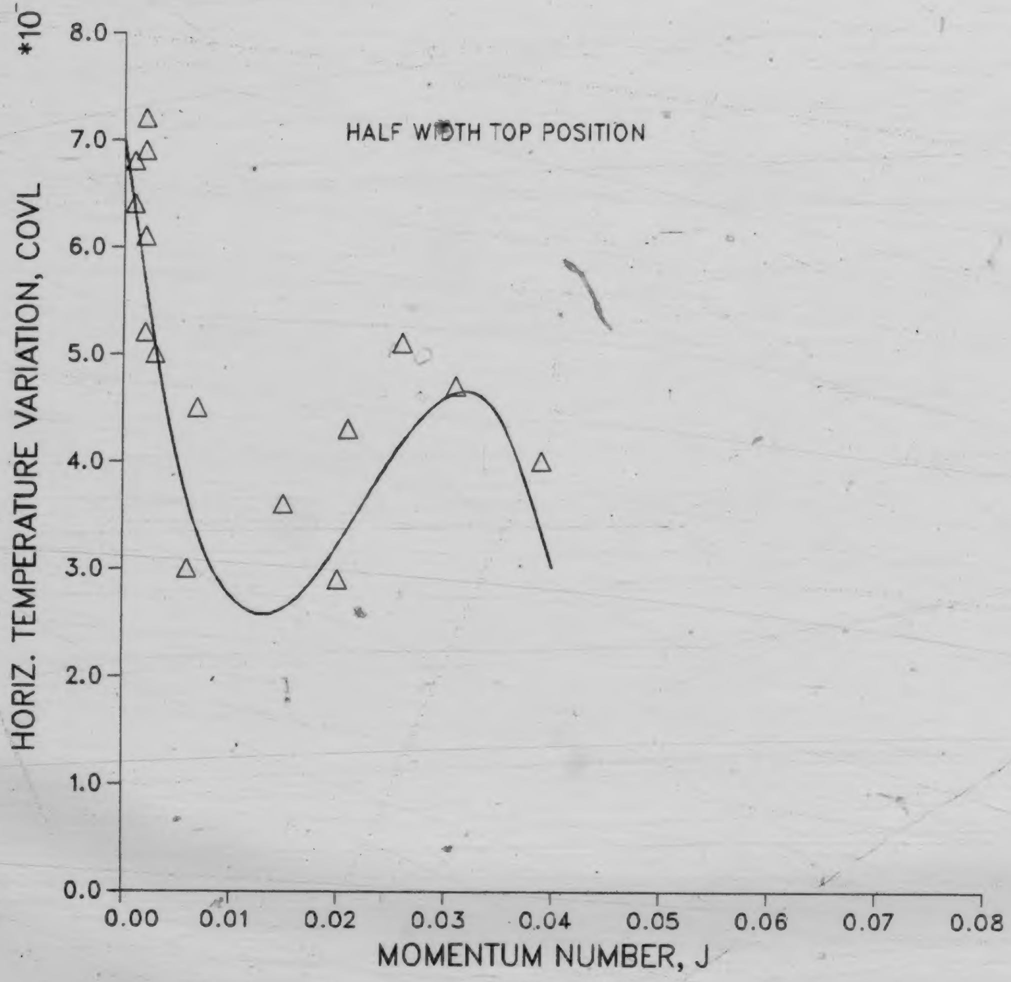

Figure 6.3 Plot of COVL versus J (half-width, ceiling inlet).

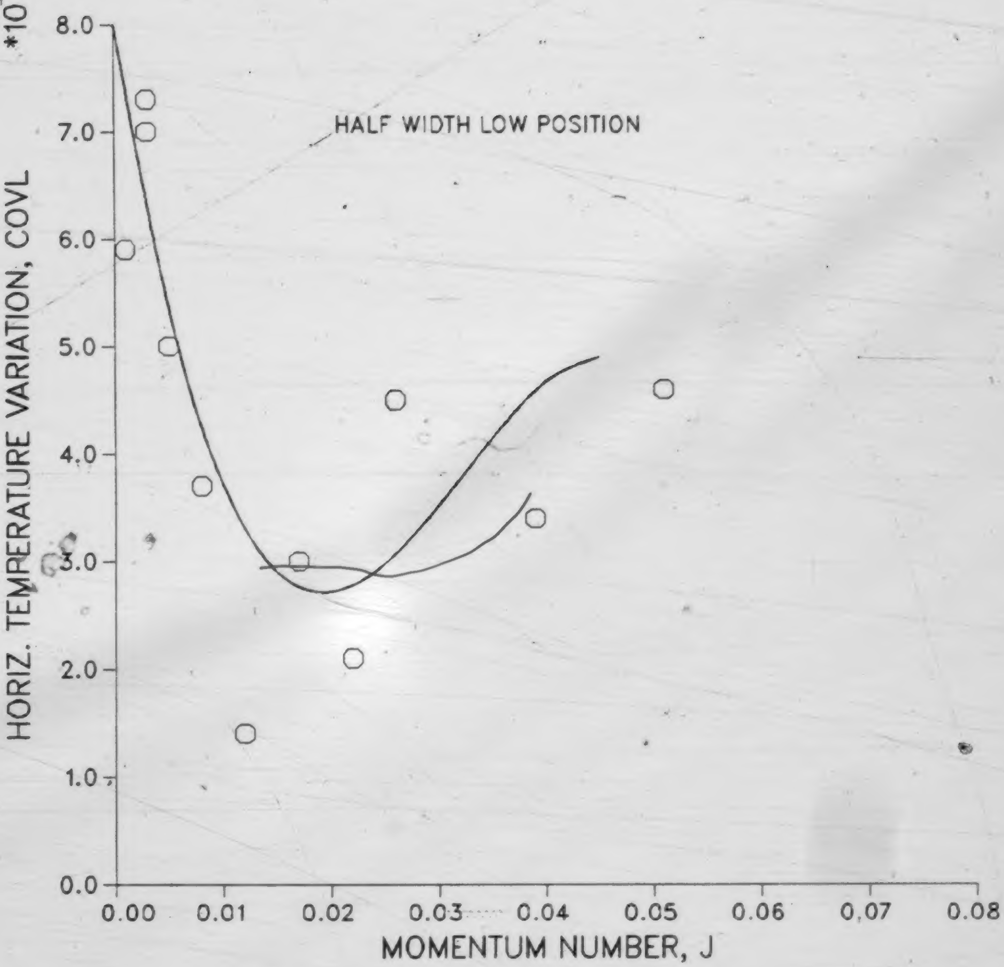

Figure 6.4 Plot of COVL versus J (half-width, lower inlet).

are given in Table 6.3 and are not necessarily the best fit equations but, rather, were used to quantify the minima that are exhibited by the data. The values of J at which these minima occur were determined by setting the derivatives of the cubic functions equal to zero and solving the resulting quadratic equations. They are as follows:

FT : $J = .002$
FL : $J = .030$
HT : $J = .013$
HL : $J = .019$

The fact that, in each case, there appears to be a value of J for which the variation in temperature is minimised is, in itself, significant. The implication of this result is that, for mixing and uniform supply of fresh air, there is an optimum ventilation rate rather than a minimum rate as proposed by Kaul *et al.* (1975) and Barber *et al.* (1982).

In fact, even the lowest momentum numbers measured were greater than the minimum values proposed by the above authors. This is noteworthy since observations and the photographic record indicated that the mixing effect of these jets was minimal, and primary eddies were not set up as predicted by the momentum number criteria that have been proposed. These criteria were developed for isothermal jets, and the results reported here seem to indicate that different criteria are required for non-isothermal conditions.

TABLE 6.3: CUBIC EQUATIONS RELATING COVL AND J.

INLET	EQUATION	R^2
FT	$COVL = 0.002+0.013J+3.76J^2-51.2J^3$	0.57
FL	$COVL = 0.005-0.19J+4.33J^2-25.6J^3$	0.81
HT	$COVL = 0.007-0.79J+42.85J^2-639.8J^3$	0.77
HL	$COVL = 0.008-0.64J+23.68J^2-244.2J^3$	0.69

The minima identified with the cubic regression functions may be taken as indicators of such criteria. For comparison, the minimum value of j recommended by Kaul *et al.* (1975) was 10^{-2} N/m³ which, when made non-dimensional, transforms into a value of $J \simeq 7.4\times10^{-4}$ for the air densities used in these experiments. This value is less than half of that required to give the minimum temperature variation for the full-width ceiling inlet which, itself, was an order of magnitude smaller than that for the other inlets.

The results from the full-width, ceiling inlet differ from those of the other inlets, not only in the much lower value of J required for minimum temperature variation but, also, in the generally lower level of variation over the range of J. These differences may be explained by the greater tendency of jets from the full-width ceiling inlet to adhere to the ceiling.

Low velocity jets from the other inlet configurations tended to drop within the first 0.5m of entry. At very low flow rates these jets would be dissipated rapidly and have little effect on temperatures at lower levels in the airspace. With a slight increase in flow rate, the jets would have sufficient energy to affect the lower level temperatures, thereby giving the peak coefficients of variation at low values of J. As the flow rate increased, the jets increasingly tended to remain elevated and to dissipate in the upper part of the airspace, thereby giving a decrease in the coefficients of variation. Beyond the COV minimum, primary circulation patterns and the spreading of the temperature profile combined to bring colder air into the lower airspace further from the inlet. This resulted in an increasing coefficient of variation.

Of the observed ceiling jets from the full-width inlet, only one had sufficiently low momentum to drop to the floor within 0.5m of entry. The coefficient of variation decreased over a much narrower range of J (Figure 6.4) since the Coanda effect became significant at lower flow rates than for other inlets and had the effect of shifting the coefficient of variation minimum to the left. Because the jets from this inlet were held in the upper airspace, especially at low velocities, the temperature variations were lower than with the other inlet configurations.

6.6.2 Vertical temperature distribution

The vertical temperature distribution was assessed using the group of sensors located 5m from the inlet wall. Again, coefficients of variation were calculated and these are plotted against J in Figures 6.5 to 6.8. Unlike those of

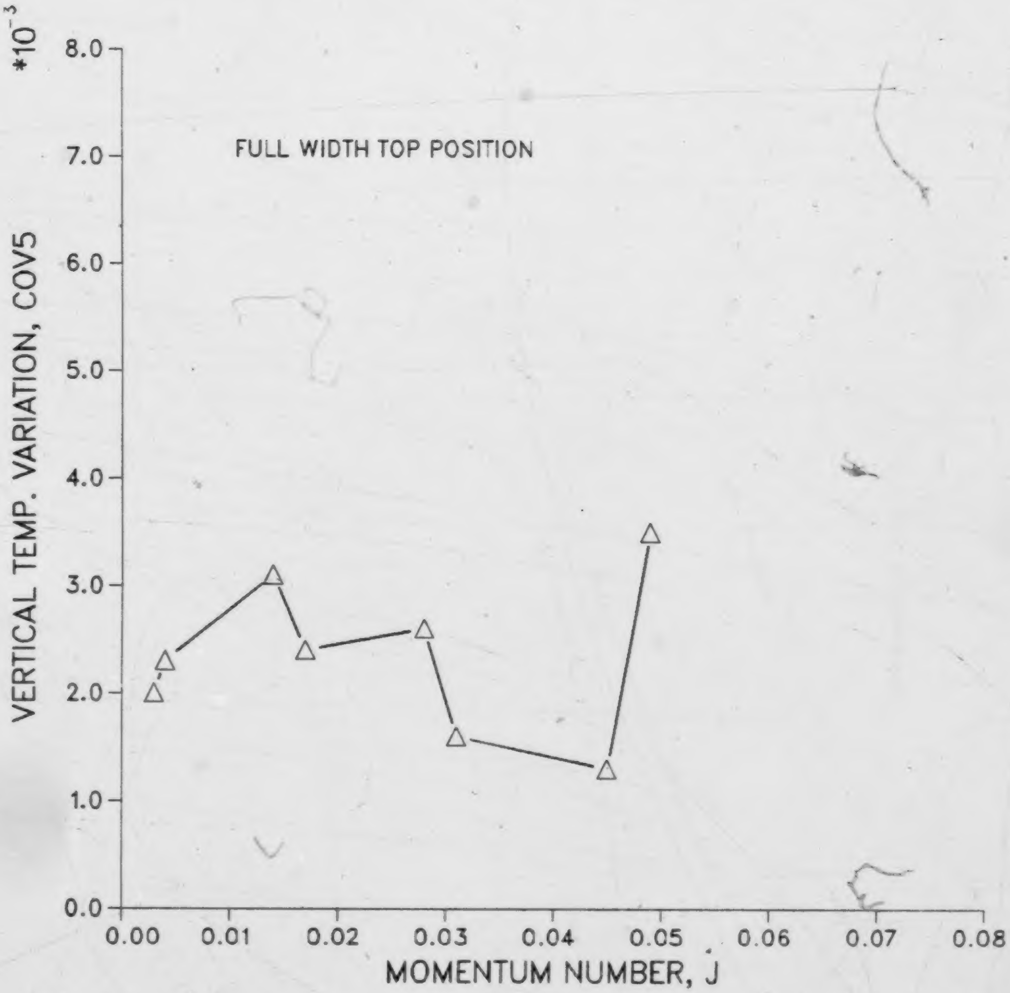

Figure 6.5 Plot of COV_5 versus J (full-width, ceiling inlet).

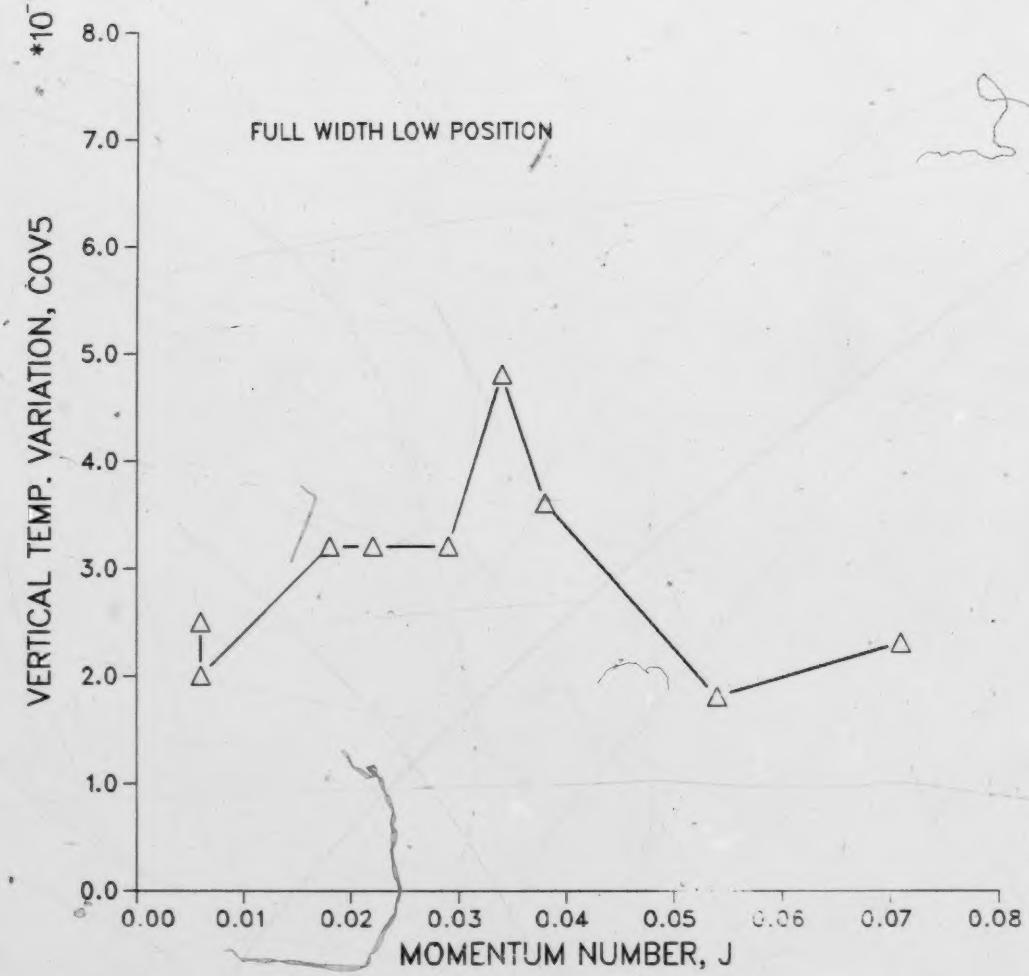

Figure 6.6 Plot of COV_5 versus J (full-width, lower inlet).

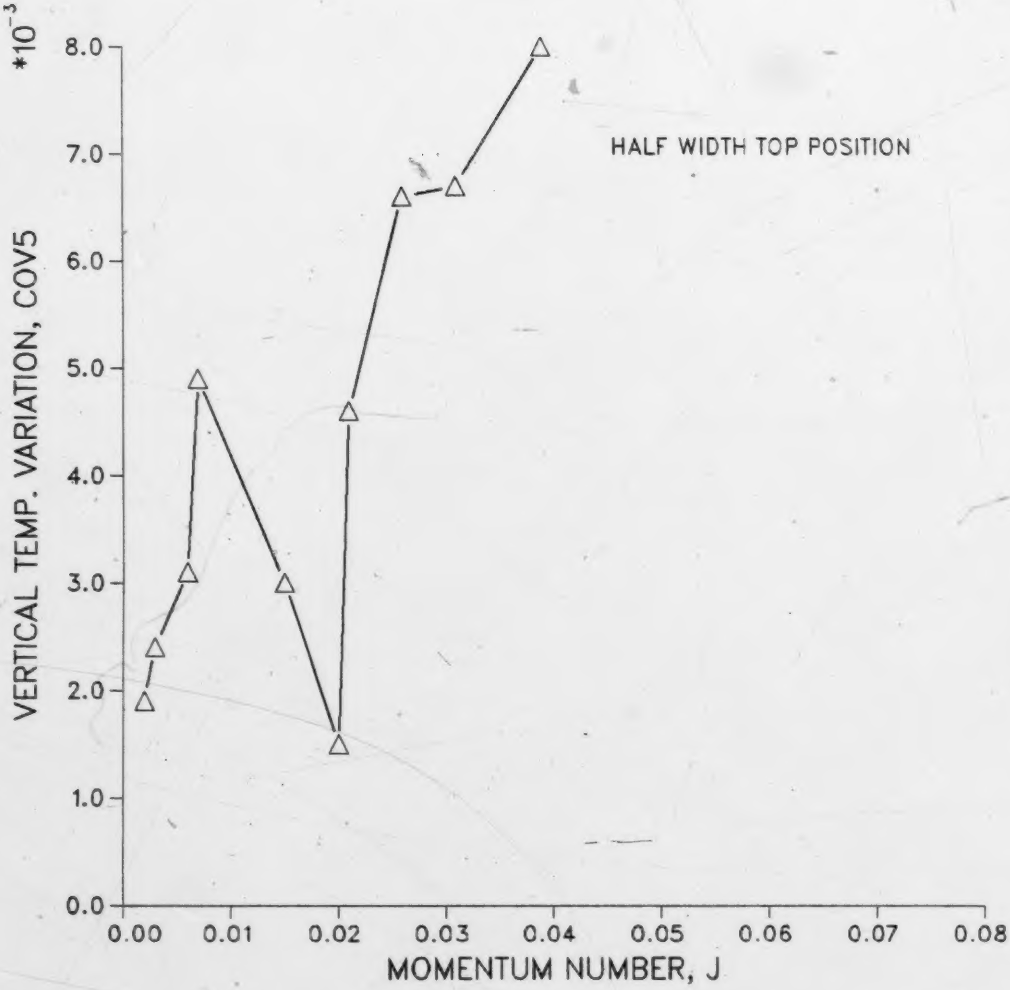

Figure 6.7 Plot of COV_5 versus J (half-width, ceiling inlet).

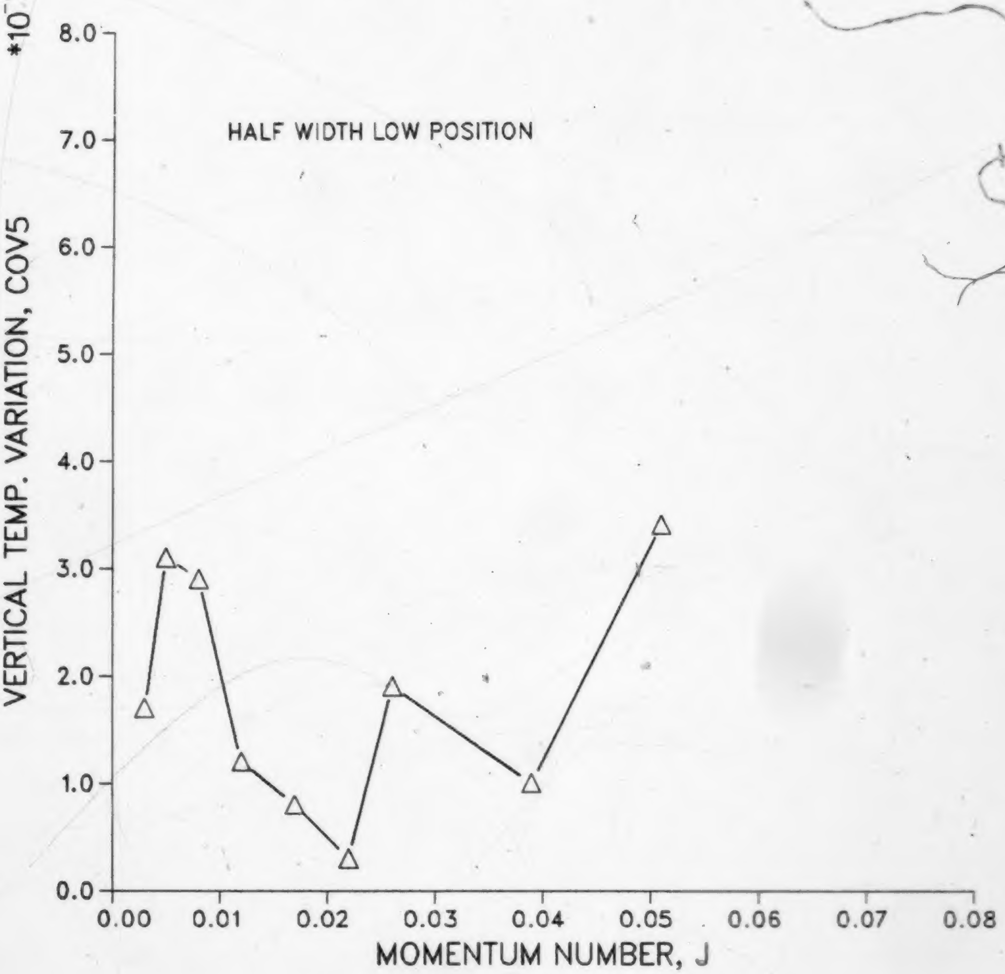

Figure 6.8 Plot of COV_5 versus J (half-width, lower inlet).

the horizontal temperature variation data, these plots show no coherent pattern and no regression curves have been fitted to the data.

The data are distorted by the fact that, of the jets with sufficient energy to penetrate to the line of sensors, some would have been adhering to the ceiling while some would have separated. The temperature profiles of separated and adhering jets would be of different shapes and, therefore, not comparable in this manner.

The jets least affected by attachment to the ceiling were those from the half-width inlet at the lower position. The data from these jets (Figure 6.8) does suggest a minimum variation in the vertical temperature distribution at values of J similar to those that gave minimum horizontal temperature variations. This suggestion is also apparent from the data for the half-width inlet in the top position, but is not apparent for the two full-width inlets.

6.6.3 Entrainment ratios

Although the temperature profile of a jet is wider than its velocity profile, the similarities between the two suggested the use of temperature to obtain an indication of the relative entrainment characteristics of the jets studied. The entrainment ratio of free isothermal jets is a function of the velocity ratio U_0/U_m and is greater for axial jets than for plane jets by a factor of approximately $\sqrt{2}$ (Section 2.1.4). On this basis, the ratio T_0/T_s was

TABLE 6.4: LINEAR EQUATIONS RELATING T_0/T_5 AND J.

INLET	EQUATION	R^2	MEAN T_0/T_5
FT	$T_0/T_5 = 0.911+0.802J$	0.91	0.930
FL	$T_0/T_5 = 0.927+0.387J$	0.44	0.941
HT	$T_0/T_5 = 0.920+1.013J$	0.73	0.941
HL	$T_0/T_5 = 0.947+0.513J$	0.85	0.957

proposed as an indicator of entrainment. This ratio was calculated for all normal tests and is plotted against J in Figures 6.9 to 6.12. Data for low velocity jets that did not penetrate 5m into the airspace are not included in these plots.

The trend of the data, for all inlets, is to increase with J and, consequently, the best-fit linear regression lines have been superimposed on the data. As with the plots of COVL against J these are not necessarily the best-fit curves but are used to provide a basis of comparison between the data from the different inlets. The equations to these regression lines are shown in Table 6.4 together with the mean values of T_0/T_5.

In general, the results show that the more "free" the jet, the worse the air entrainment and the greater the decrease in entrainment with flow rate. The means give an indication of the relative entrainment characteristics of each inlet. The worst entrainment occurred with jets from the lower, half-width inlet while the best entrainment occurred with the top, full-width inlet. While the other two inlets have the same mean, if these were corrected for the

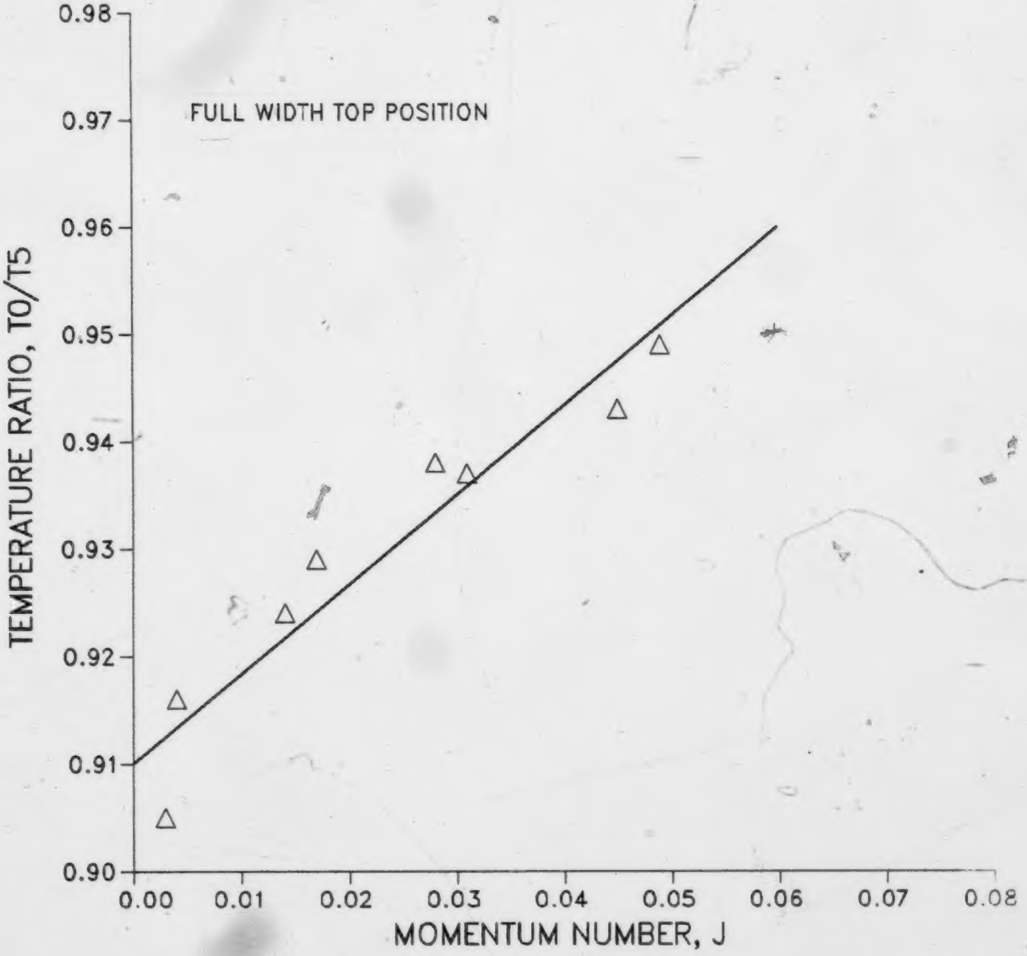

Figure 6.9 Plot of T_0/T_5 versus J (full-width, ceiling inlet).

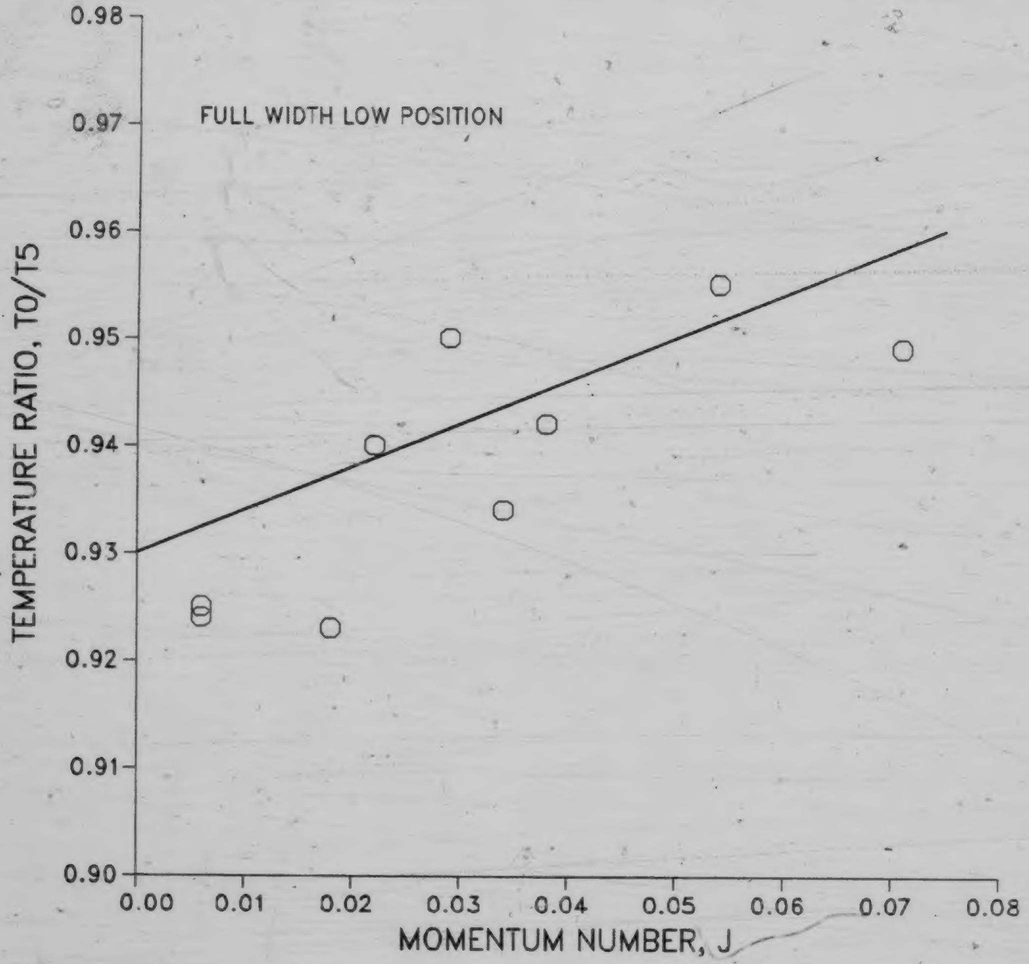

Figure 6.10 Plot of T_0/T_5 versus J (full-width, lower inlet).

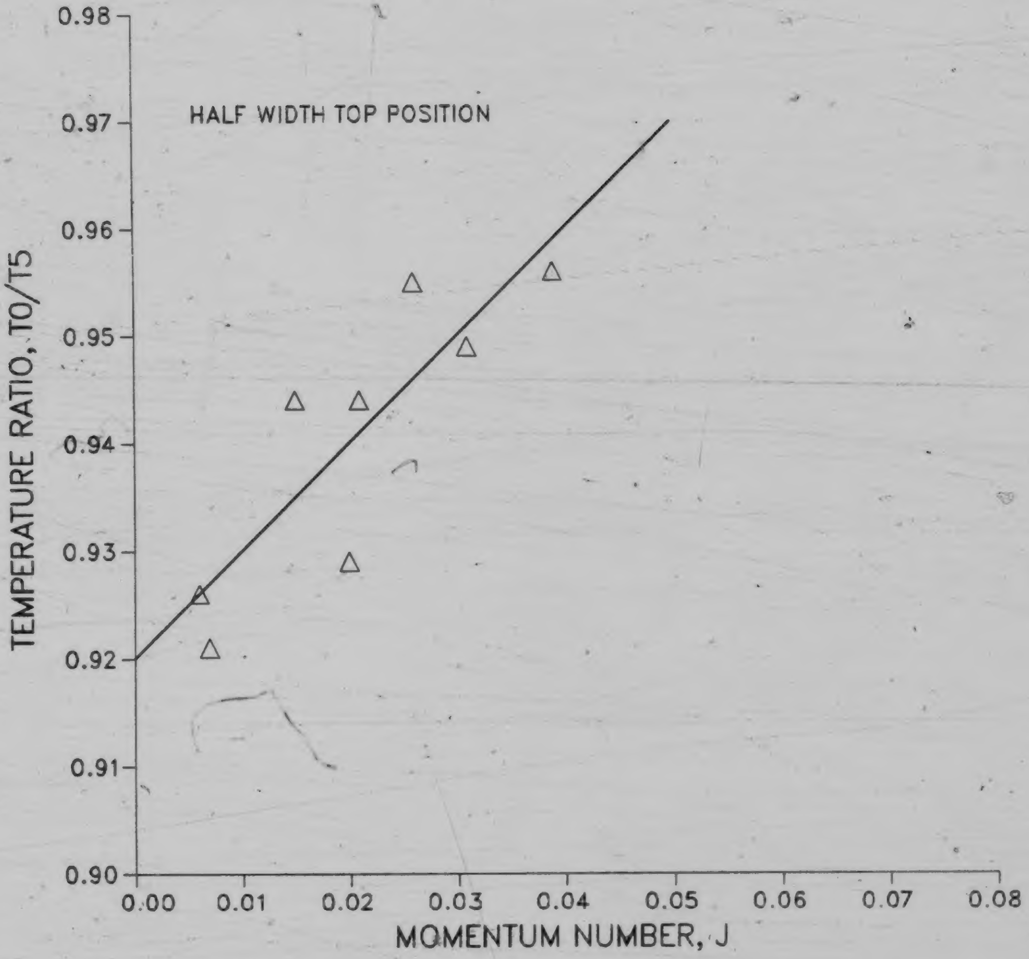

Figure 6.11 Plot of T_0/T_5 versus J (half-width, ceiling inlet).

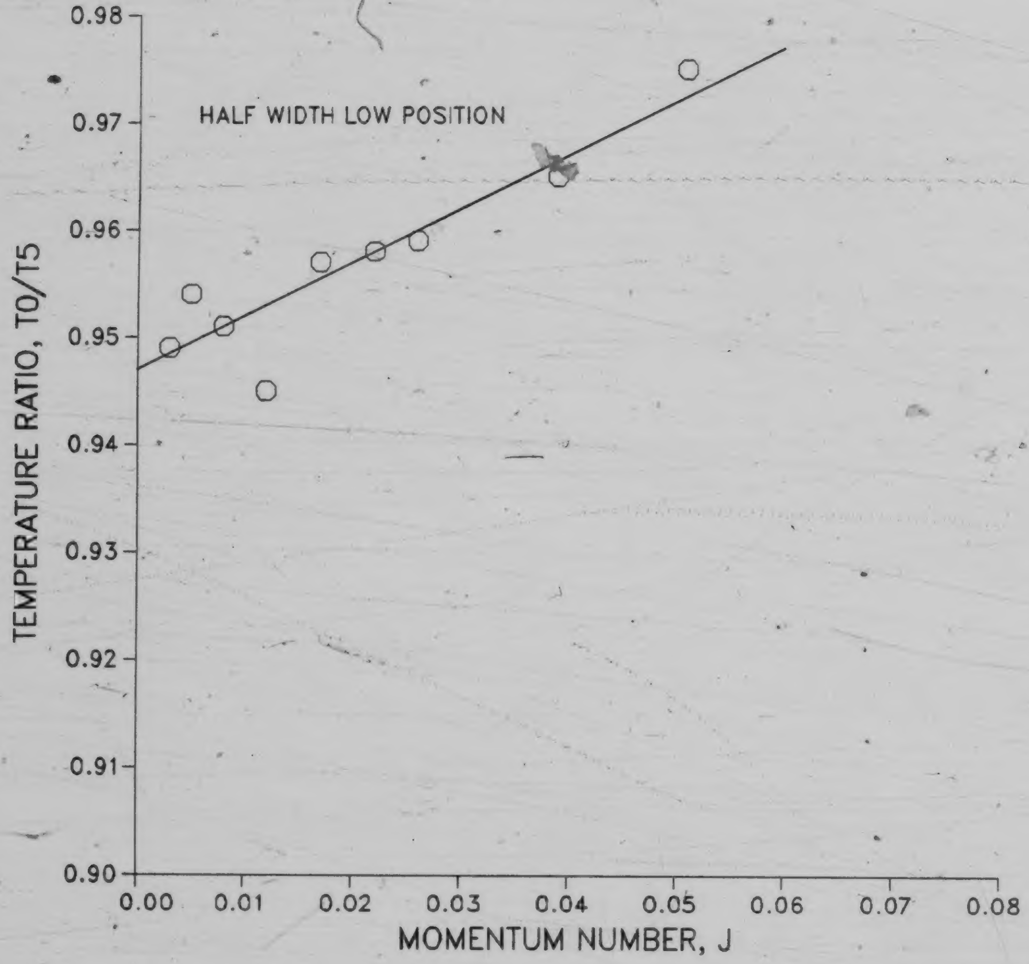

Figure 6.12 Plot of T_0/T_5 versus J (half-width, lower inlet).

difference in range of J, the top half-width inlet would exhibit inferior entrainment than the lower full-width inlet. These observations are completely opposite to the trend expected from established knowledge of entrainment in plane and axial jets and the effect of solid boundaries on entrainment.

Since the means of T_0/T_5 follow the same trend as the tendency of jets from the various inlets to drop, and since this is related to the Coanda effect, T_0/T_5 appears to be influenced more by heat exchange between the jet and the ceiling than between the jet and the room air. The slopes of the regression lines tend to support this theory since jets from the two full-width inlets, where the flow per unit width of heat exchange area is less, exhibit less deterioration in "entrainment" than the corresponding half-width inlets. The general deterioration in "entrainment" is due to the cooling of the ceiling during the course of the series of tests which were carried out in order of increasing J.

The fact that the slopes of the regression lines are lower for the low inlet positions could be due to partial compensation of the decrease in ceiling heat exchange by actual entrainment of room air. This would occur with all inlets but the effect would be more noticeable with the lower inlets.

The ratio T_0/T_5 does not appear to be suitable for evaluating the actual entrainment performance of the various jet types. However, the above hypothetical discussion points to further areas that could be investigated with relation to modifying the temperature of inlet air as it enters the ventilated space. Evaluation of air entrainment in the jets could be accomplished by means of velocity measurements or the use of more extensive temperature measurements at a location closer to the inlet wall.

7. DESIGN IMPLICATIONS

7.1 Archimedes Number Criteria for Jets

Examination of all the temperature-derived trajectory plots indicated that all jets with a drop coefficient, Z, greater than 0.5 fell to the floor within 0.5m of entry. Also, all those jets with Z greater than 0.25 fell at least 1m within 1.5m of entry. Thus, depending on what value of Z is considered acceptable, design values of Ar may be determined from the regression equations of Table 5.1. Some sample values are tabulated in Table 7.1 for each inlet configuration and for the two values of Z mentioned above.

Thus, if a design required that Z be kept less than 0.25, then the maximum values of Ar would be similar for the two inlets at the ceiling and for the two removed from the ceiling. The values reflect the tendencies of jets from the two locations to drop and the value of Ar=30 (Ar_d=16), proposed by Randall and Battams (1979), would be applicable to ceiling inlets while that of Ar=20 (Ar_d=10) would be more appropriate for the lower inlets.

However, the requirement that Z be less than 0.25 is, perhaps, too stringent for many ventilation systems, where it is sufficient simply to prevent a jet dropping to the floor on entry. In these cases, the less stringent requirement of $Z<0.5$ could be quite acceptable and would allow considerably higher values of Ar. For instance, on the basis of the results of these experiments, Ar values of 50

TABLE 7.1: MAXIMUM Ar FOR Z<0.25 AND Z<0.5.

INLET CONFIGURATION	Z<0.25	Z<0.5
FT	30	60
FL	22	53
HT	32	55
HL	22	39
ALL DATA	27	53

(Ar_d=27) could be tolerated for all inlets, except those removed from both ceiling and walls, where a maximum value 40 (Ar_d=21) would be appropriate.

The general agreement of the observed jet behaviour with the results of Randall and Battams (1979) indicates that Archimedes number criteria may be applied over a wide temperature range. Extrapolation to cover inlet temperatures as lowas -35°C does not seem unreasonable.

7.2 Mixing Criteria

Analysis of horizontal temperature distributions in the ventilated room (Section 6.6.1) indicates that, even if the trajectory criteria given above are satisfied, mixing and uniformity of air distribution in the lower airspace may be impaired if Ar is too small. Optimum mixing occurred at different values of J(or Ar), depending on inlet type, while the variation of temperature associated with these flow rates depended also on the inlet type.

Although optimum values of Ar could be applied for each type of inlet, for design purposes a general rule or single value of Ar that could be applied universally, regardless of inlet type, would be desirable. Examination of Figures 6.1 to 6.4 and the equations of Table 6.3 leads to the conclusion that a value of $Ar=10$ ($Ar_d=5$) would give good mixing performance in all cases. This corresponds to a value of $J=0.013$ which, when substituted in the equations of Table 6.3, would give a coefficient of variation of temperature of approximately 0.003.

The above discussion is based on observed, albeit limited, experimental evidence. However, the experimental observations were carried out under idealized conditions and may not translate easily into practical designs. An analysis of what these criteria mean in terms of actual inlet design and operation is, therefore, appropriate.

7.3 Inlet Design

One of the most widespread inlet designs in current use in animal housing is that of a continuous slot discharging at ceiling level. These slots extend for the entire length of the ventilated space and may be located along the walls discharging inwards or, at the centre of the ceiling, discharging towards the walls. Usually, there is some provision for varying the width of the inlet, h, in response to varying ventilation requirements. A minimum width is required during periods of minimum ventilation which, in turn, usually coincide with low inlet air temperatures. The actual minimum width of inlet required is of interest since this defines the required accuracy of construction and control of the inlet.

In order to get some idea of typical requirements, data were used from environment monitoring studies of a broiler barn (Leonard *et al.*, 1984b), a layer rearing barn (Glennon *et al.*, 1984), a laying barn (Feddes *et al.*, 1984) and a swine finishing barn (Clark *et al.*, 1984). All of the barns concerned had continuous slot inlets. From these studies data were obtained on the minimum ventilation rates monitored together with inside and outside temperatures. Since some of the barns had supplementary heating systems, the use of Archimedes number criteria based on exhaust temperatures was more appropriate than the use of those based on a heated surface temperature. Thus, equation 6.2 was used to calculate the inlet openings required to satisfy the trajectory criterion (Ar_d=27) and the mixing criterion (Ar_d=5). The results of these calculations are shown in Table 7.2.

The largest opening satisfying the trajectory criterion was 1.2 mm while, when the mixing criterion was applied, the largest opening was 0.22 mm. On other barns, required openings were at least an order of magnitude smaller. Openings of this size are impractical to construct or control and, in all likelihood, would be dominated in effect by other openings in the structure such as those around doors. In the barns from which the data were obtained, the ventilation inlets were set at much wider openings and, in

TABLE 7.2: OPENING WIDTHS REQUIRED FOR FULL-WIDTH SLOTS UNDER MINIMUM VENTILATION IN ACTUAL BARNS.

BARN TYPE	VENT. RATE m^3/s	TEMPERATURES (°C)		OPENING (mm)	
		INLET	EXHAUST	$Ar_d<27$	$Ar_d<5$
REARING	0.62	-7	27	0.098	0.018
BROILER	0.26	-13	30	0.015	0.003
LAYING	1.79	-9	13	1.2	0.22
SWINE	0.78	-20	15	0.052	0.097

the laying barns, vertical temperature gradients of approximately 1°C/m were observed. In the other barns, the effects of the wide openings were modified by the location of supplemental heat sources and air mixing fans.

Another important factor to consider is the characteristics of the ventilation fan to be used. Considering the case of the laying barn in Table 7.2, which required the largest ventilation openings, an estimate was obtained of the pressure that a fan would have to work against under the specified conditions. This estimate was obtained by treating the inlet as a simple orifice for which the relationships between flow, pressure and orifice area are well known (Ower and Pankhurst, 1977). The simplified expression for pressure difference, P, that was used may be written as:

$$P = Q^2\rho/2(C_dA)^2 \qquad 7.1$$

After substitution of the pertinent values, the required pressure difference was calculated to be 1.67 kPa

(170 mm H_2O) to satisfy the trajectory criterion and 49.6 kPa (5057 mm H_2O) to satisfy the mixing criterion. Since ventilation fans are often rated at 31.1 Pa, the achievement of these pressures with standard equipment is obviously unrealistic. Also obvious is the need for a rational design procedure that will avoid such glaring inconsistencies.

There are, in fact, three sets of conditions that must be satisfied simultaneously. These are the Archimedes number criterion, the system characteristics and the fan characteristics. The Archimedes number criterion is expressed mathematically in equation 6.2 and, in the absence of experimental data, equation 7.1 may be used to approximate the system characteristics. The fan characteristic that is of interest is the relationship between static pressure and airflow. This may be obtained from fan test data such as those published by the Prairie Agricultural Machinery Institute (e.g., PAMI, 1984). Such relationships may be approximated by a straight line over the range of normal operating pressures and, hence, the third design equation will be in the form:

$$P = I - EQ \qquad 7.2$$

where I and E are constants dependent on the particular fan.

Equations 6.2, 7.1 and 7.2 now may be solved for Q, P and A to determine the limiting operating conditions at which the Archimedes number criterion can be satisfied at a given inlet temperature T_0. Rigorous solution of these

TABLE 7.3: FAN TEST DATA (PAMI, 1984/85).

MAKE AND MODEL	EQUATION CONSTANTS		OPERATING RANGE (m^3/s)	
	I	E	Qmin	Qmax
ZIEHL 562-6	300	100	2.0	2.9
" 501-6	210	120	1.2	1.7
" 631-6	350	90	2.5	3.7
" 451-4	425	215	1.5	2.0
" 451-6	130	110	0.7	2.0
KOENDERS KV20	300	150	1.0	2.0
" KV18	250	190	0.7	1.2
" KV15	200	290	0.5	0.7
" KS18	260	190	0.7	1.2
CYCLONE 60AG0000	270	160	1.3	1.7
EMI WLA 4/50	310	150	1.5	2.0
PRAIRIE PRIDE TR12	140	200	0.5	0.7
" " TR18	160	70	1.9	2.4
" " TR24	180	80	1.6	2.3

equations, however, can give results that, while mathematically correct, are not achievable in practice. For example, solutions may include negative values of A and values of P that are more appropriate to vacuum pumps than ventilation fans.

Nevertheless, if flow rates (or pressure differentials) are specified that are within the normal operating range of a given fan, the above equations can be applied to determine allowable inlet temperatures and required inlet areas. Using a computer, this procedure may be used to generate sets of curves such as those shown in Figures 7.1 and 7.2 for any given fan. These figures indicate the limiting conditions beyond which the criteria for the jet trajectory ($Ar_d<27$) and mixing ($Ar_d<5$) cannot be satisfied with the fan concerned. For example, Figure 7.1 indicates that, with a

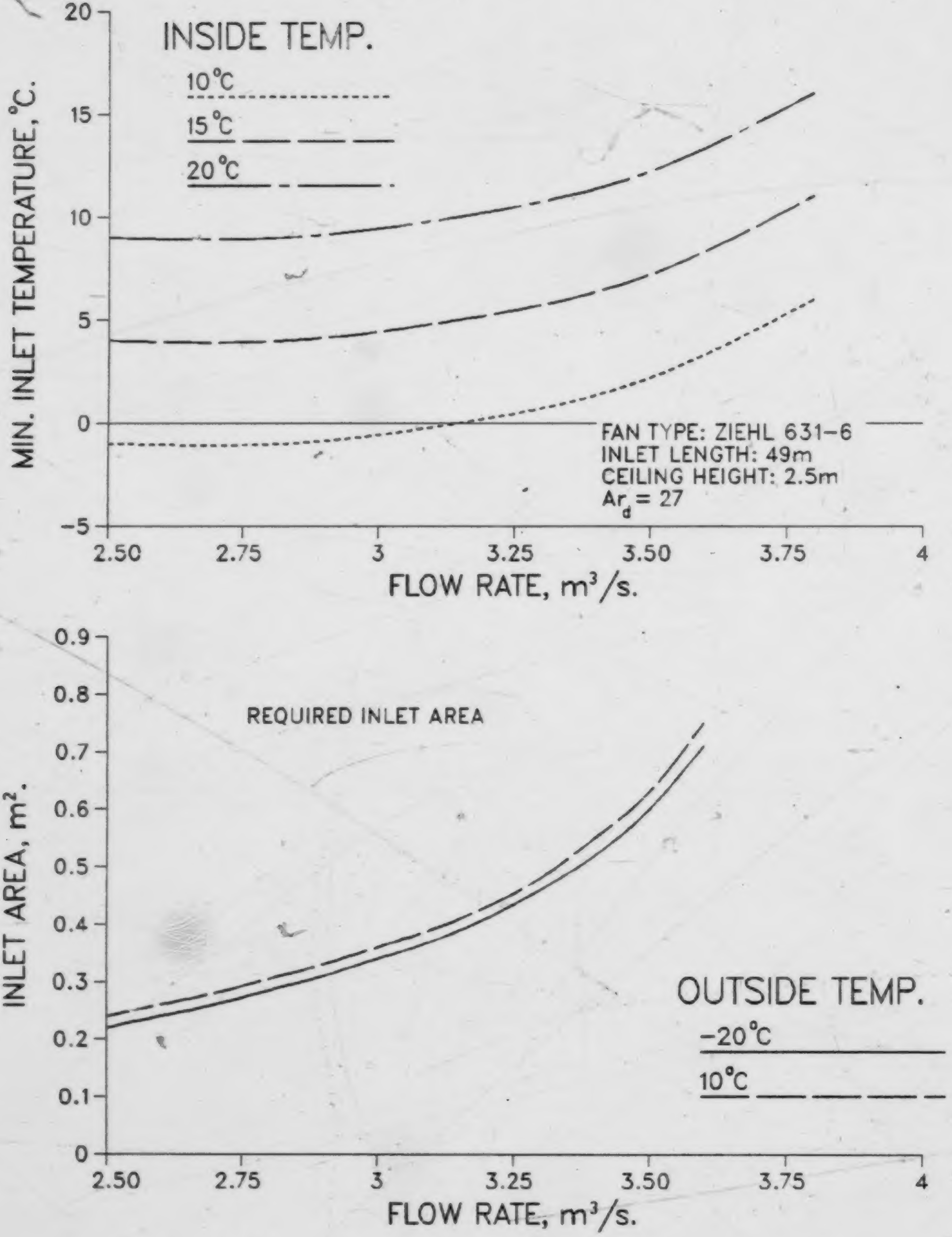

Figure 7.1 Plot of conditions to satisfy Ar_d<27

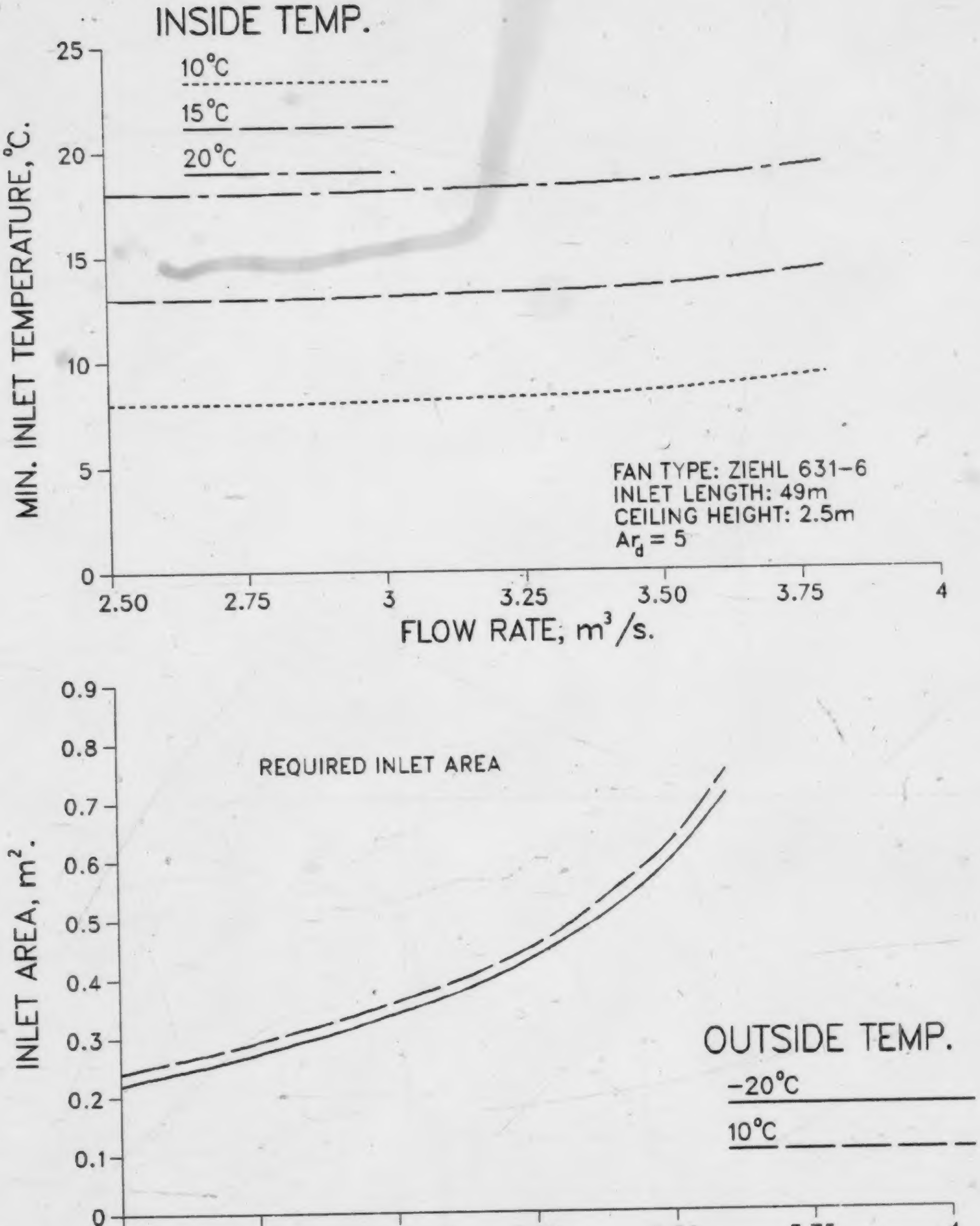

Figure 7.2 Plot of conditions to satisfy $Ar_d<5$

Ziehl 631-6 fan operating at constant speed, it is not possible to achieve $Ar_d<27$ when the inside temperature is 10°C (283°K) and the ventilation rate is 2.5 m^3/s if the inlet temperature is less than -1°C (272°K). Similarly, Figure 7.2 indicates that the inside and inlet temperatures must be very close to meet the much more stringent requirement of $Ar_d<5$.

Assuming that the temperature requirements can be met, the above figures also indicate the inlet area required to produce the required flow rate for the constant speed fan. For variable speed fans, a set of curves would be required for each speed setting since, for each speed, the values of the constants in equation 7.2 would be different.

Analyses similar to that described above were carried out using published data from 14 fan tests (PAMI, 1984/85) which are summarised in Table 7.3. These fans were assessed for possible application to the ventilation conditions and requirements of the laying barn in Table 7.2. None of these fans, under the given temperature conditions, could satisfy either of the Archimedes number criteria at the given ventilation rates when used either singly or in parallel. Thus, while systems could be designed to satisfy the criteria using high-pressure fans and aerodynamically shaped inlets, negative pressure ventilation systems, using conventional fans and inlets, are unlikely to satisfy the Archimedes number criteria at minimum ventilation rates and low inlet temperatures.

The difficulty of satisfying Archimedes number criteria under Prairie winter conditions was understood, although not fully described, by Barber *et al.* (1982). These authors pointed out that, in practice, at least partial solutions to the problem have been achieved by the use of air mixing fans and recirculation systems. In addition, they proposed the use of preheating the inlet air in order to decrease the effective value of the Archimedes number.

The above authors suggested the use of plenums for preheating the air and, indeed, this method has been adopted in practice where outside air is drawn into a central corridor before discharging into ventilated spaces on either side. In view of the results pertaining to entrainment ratio that have been discussed in section 6.6.3, an alternative method of "preheating" the inlet air would be to heat the ceiling in the vicinity of the air inlet. Heat exchange between the ceiling and the air could be promoted by attaching thin fins to the ceiling, running parallel to the air flow, in order to increase the heat exchange area.

An indirect method of heating the ceiling, which is used in some barns, is by means of hot water pipes mounted on a rack, parallel to the ceiling but below the air inlet. With this arrangement, heat is transferred to the ceiling by radiation and then to the top of the jet by convection. At the same time heat is transferred to the bottom of the jet, also by convection. Further experimental work is required to determine the relative effectiveness of, and values of relevant design parameters for, these methods.

Assuming that a suitable pre-heat system were available, a system could be built that would be controlled on the basis of the outside, inside and inlet jet temperatures. The control of such a system is described in the following section but, although preheating techniques are feasable, they are not appropriate to situations, such as poultry laying barns, where supplementary heating normally is not supplied. A design is required that does not involve the addition of heat.

The limiting factor in the design of conventional systems is the performance characteristics of the fans that normally are used. Whilst these fans are capable of providing large flows at low pressures, they are unsuitable for providing the low flows at high pressures that are required to satisfy Archimedes number criteria under minimum ventilation conditions during the Prairie winter. An alternative system is proposed in which a high pressure fan is used to provide these minimum ventilation requirements.

This fan, which would probably be of centrifugal design, would discharge into a pressurised plenum running the length of a barn, possibly in the attic space. From the plenum, the pressurised air would enter the barn through inlets designed to produce flows satisfying Archimedes number criteria. Air would exit through the backdraught shutters of conventional propeller fans. The design of suitable inlets, especially if they were to be adjustable, would require some research and innovation but, nevertheless, such a system would have some significant advantages including:

1. Some preheating of inlet air as it passed through the fan.
2. No need for supplementary preheating of the inlet air.
3. The pressurised part of the system would be isolated and would use dry, cold air. This would eliminate the problems of moisture diffusion into insulation that are associated with positive pressure ventilation.
4. Relatively simple retro-fitting to existing barns.
5. Simplicity of control.

7.4 Control

Regardless of the type of system used, the control of ventilation in animal housing should always embody certain features such as the interlocking of fans, inlets and supplementary heating systems. Beyond this level of commonality, however, the type of control sytem and the strategy or logic used in the implementation of the controls may vary widely, even between physically similar systems, depending on factors such as management practice and expertise and the desired level of technical sophistication. The following discussion, therefore, presents conceptual possibilities, rather than rigid outlines, for the design of the systems discussed in the preceding section.

In the case of the system based on preheating inlet air, the assumption is made that the controlled system would consist of a number of identical single-speed fans with inlets consisting of a number of variable-opening slots. Each fan would be associated, for control purposes, with one slot. In order for the fans to operate only over an efficient pressure range, the slot lengths would be determined on the basis of the fan characteristics (e.g., using curves such as those in Figures 7.1 and 7.2) to provide the minimum area required at a practical value of opening (h). The maximum opening required then would be determined from the maximum area required.

At minimum ventilation rates in cold weather, one fan/inlet unit would provide the total ventilation required with the inlet air being preheated. The energy supply for preheating would be regulated on the basis of the jet temperature to satisfy the Archimedes number criteria and the inlet would be open to the position giving minimum inlet area. All other inlets would be closed but, to provide uniformity of air distribution over time, single fan/inlet units could be run cyclically or, alternatively, different slots could be opened on a rotational basis while the same fan provided air movement.

If the inside temperature rose beyond a preset limit, more ventilation would be required and additional fan/inlet units would be brought into play with inlets open to the minimum area and preheat in operation. The system would continue to operate in this fashion until the outside temperature was high enough to allow the Archimedes number criteria to be satisfied without preheating the inlet jet. At this point, further ventilation demand would result in an increase in inlet area rather than the activation of additional fans. All operating inlets would be opened together and, only when they were fully open, would further fan/inlet units be activated.

An advantage of the above scheme is that it does not depend on the measurement of a pressure difference which can be affected by winds and thereby lead to instability in the system. Temperatures, on the other hand, are easier to measure and tend to vary much more slowly than pressure differentials. Consequently, a temperature-based control system is likely to be cheaper and inherently more stable.

A disadvantage of the scheme is that the control logic is relatively complex when compared with conventional, thermostat-operated systems. The complexity is a result firstly, of the need to provide complete interlocking of the fan, inlet and heating systems. Secondly, the complexity arises out of the need to satisfy simultaneously the requirements summarised in equations 6.2, 7.1 and 7.2.

Nevertheless, although the required control strategy is more complex than that normally found in animal housing, it is not complex when judged in absolute terms. In principle, such a scheme could be implemented quite easily using a microprocessor-based controller, assuming that the pressure/flow characteristics of both inlets and fans were known. Further work is required to develop cost-effective hardware for such a system together with suitable software.

The system based on the use of a high-pressure fan to provide minimum ventilation rates also would require slightly more control sophistication than is normal in animal housing. However, as with the heated-inlet system, this sophistication is within the capabilities of existing technology and could be implemented with a modest amount of further work.

The high-pressure fan would be required to operate only over that range of outside temperatures that precluded propeller-fan operation. Over this range, the maximum opening of the high-pressure inlets would be controlled on the basis of plenum temperature to satisfy the Archimedes number criteria.

When the outside temperature was sufficiently high, the high-pressure system would be shut off and a conventional, propeller-fan system would take over. This system would be controlled in the same way as described for the heated-inlet system above except that control of supplemental heat would not be required.

8. SUMMARY AND CONCLUSIONS

The experiments described in previous sections were carried out to address the aims of this project as detailed in section 2.3.4. The results of the experiments, together with the analyses and discussion that is detailed in subsequent sections, give rise to the following conclusions:

8.1 The Drop Coefficient

A general equation to describe the trajectories of confined cold air jets was not defined. Nevertheless, a measure of the degree to which jets dropped was provided by the drop coefficient, Z. Evidence was shown to exist of linear relationships between Z and an Archimedes number, Ar, with the slopes of these lines being dependent on the inlet position and width. On this basis, Z appeared to be a useful tool in the comparison of inlets and in describing the behaviour of non-isothermal ventilation jets.

8.2 Criteria for Jet Trajectories

Jets that dropped at least 1m within 1.5m of entry had drop coefficients greater than 0.25 while, for those that dropped to the floor within 0.5m of the inlet wall, Z was greater than 0.5. If Z were to be limited to values less than 0.5, the maximum allowable values of Ar would be 30 and 20 for inlets at the ceiling and 30mm from the ceiling, respectively. This result is in agreement with the work of Randall and Battams (1979).

The proposal is made, however, that the above requirement may be too stringent and that Z need be limited only to values of less than 0.25. If this were the case, Ar values of up to 50 would be allowable for all inlets, except those removed from both ceiling and walls, where Ar should be limited to values of less than 40. These values are applicable for inlet air temperatures as low as -35°C.

8.3 Effect of Heated Area

The effects of the extent and location of exposed heated area within the room were found to be small but generally in agreement with the observations of previous researchers (Randall and Battams , 1979; Mullejans, 1966). Jets showed a decreased tendency to drop as the heated area was reduced. This tendency was more noticeable with low-velocity jets. There was some evidence to indicate that jets were most sensitive to changes in heated area occurring close to the inlet wall.

8.4 Modification of Archimedes Number

While Ar is a useful number, there is scope for work to be done towards simplificiation and clarification of its constituent geometric terms. In the interests of simplifying temperature terms, exhaust air temperature was shown to be a feasible and desirable alternative to the heated surface temperature previously used in the calculation of Ar. The resulting number, Ar_a, had values approximately half those of Ar and gave, if anything, a better linear correlation with Z.

8.5 Criteria for Air Mixing

The use of a momentum number, J, proposed by Barber *et al.* (1982), as a mixing criterion was shown to be superfluous by virtue of a clear relationship between Ar and J.

The degree of air mixing, evaluated by analysing the variation in temperature in the lower part of the ventilated space, was not independent of jet velocity. With each inlet configuration tested, an optimum ventilation rate for air mixing was apparent. These rates corresponded to values of J that were much larger than the criteria proposed by previous researchers (Kaul *et al.*, 1975; Barber *et al.*, 1982) using isothermal jets. For all inlet types, jets with Ar values of less than 10 would give good mixing performance.

8.6 Heat Transfer from the Ceiling

An attempt to assess the relative entrainment performance of jets from different inlet configurations by means of analysing centreline temperatures gave results that were the inverse of those expected. This discrepancy can be explained if substantial heat transfer from the ceiling to the jet is assumed.

8.7 Design Implications

Rational design of ventilation systems using the Archimedes number criteria requires that conditions specified by the fan characteristics, the inlet (or system) characteristics and the Archimedes number be satisfied simultaneously. Generally, this will not be possible when propeller-fans are used to provide minimum ventilation rates for animal housing under Prairie winter conditions.

Ways to overcome this problem using recirculation, pre-heat and high-pressure systems have been discussed. Two hypothetical systems, one using pre-heating of inlet air and fans uniquely associated with controlled inlets, and one using a high-pressure fan to provide minimum ventilation have been described. Such systems would embody control requirements of a complexity that would be suited to operation by computer or computer-based controller.

9. RECOMMENDATIONS FOR FURTHER WORK

9.1 Modification of Experimental Facilities

Despite the fact that the experimental facility proved adequate for the experiments described in this thesis, improvements could be made in a number of areas. Most of these improvements have been alluded to previuosly but, nevertheless, are listed below to provide a comprehensive picture of future requirements.

9.1.1 Thermistor circuits

In order to obtain sufficient resolution from the circuits used, a high excitation voltage was required. This resulted in excessive current through the thermistors which, in turn, caused "self heating" and gave rise to considerable calibration problems.

The deficiency in the thermistor circuits could be remedied by incorporating a constant current source to supply the thermistors. A convenient way of doing this would be to use one of the integrated circuits that are commercially available for this purpose. An example of such a device is the LM334Z (National Semiconductor Corp., Santa Clara, CA.).

9.1.2 Thermistor placement

In the experiments described above, the location of some of the trajectory-delineating thermistors was changed for different inlet locations. The rationale for doing this was to maximise the accuracy with which the jet centreline could be located. However, this objective was not necessarily realised and, in fact, the procedure resulted in some uncertainty about the trajectories in the upper part of the ventilated space. Also, changing thermistor locations inhibited the direct comparison of trajectories from different inlet locations.

In future work, therefore, the location of thermistors should be kept constant for all inlet types and locations. The problem of reducing the uncertainty of trajectories could be addressed by using more thermistors. This would involve multiplexing inputs to the data-logging computer or, alternatively, purchasing additional analog-to-digital conversion boards.

9.1.3 Air velocity probe array

The use of temperature sensors to delineate the trajectories has provided a good compromise between economy and performance. These sensors, however, did not prove adequate in the determination of entrainment ratios and could not, without considerable effort, be used to give an indication of air velocities in the room. On this basis, some consideration should be given to installing an array of low-velocity flow sensors in the experimental room. Such an installation could provide quantitative information on entrainment ratios and the degree of stagnation or turbulent mixing in the lower part of the air space. A commercially available system that has promising specifications is the Model 5410 Multichannel Flow Analyzer (DISA Elektronik A/S, Copenhagen, Denmark).

9.1.4 Heating pad water circulation

Although the heating pads provided an economical method for simulating the effect of animals in the ventilated space, this simulation would be enhanced by improving the surface temperature uniformity with respect to both time and location. This enhancement could be realised by connecting the pads with hose and circulating water through them with a small pump.

Circulation of the water would increase heat transfer from the heating elements, thereby decreasing the rate at which surface temperatures decayed and better utilising the capacity of the heaters. In addition, circulation of water among the pads would tend to provide uniform temperatures over the entire heated surface area.

9.2 Topics for Future Investigation

Whereas this thesis can claim to have answered some questions regarding the behaviour of cold air jets, other questions remain unanswered or have been raised. These questions vary in nature from the fundamental to the applied but, nevertheless, point to avenues for future investigation. Some of these avenues are presented below.

9.2.1 Trajectory equations

From the point of view of the designer attempting to provide functional and cost-effective internal layouts for animal housing, an equation, or set of equations, describing jet trajectories would be most useful. Whilst further, detailed analysis of the available data might furnish some approximate equations, additional data are required for a more rigourous approach. Such an approach would, ideally, involve the development and verification of computer models in a similar way to that taken by Fan and Brooks(1969) and Cederwall(1971) for analysis of effluent plumes.

The effects of room boundaries and other flow obstructions would complicate the mathematical models involved, however, and, except for the simplest cases, practicality may dictate a purely empirical approach based on physical models or further, full scale studies.

9.2.2 Limits of the Coanda Effect

The fact that inlet jets are attracted to the ceiling gives the building designer some latitude in the location of inlet structures. However, the limits of this latitude are not established and need to be investigated in order to determine a coherent design procedure.

Such an investigation would aim at establishing, for various inlet widths and geometries, the limiting combination of Archimedes number and ceiling-inlet distance beyond which jets would not become attached to the ceiling.

The existing experimental facility could be used for this work with a minimum of modification.

9.2.3 Development of a universal Archimedes number

The Archimedes number as used in this thesis is an expression of buoyancy and inertia forces acting on a ventilating air jet. Although attempts have been made to correct for the influence of room boundaries, the effects of inlet geometry and location are not accounted for. This has led to the necessity of specifying criteria for the control of jets removed from walls and ceilings that are different to those for either full-width or ceiling jets. Ideally, a single criterion could be used for all jets.

In order to obtain a single criterion, further work is required to quantify the effects of inlet geometry and location. The aim of such work, which would be complimented by the Trajectory and Coanda Effect investigations described above, would be to develop a form of Archimedes number that would embody inlet geometry and location factors. This could be used subsequently to define a single criterion for all inlet jets.

9.2.4 Heat transfer from ceiling

The failure of attempts to evaluate entrainment ratios for the various inlets using temperature data has been explained by assuming significant heat transfer from the ceiling to the air jet. Because data were not available on ceiling temperatures, this hypothesis could not be tested. Instumentation should, therefore be installed to investigate this mode of heat transfer. Experiments then could be carried out to evaluate the effect of different ceiling types and heating methods on the preheating of incoming air.

9.2.5 Mixing in the ventilated space

Two aspects of air mixing have not been investigated fully in this work. Firstly, the relative efficiencies with which jets from the various inlets entrained surrounding air were not established. Secondly, although evidence existed of optimum, rather than minimum, levels of jet momentum required to promote mixing, the data were insufficient for a definitive assessment of these levels.

Further work is required, using tracer gas techniques coupled with velocity measurements, to measure both entrainment ratios and air mixing in the lower part of the ventilated space. This work could be carried out, initially, in the existing facility but should be confirmed by additional work in larger rooms.

9.2.6 Development of inlets and control systems

Although Archimedes number criteria have been established for the control of ventilation jets, these criteria are not achievable with conventional, slot inlets under winter conditions. Work is required to perfect existing, alternative inlet systems using recirculation and preheating. In addition, there is considerable scope for work in the design of new controllable inlet structures that are capable of satisfying the above criteria. An important aspect of this modification and design work will be associated with the control of the inlet systems. These should be integrated with the overall heating and ventilation systems to provide failsafe operation and optimum energy efficiency while, at the same time, attempting to achieve an optimum indoor environment on both macro and micro scales.

10. REFERENCES

Abraham, G. 1963. Jet Diffusion in Stagnant Ambient Fluid. Publication No. 29. Delft Hydraulics Laboratory, Netherlands.

Abramovich, G.N. 1963. The Theory of Turbulent Jets. (English translation edited by L.H. Schmidel). M.I.T. Press, Cambridge, MA.

Albright, L.D. and N.R. Scott. 1974. The low-speed non-isothermal wall jet. J. Agric. Engng. Res. 19: 25-34.

AMCA. 1974. Laboratory methods of testing fans for rating. Standard 210-74. Air Movement and Control Association Inc. Arlington Heights, IL.

ASHRAE. 1981. Fundamentals Handbook. Am. Soc. Heat. Refrig. and Air Cond. Engnrs., Atlanta, GA.

Barber, E.M. 1981. The nature and importance of air distribution in ventilated livestock buildings. Paper presented at seminar on Ventilation of Confined Livestock Buildings in the Prairie Climate, University of Saskatchewan, Saskatoon, SK.

Barber, E.M. and J.R. Ogilvie. 1982. Incomplete mixing in ventilated airspaces. Part I. Theoretical Considerations. Can. Agric. Eng.24:25-29.

Barber, E.M., S.Sokhansanj, W.P.Lampman and J.R.Ogilvie. 1982. Stability of airflow patterns in ventilated airspaces. ASAE Paper No. 82-4551, Am. Soc. Agric. Eng., St. Joseph, MI.

Baturin, V.V. 1972. Fundamentals of Industrial Ventilation. 3rd Ed. (English translation by O.M. Blunn). Pergamon Press of Canada. Toronto, ON.

Baxter,S. 1984. Intensive Pig Production: Environmental Management and Design. Granada, London, England.

Black, T.C., J.N. Walker and G.M. White. 1970. Plane non-isothermal air jets discharging along a smooth ceiling. Trans. Am. Soc. Agric. Eng. 13: 774-778.

Bond, T.E., H. Heitman, Jr. and C.F. Kelly. 1965. Effects of increased air velocities on heat and moisture loss and growth of swine. Trans. Am. Soc. Agric. Eng. 8: 167-174.

Boon, C.R. 1978. Airflow patterns and temperature distribution in an experimental piggery. J. Agric. Engng. Res. 23:129-139.

Brannigan, P.G. and J.B. McQuitty. 1971. The influence of ventilation on distribution and dispersal of atmospheric gaseous contaminants. Can. Agric. Eng. 13:69-75.

Bruce, J.M. 1981. Ventilation and temperature control criteria for pigs. In: J.A. Clark (Ed.), Environmental Aspects of Housing for Animal Production. Butterworths, London, England.

Clark, P.C., J.B. McQuitty, and J.J.R. Feddes. 1984. Heat and moisture loads in swine finishing barns in Alberta. Can. Agric. Eng. 26:171-176.

Cederwall, K. 1971. Buoyant slot jets into stagnant or flowing environments. Report No. KH-R-25, W.M. Keck Laboratory of Hydraulics and Water Resources, California

Institute of Technology, Pasadena, CA.

Dybwad, I.R., M.A. Hellickson, C.E. Johnson and D.L. Moe. 1974. Ridge vent effects on model building ventilation characteristics. Trans. Am. Soc. Agric. Eng. 17: 366-370.

Esmay, M.L. 1978. Principles of Animal Environment. Textbook Edition. AVI, Westport, CT.

Fan, L-N. and N.H.Brooks. 1969. Numerical solutions of turbulent buoyant jet problems. Report No. KH-R-18, W.M. Keck Laboratory of Hydraulic and Water Resources, California Institute of Technology, Pasadena, CA.

Farquharson, I.M.C. 1952. The ventilating air jet. J. Heat. Vent. Engnrs. 19:449-469.

Feddes, J.J.R., J.B.McQuitty, and P.C.Clark. 1985. Laying hen heat and moisture production under commercial conditions. Can. Agric. Eng. 27:21-29.

Frean, D.H. and N.S.Billington. 1955. The ventilating air jet. J. Heat. Vent. Engnrs. 23: 313-334.

Furry, R.B. and T.E.Hazen. 1967. A constant temperature model for the ventilation-dilution phenomenon. Trans. Am. Soc. Agric. Eng. 10:188-195.

Glennon C.R., J.B.McQuitty, and P.C.Clark. 1984. Heat and moisture loads and air quality in commercial poultry rearing facilities. CSAE Paper No. 84-405. Can. Soc. Agric. Engng., Ottawa, ON.

Hinze,J.O. 1959. Turbulence, an Introduction to its Mechanism and Theory. McGraw-Hill Book Co. Inc., Toronto, ON.

Jackman, P.J. 1970. Air movement in rooms with side-wall mounted grilles - a design procedure. Laboratory Report No. 65, Heat and Vent. Res. Assoc., Bracknell, England.

Jorgensen, R. 1983. Fan Engineering. 8th Edition. Buffalo Forge Company, Buffalo, NY.

Kaul, P., W.Maltry, H.-J.Muller and V.Winter. 1975. Scientific-technical principles for the control of the environment in livestock houses and stores. Translation 430, Brit. Soc. for Res. in Agr. Engng., N.I.A.E., Silsoe, England.

Koestel, A., P.Hermann and G.L.Tuve. 1950. Comparative study of ventilating jets from various types of outlets. Trans. Am. Soc. Heat. and Vent. Engnrs. 56: 459-355.

Koestel, A. 1955. Paths of horizontally projected heated and chilled air jets. Trans. Am. Soc. Heat. and Vent. Engnrs. 61: 213-232.

Leonard, J.J., J.J.R.Feddes and J.B.McQuitty. 1984a. Measurement of ventilation rates using a tracer gas. Can. Agric. Eng. 26(1):49-51.

Leonard, J.J., J.J.R.Feddes, and J.B.McQuitty. 1984b. Air quality in commercial broiler housing. Can. Agric. Eng. 26:65-71.

Leonard, J.J., and J.B.McQuitty. 1986. Computer control of the environment in animal housing. In: Clark, J.A., K. Gregson and R.A. Saffell (Eds.), Computer Applications in Agricultural Environments. Butterworths, London, England.(In Press).

Linke,W. 1966. Aspects of Jet Ventilation. Translation 103, Heat. and Vent. Res. Assoc., Bracknell, England.

Mullejans,H. 1966. The similarity between non-isothermal flow and heat transfer in mechanically ventilated rooms. Translation 202, Heat. and Vent. Res. Assoc., Bracknell, England.

Nottage H.B., J.G.Slaby and W.P.Gojsza. 1952a. Isothermal ventilation-jet fundamentals. Trans. Am. Soc. Heat. and Vent. Engnrs. 58: 107-138.

Nottage, H.B., J.G.Slaby and W.P.Gojsza. 1952b. Exploration of a chilled jet. Trans. Am. Soc. Heat. and Vent. Engnrs. 58: 357-376.

Nottage, H.B., J.G.Slaby and W.P.Gojsza. 1952c. A smoke-filament technique for experimental research in room air distribution. Trans. Am. Soc. Heat. and Vent. Engnrs. 58: 399-404.

PAMI. 1984/5. Evaluation reports. Nos. 339, 344-347, 378-386. Prairie Agricultural Machinery Institute, Humboldt, SK.

Ower, E. and R.C.Pankhurst. 1977. The Measurement of Airflow. 5th Edition. Pergamon Press, Toronto, ON.

Pattie, D.R. and N.K.Kagio. 1981. The reduction of ventilation heat loss by porosity. Trans. Am. Soc. Heat. Refrig. and Air Cond. Engnrs. 87(1):222-234.

Pattie, D.R. and W.R.Milne. 1966. Ventilation air-flow patterns by use of models. Trans. Am. Soc. Agric.

Engnrs. 9:646-649.

Rajaratnam, N. 1976. Turbulent Jets. Elsevier Scientific Publishing Co., NY.

Randall, J.M. 1975. The prediction of airflow patterns in livestock buildings. J. Agric. Engng. Res. 20:199-215.

Randall, J.M. 1980. Selection of piggery ventilation systems and penning layouts based on the cooling effects of air speed and temperature. J. Agric. Engng. Res. 25:169-187.

Randall, J.M. and V.A.Battams. 1976. The observed influence of surface obstructions on the airflow pattern within livestock buildings. J. Agric. Engng. Res. 21: 31-39.

Randall, J.M. and V.A.Battams. 1977. Theoretical prediction of the initial path of air jets in ventilated livestock buildings. DN/En/714/10003, Nat. Inst. Agric. Engng., Silsoe, England. (Unpubl.)

Randall, J.M., and V.A.Battams. 1979. Stability criteria for airflow patterns in livestock buildings. J. Agric. Engng. Res. 24: 361-374.

Sainsbury, D. 1980. Poultry Health and Management. Granada. London, England.

Sällvik, K. and K.Walberg. 1984. The effects of air velocity and temperature on the behaviour and growth of pigs. J. Agric. Engng. Res. 30:305-312.

Smith, C.V. 1972. Some environmental problems of livestock housing. Technical Note No. 122, World Meteorological Organization, Geneva, Switzerland.

Timmons, M.B. 1980. Use of models to predict fluid motion in mechanically ventilated structures. ASAE Paper No. 80-4018, Am. Soc. Agric. Engnrs., St. Joseph, MI.

Turnbull, J.E. and N.A.Bird. 1980. Confinement Swine Housing. Publ. 1451, Agriculture Canada, Ottawa, ON.

Tuve, G.L. 1953. Air velocities in ventilating jets. Trans. Am. Soc. Heat. and Vent. Engnrs. 59: 261-282

Van Gunst, E., P.J.Erkelens and W.P.J.Coenders. 1967. Some results of investigations regarding the supply of cooled air in a test room. Proc. 4th Int. Conf. of Heat. and Air Cond. Paris, France.

Walker, J.N. 1977. Review of the theoretical relationships of isothermal ventilating air jets. Trans. Am. Soc. Agric. Engnrs. 20: 517-522.

Wathes, C.M., C.D.R.Jones and A.J.F.Webster. 1983. Ventilation, air hygiene and animal health. Veterinary Record 113:554-559.

Webster, A.J.F. 1981. Optimal housing criteria for ruminants. In: J.A.Clark (Ed.),Environmental Aspects of Housing for Animal Production. Butterwoths, London, England.

Wilson, J.D., M.L.Esmay and S.Persson. 1970. Wall-jet velocity and temperature profiles resulting from a ventilation inlet. Trans. Am. Soc. Agric. Engnrs. 13:77-81.

Winchell, W. 1982. Poultry Housing Facilities. Alberta Agriculture, Edmonton, AB.

11. APPENDIX I - CIRCUIT DIAGRAMS

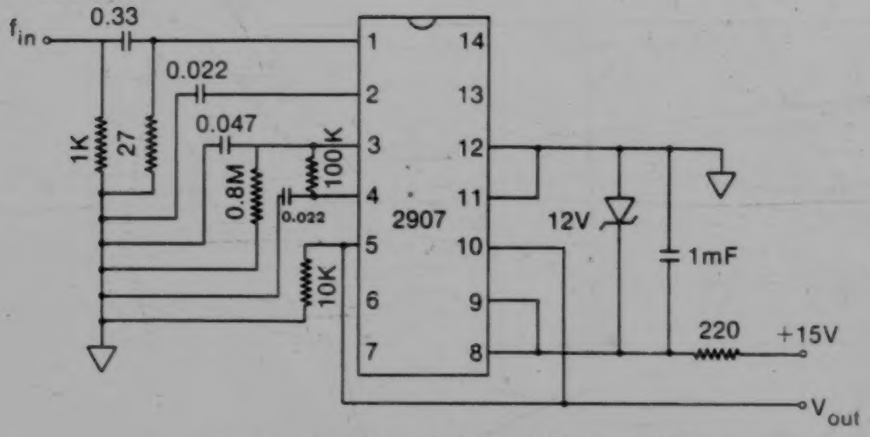

f_{in}
0.33
0.022
0.047
1K
27
100K
0.8M
0.022
10K
2907
1
2
3
4
5
6
7
8
9
10
11
12
13
14
12V
1mF
220
+15V
V_{out}

Frequency to Voltage Converter

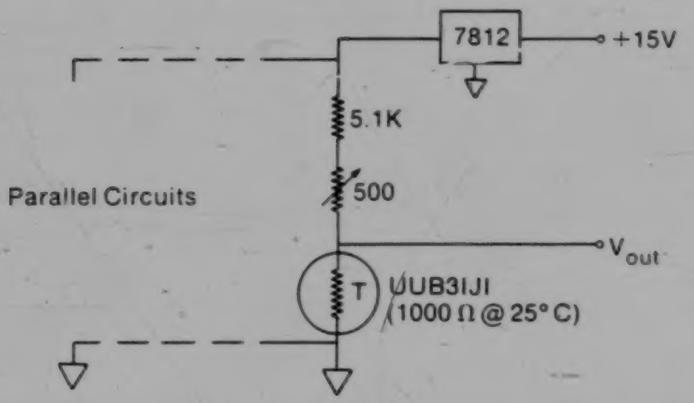

7812
+15V
5.1K
Parallel Circuits
500
V_{out}
T
UB3IJI
(1000 Ω @ 25° C)

Thermistor Circuit

12. APPENDIX II - CALIBRATION EQUATIONS

A. FAN SPEED

$$R = 150.6(V-0.347)$$

Where: R = Fan Speed (RPM), and
V = Observed voltage from F/V converter.

B. FAN PERFORMANCE

Symbols: Q = Flow rate (m^3/s)

R = Speed (RPM)

P = Static pressure (mm H_2O)

INLET TYPE	EQUATION	r^2
FT	$Q = 0.00182R$	0.9906
	$P = 3.0336Q^2+0.7834Q-0.2878$	0.9968
FL	$Q = 0.00205R$	0.9833
	$P = 2.8281Q^2-0.0908Q+0.0086$	0.9728
HT	$Q = 0.00193R$	0.9989
	$P = 3.3681Q^2-0.7367-0.1239$	0.9943
HL	$Q = 0.00206R$	0.9925
	$P = 3.3617Q^2-0.4271-0.2098$	0.9979

C. DIGITAL THERMOMETER

$T = -0.0464 + 1.0049T_m$

Where: T = Actual Temperature °C, and
T_m = Observed Temperature °C

13. APPENDIX III - COMPUTER PROGRAMS

A. PROGRAM FOR DATA AQUISITION

Runs on AIM65 with 64K memory.

Language is AIM BASIC with assembly language routines "POKED" in at the start of each run.

```
 10 REM DATA LOGGER PROGRAM
 20 REM DLOG 2A 0-30
*
* INITIALISATION
*
100 REM LOAD TIME ROUTINE AT LOCATIONS $0FCD-$0FFF
110 FORI=1TO50:READX
120   POKE4044+I,X:NEXTI
130 REM LOAD TAPE ROUTINE AT LOCATIONS $0F0C-$0FCA
135 POKE4044,6              :REM TIME OVERHEAD AT $0FCC
140 POKE41993,32            :REM TAPEGAP AT $A409
150 POKE4,18                :REM 12
160 POKE5,15                :REM 0F
170 FORI=1TO191:READX
180   POKE3851+I,X
190 NEXTI
200 AR=42010                :REM DATA ADDRESS AT $A41A
210 DH=10:DL=0
211 POKEAR,DL
212 POKEAR+1,DH
220 N=65                    :REM INITIAL FILE ID="A"
230 FORI=1TO112:POKE3711+I,0
240 NEXTI                   :REM CLEAR BUFFER $0E80-$0EF0
*
* START UP ROUTINE
*
250 INPUT"BITS=8 OR 12";BT
260 BF=0:IFBT=8THENBF=2
270 INPUT"PRINTOUT Y/N";P$
280 P=0:IFP$="Y"THENP=1
290 DIMT(3)
300 INPUT"START=HH,MM,SS",T(1),T(2),T(3)
320 INPUT"INTERVAL=HH,MM,SS";PH,PM,PS
340 INPUT"HIT 1 TO START";G
350 IFG=1GOTO390:GOTO340
390 FORI=1TO3                 :REM INITIALISE TIMER
400 POKE219+I,T(I):NEXTI
410 POKE40974,192
420 POKE40971,64
```

```
430 POKE41984,205
440 POKE41985,15
450 POKE40964,34
460 POKE40965,244
470 GOSUB600                  :REM TIME CALCULATION
480 HR=PEEK(220)
490 MN=PEEK(221)
500 SC=PEEK(222)
510 IFSC<ESGOTO480           :REM CHECK TIMEOUT
520 IFMN<EMGOTO480
530 IFHR<EHGOTO480
540 T(1)=HR:T(2)=MN:T(3)=SC
550 GOSUB600
560 GOSUB800                  :REM READ TAPE
570 GOTO480
*
* TIME CALCULATION ROUTINE
*
600 ES=T(3)+PS
610 IFES<60THEN640
620 ES=ES-60:CM=1
630 GOTO650
640 CM=0
650 EM=T(2)+PM+CM
660 IFEM<60THEN690
670 EM=EM-60:CH=1
680 GOTO700
690 CH=0
700 EH=T(1)+PH+CH
710 RETURN
*
* DATA RECORDING ROUTINE
*
800 PRINTHR;":";MN;":";SC      :REM TIME LABELS
810 FORI=1TO3
820 POKE3812-I,T(I):NEXTI
830 REM SET UP A/D
840 FORK=1TO3                  :REM FOR EACH BOARD
850  BASE=24576+(K*4096)       :REM BASE ADDRESS CALCN
860  AL=BASE
870  AH=BASE+1
880  AM=BASE+2
890  ST=BASE+3
900  CT=BASE+3
910  IFP=0THEN920
920  FORI=1TO16:MX=1            :MUX CONTROL- 16 CHANNELS
930    MX=INT(MX-1)*16)
940    POKECT,BF                :REM NO. OF BITS
950    GOSUB1100                :REM READ DATA FROM A/D
960  NEXTI
970 NEXTK
980 POKE3857,N
985 POKE3812,N                  :REM FILE ID  AT $0EE4
990 GOSUB1500                   :REM INCREMENT FILE ID
```

```
1020 X=USR(0)                    :REM OUTPUT BUFFER TO TAPE
1030 RETURN
*
* A/D READ SUBROUTINE
*
1100 REM DATA READ ROUTINE
1110 POKEAM,MX
1120 CN=I+16*(K-1)               :REM CHANNEL NUMBER
1130 BUFF=3808-2*(CN-1)          :REM START OF BUFFER AT $0EE0
1140 Y=PEEK(AH)                  :REM START A/D CONVERSION
1150 WAITST,64,255-64
1160 H=PEEK(AH)
1170 L=PEEK(AL)
1180 POKEBUFF,H
1190 POKEBUFF-1,L
1195 IFP=0GOTO1240               :REM NO PRINT/DISPLAY
1200 V=(H*256+L)/16              :REM CONVERT HEX TO VOLTS
1210 VD=(V-2048)/2048
1220 VD=INT(VD*1000+.5)/100
1230 PRINTCN,VD
1240 RETURN
1500 REM SUBROUTINE TO CHANGE DATA ADDRESS
1510 N=N+1
1515 IFN=91THENN=65               :REM FILE ID'S FROM A-Z
1590 RETURN
*
* TIMER OBJECT CODE CONVERTED TO DECIMAL
*
2000 REM TIME ROUTINE
2010 DATA72,138,72,230,223,166,223,224,16,208,32
2020 DATA169,0,133,223,230,222,162,60,2
28,222,208,20
2030 DATA133,222,230,221,228,221,208,12
2040 DATA133,221,230,220,162,24,228,220,208,2
2050 DATA133,220,104,170,173,4,160,104,64
*
* RECORDING OBJECT CODE CONVERTED TO DECIMAL
*
3000 REM TAPE OUTPUT ROUTINE
3010 DATA0,68,65,84,65,0,169,84,141,19
3020 DATA 164,173,12,15,141,53,164,160,4,185
3030 DATA13,15,153,46,164,136,16,247,32,111
3040 DATA 229,162,112,169,0,141,30,164,141,31
3050 DATA164,169,16,72,32,186,233,104,141,25
3060 DATA164,32,78,229,32,139,241,173,27,164
3070 DATA32,78,229,32,139,241,173,26,164,32
3080 DATA78,229,32,139,241,189,128,14,32,78
3090 DATA229,32,139,241,32,93,229,202,206,25
4000 DATA164,208,238,173,32,164,32,139,241,173
4010 DATA30,164,32,139,241,32,102,229,224,0
4020 DATA240,3,76,45,15,32,186,233,162,2
4030 DATA169,0,32,139,241,173,7,1,32,139
4040 DATA241,173,6,1,32,139,241,202,208,241
4050 DATA32,240,233,32,10,229,169,207,45,0
```

```
4060 DATA168,141,0,168,172,204,15,169,0,162
4070 DATA60,230,222,228,222,208,20,133,222,230
4080 DATA221,228,221,208,12,133,221,230,220,162
```

B. PROGRAM FOR DATA CONVERSION

Runs on IBM PC using BASIC 2.0

```
0  '
10 'PROGRAM: PROC
20 'PURPOSE: To convert hex ASCII to meaningful numbers
30 'CREATION; 25 APRIL 85
40 'PROGRAMMER: J.LEONARD
50 'REVISION: 06 MAY 85
100 'BASED ON MASS2 - NEW INPUT AND TEMP. PARAMETER CALC.
110 '               - EXCITATION VOLTAGE ON CHANNEL 5
120 '               -SEPARATE CALIBRN FOR BED & AIR TEMPS
125 '               - LATEST AIR TEMP CALIBN EQNS 13 FEB 85
130 GOSUB 2000
170 DIM T(3) , TEM(48) , DT(48) , TR(48)
180 OPEN D$ FOR INPUT AS #1
190 OPEN V$ FOR OUTPUT AS #2
200 CHARP=6                   'INITIALISE CHARACTER POINTER
210 LINE INPUT #1,LIN$
220  GOSUB 1100
230  IF C$="AA" THEN 240 ELSE 220      'IDENTIFY RUN START
240  GOSUB 1100
250  IF C$="00" THEN 260 ELSE 220
260  IF (CHARP>44) THEN 270                'FIND DATA START
265  CHARP=CHARP+22 :GOTO 290
270  LINE INPUT #1,LIN$
280  CHARP=CHARP-38
290  FOR I=1 TO 3                         'CONVERT RUN TIME
300   GOSUB 1100
310   GOSUB 1200
320   T(I)=DEC
330  NEXT I : PRINT"TIME";T(1);":";T(2);":";T(3)
335  PRINT #2,"TIME";T(1);":";T(2)":";T(3)
340  FOR I=1 TO 48                     '48 CHANNELS OF DATA
350   GOSUB 1100                        'GET TWO CHARACTERS
360   GOSUB 1200                        'CONVERT TO DECIMAL
370   H=DEC                             'HIGH BYTE
380   GOSUB 1100                        'GET TWO CHARACTERS
390   GOSUB 1200                        'CONVERT TO DECIMAL
400   L=DEC                             'LOW BYTE
410   GOSUB 1300                        'CONVERT TO VOLTS
412   IF I=1 THEN TEM(I)=INT((4-VD)/.0033) 'WIND DIRN DEG
414   IF I=2 THEN TEM(I)=11.39*VD          'WIND SPEED M/S
416   IF I=3 THEN TEM(I)=150.6*(VD-.347)   'FAN SPEED
418   IF I=4 THEN TEM(I)=3*VD              'DIFF PRESS
420   IF I=5 THEN TEM(I)=2*VD              'THERM EXITN V
422  'IF I=5 THEN TEM(I)=2*6.056 '*USE WITH OLD DATA ONLY*
425   IF I>5 GOTO 1400
430 NEXT I
440 DZ=TEM(46)-TEM(47)             'INLET-OUTLET TEMP DIFF
450 FOR I=12 TO 48
460  DT(I)=TEM(I)-TEM(47)          'ROOM-OUTLET TEMP DIFF
```

```
470  TR(I)=DT(I)/DZ                     'DIMENSIONLESS TEMP DIFF
480 NEXT I
490 IF X$="Y" GOTO 1500                   'ARCH. NO. SUBROUTINE
500 GOSUB 3000                            'PRINTOUT SUBROUTINE
510 GOTO 220
520 CLOSE
530 END
540 '
550 'SUBROUTINES
560 '
1079 'SUBROUTINE TO GET TWO CHARACTERS
1080 CHARP=6
1090 IF EOF(1) THEN 520 ELSE LINE INPUT #1,LIN$
1100 CHARP=CHARP+2
1110 IF CHARP>66 THEN 1080
1120 C$=MID$(LIN$,CHARP,2)
1130 RETURN
1140 '
1150 '
1190 'SUBROUTINE TO CONVERT HEX ASCII TO DECIMAL
1200 DEF FND(N)=N MOD 17+10*INT(N/17)
1210 A$=LEFT$(C$,1)
1220 B$=RIGHT$(C$,1)
1230 DEC=FND(ASC(A$)-48)*16+FND(ASC(B$)-48)
1240 RETURN
1250 '
1260 '
1290 'SUBROUTINE TO CONVERT HIGH AND LOW BYTES TO VOLTS
1300 V=(H*256+L)/16
1310 VD=(V-2048)/2048
1322  VD=INT(VD*10000+.5)/1000
1330 RETURN
1340 '
1350 '
1400  'SUBROUTINE TO CONVERT VOLTS TO CELSIUS TEMPERATURE
1405 VI=TEM(5)
1407 Q=2000                             'POWER DISSIPN CONST
1410 A=.001379588514#
1420 B=.0002758512252#
1430 C=.000000209099055#
1440 R=(5400*VD/(VI-VD))-2.8  '2.8 = LEAD RESISTANCE FOR 50'
1445 R=.5*(R+SQR(R**2+4*Q*VI**2)) 'R CORRECTED FOR SELF-HEAT
1450 TEM(I)=1/(A+B*LOG(R)+C*(LOG(R))**3)-273.15
1455 TEM(I)=TEM(I)-.4+8.429999E-02*TEM(I) 'LINEAR TEMP CORRN
1460 IF I>11 GOTO 430
1470 IF TEM(I)<17 GOTO 430
1480 TEM(I)=1.9*((TEM(I)+.4-8.429999E-02*TEM(I))-8)
1485 'ADJUST HEAT DISSIP BED THERMSTRS
1490 GOTO 430
1492 '
1495 '
1497 '
1500 'SUBROUTINE TO CALCULATE CORRECTED ARCHIMEDES NUMBER
1505 IF BT=6 GOTO 1510        'ALLOW FOR BAD BEDS IN CDAT7
```

```
1507 TW=(TEM(6)+TEM(7)+TEM(8)+TEM(11))/4 : GOTO 1520
1510 TW=(TEM(6)+TEM(7)+TEM(8)+TEM(9)+TEM(10)+TEM(11))/6
'MEAN BED TEMP
1520 TC=TEM(46)                           'MEAN INLET TEM
1530 WR=5.4 :HR=1.825                     'ROOM WIDTH, HEIGHT
1540 CD=.6                               'INLET ORIFICE COEFF.
1560 QF=AF*TEM(3) : VF=QF/(AI*CD)
1565 GOSUB 1700
1570 ARF=9.8*(TW-TC)*CD*AI*WR*HR*(WR+HR)/(QF**2*(546+TW+TC)
1580 ARP=ARF*QF**2/QP**2
1585 IF QP=9999 THEN ARP=ARF
1590 ARM=(ARP+ARF)/2
1600 GOTO 500
1610 '
1620 '
1700 'SUBROUTINE TO CALCULATE FLOW FROM PRESSURE EQUATION
1710 P=TEM(4)*298/(TEM(47)+273)  'CORRECTED PRESSURE DIFF
1720 DET=(BP**2-4*AP*(CP-P))
1725 IF DET<0 THEN 1790            'IGNORE UNREAL ROOTS
1730 QP1=(-BP+SQR(DET))/(2*AP)     'ROOT #1 OF FLOW EQN
1740 QP2=(-SQR(DET)-BP)/(2*AP)     'ROOT #2 OF FLOW EQN
1750 D1=ABS(QF-QP1)                'CHOOSE CLOSEST ROOT...
1760 D2=ABS(QF-QP2)
1770 IF D1>D2 THEN QP=QP2 ELSE QP=QP1
1775 VP=QP/(AI*CD)
1780 RETURN
1790 QP=9999 :RETURN
1800 '
1900 '
2000 'INITIALISATION SUBROUTINE TO SET INLET VARIABLES ETC.
2010 PRINT "            INLET TYPES"
2020 PRINT "FULL WIDTH TOP...................1"
2030 PRINT "FULL WIDTH MID...................2"
2040 PRINT "HALF WIDTH TOP...................3"
2050 PRINT "HALF WIDTH MID...................4"
2060 INPUT "INLET NO. FOR THIS RUN ?        ",N
2070 IF N=1 GOTO 2080 : IF N=2 GOTO 2090
: IFN=3 GOTO 2100 :IF N=4 GOTO 2110
2075 'INLET AREA, COEFFS FOR PV=A*QP**2+B*QP+C AND QF=A*FV
2080 AI=.143 : AP=3.0336 : BP=.7834
: CP=-.2878 : AF=.00182 :GOTO 2130
2090 AI=.134 : AP=2.8281 : BP=-.0908
: CP=.0086 : AF=.00205 :GOTO 2130
2100 AI=.166 : AP=3.3681 : BP=-.7367
: CP=-.1239 :AF=.001931 :GOTO 2130
2110 AI=.166 : AP=3.3617 : BP=-.4271
: CP=-.2098 :AF=.00206
2130 INPUT "HOW MANY BED TEMPERATURES ?    ",BT
2140 INPUT "INPUT FILE ? (B:CDATXX.TXT)    ",D$
2150 INPUT "OUTPUT FILE ? (B:CVALXX.TXT)   ",V$
2160 INPUT "DISPLAY OUTPUT ON SCREEN ? (Y OR N) ",P$
2170 INPUT "IS AR NO. REQUIRED ? (Y OR N)       ",X$
2171 PRINT " ":PRINT " "
2180 RETURN
```

```
2190 '
2200 '
2300 '
3000 'SUBROUTINE FOR PRINTING OUTPUT
3005 IF P$="N" THEN 3008
3007 PRINT "CHAN.       VALUE       DT          DT/DZ"
3008 PRINT #2,"CHAN.     VALUE        DT          DT/DZ"
3010 FOR I=1 TO 11
3020  IF P$="N" THEN 3040
3030  PRINT USING "####.##     "; I,TEM(I)
3040  PRINT #2,USING"####.##      "; I,TEM(I)
3050 NEXT I
3060 FOR I=12 TO 48
3070  IF P$="N" THEN 3090
3080  PRINT USING "###.###    ";I, TEM(I), DT(I), TR(I)
3090  PRINT #2,USING"###.###   "; I,TEM(I),DT(I),TR(I)
3100 NEXT I
3110 IF X$="N" GOTO 3190
3120 IF P$="N" GOTO 3160
3130 PRINT "ARP=";ARP;"QP=";QP;"VP=";VP
3140 PRINT "ARF=";ARF;"QF=";QF;"VF=";VF
3150 PRINT "ARM=";ARM :PRINT" "
3160 PRINT #2, "ARP=";ARP;"QP=";QP;"VP=";VP
3170 PRINT #2, "ARF=";ARF;"QF=";QF;"VF=";VF
3180 PRINT #2, "ARM=";ARM :PRINT #2," "
3190 RETURN
```

B. PROGRAM FOR READING RAW DATA FROM TAPE TO AIM 65/40

Assembler listing of object and source code.

Object code stored on tape as TARO.

Source code stored on tape as TAR.

```
PAGE 0001
ADDR OBJECT     SOURCE
0800             INDEV=$0273
0800             OFFSET=$02E5
0800             TRDRNO=$0314
0800             NAME=$0300
0800             SPOPEN=$F993
0800             LOADX=$ABBC
0800                    *$09B0
09B0             LABL   *=*+5
09B5 A9 02              LDA #2
09B7 8D 73 02           STA INDEV
09BD A9 00              LDA #0
09BF 8D E5 02           STA OFFSET          OFFSET=0
09C2 8D E6 02           STA OFFSET+1
09C5 A9 44              LDA #$44              "D"
0907 8D B0 09           STA LABL
09CA A9 4A              LDA #$41              "A"
09CC 8D B1 09           STA LABL+1
09CF 8D B3 09           STA LABL+3
09D2 8D B4 09           STA LABL+4
09D5 A9 54              LDA #$54              "T"
09D7 8D B2 09           STA LABL+2
09DA A0 04              LDY #4
09DC B9 B0 09   NAM     LDA LABL,Y          LOAD FILE ID
09DF 99 00 03           STA NAME,Y
09E2 88                 DEY
09E3 10 F7              BPL NAM
09E5 20 93 F9           JSR SPOPEN          OPEN TAPE INPUT
09E8 20 BC AB           JSR LOADX           LOAD FROM TAPE
09EB EE B4 09           INC LABL+4          INC FILE ID
09EE AD B4 09           LDA LABL+4
09F1 C9 5B              CMP #$5B            FILE ID=Z ?
09F3 30 05              BMI LOOP            NO:GET NXT FILE
09F5 A9 41              LDA #$41            YES:RESET ID=A
09F7 8D B4 09           STA LABL+4
09FA 4C DC 09   LOOP    JMP NAM
09FD                     END
 ERRORS=0000
```

C. PROGRAM FOR DUMPING RAW DATA FROM AIM 65/40 TO IBM PC

Assembler listing of object and source code.

Object code stored on tape as RSOBJ.

Source code stored on tape as RSOUT.

```
PAGE 0001
ADDR OBJECT    SOURCE
0800                     *=$FFD0
FFD0              RACIA  *=*+1
FFD1              STATUS *=*+1
FFD2              CMND   *=*+1
FFD3              CTRL   *=*+1
FFD4              CMD=$0B
FFD4              CTL=$16
FFD4                     *=$0206
0206 00 08        IOVS   WOR SOUT
0208                     *=$0800
0800 4C 09 08     SOUT   JMP OPEN
0803 4C 17 08            JMP SEND
0806 4C 28 08            JMP CLOSE
0809 A9 0B        OPEN   LDA #CMD
080B 8D D2 FF            STA CMND
080E A9 16               LDA #CTL
0810 8D D3 FF            STA CTRL
0813 AD D0 FF            LDA $FFD0
0816 60                  RTS
0817 48           SEND   PHA
0818 20 22 08     TEM    JSR OUTYET
081B F0 FB               BEQ TEM
081D 68                  PLA
081E 8D D0 FF            STA $FFD0
0821 60                  RTS
0822 AD D1 FF     OUTYET LDA STATUS
0825 29 10               AND #$10
0827 60                  RTS
0828 60           CLOSE  RTS
0829                      END
 ERRORS=0000
```

14. APPENDIX IV - DATA SAMPLES

A. Raw Data

```
;1E0A70AA000000000000000000000042000
400B6E070A08F208070CDB0959094300933
;1E0A8E93609430975095D0A9A0A8E0A830A
790A7A0A910A990A970A750A770A8B01151
;1E0AACA7D0A7B0A730A7C0A6D0A540A4F0A
500A5A0A6A0A780A770A740A520A55011DE
;1E0ACAA640A600A670A650A600A520D4D0D
1E0D470AAD0AC50AA000000000000000DAE
;1E0AE80000000043000600B61074F090708
030CDB09660954093A094E097A096800D6F
;1E0B06AD60ACA0AC00ABE0AB60ACF0AB90A
B00AF40AEE0AD50AC50AC20AB00AB801064
;1E0B24AB20A8F0A8A0A8C0A930AAC0AB50A
BE0AB80A920A9F0A980A990AAF0AA00125C
;1E0B42AB40AA80D5F0D2D0D420ACF0AFB0
```

B. Corresponding Numerical Values

TIME 0 : 4 : 0 Time from run start

CHANNEL	VALUE		
1	140.00	Wind direction	(°)
2	3.11	Wind speed	(m/s)
3	139.61	Fan speed	(RPM)
4	0.22	Pressure difference	(mm H_2O)
5	12.13	Thermistor voltage	(V)
6	27.59	Heat pad temperatures	(°C)
7	26.93		
8	28.98		
9	15.88		
10	14.03		
11	26.62		
12	7.756	Air temperatures (Group 1) (°C)	
13	8.502		
14	9.545		
15	9.596		
16	9.390		
17	8.797		
18	7.616		
19	7.756		
20	10.563	Air temperatures (Group 2) (°C)	
21	10.667		
22	9.493		
23	10.104		
24	9.390		
25	9.246		
26	8.797		

27	9.596	
28	10.301	Air temperatures (Group 3) (˚C)
29	10.458	
30	10.104	
31	9.751	
32	9.596	
33	9.246	
34	9.751	
35	9.844	
36	10.762	Air temperatures (Group 4) (˚C)
37	10.814	
38	10.208	
39	10.156	
40	9.648	
41	9.246	
42	8.451	
43	8.350	
44	-22.715	Inlet air temperatures (˚C)
45	-21.988	
46	-24.489	Outside air temperature (˚C)
47	6.128	Fan duct air temperature (˚C)
48	2.587	Wet-bulb temperature (˚C)

15. APPENDIX V - PHOTOGRAPHY

A. PROCEDURES

All photographs were taken with a Nikon FE camera fitted with a Nikon 50mm, f2.8 lens. Kodak Tri-X pan, 400 ASA film was used throughout the series of experiments. This film was used because of ready availabity, even though it was not ideal for the limited lighting conditions in the experimental room.

By a process of trial and error, the following camera settings were shown to give good results and were used subsequently throughout the series of experiments:

ASA	800
Aperture	1.8
Exposure	0.15s

Processing of the film required "pushing" to 800 ASA.

B. SAMPLE PHOTOGRAPHS

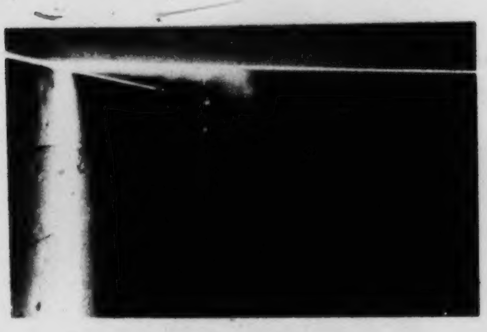

Full width inlet at ceiling with $Ar \approx 80$

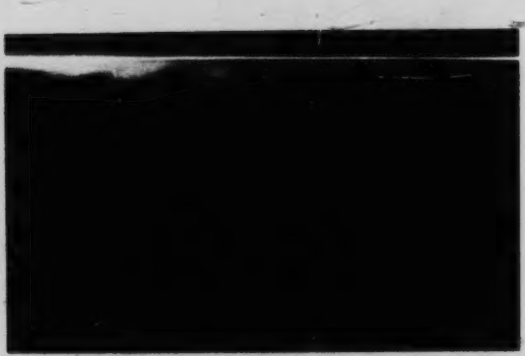

Full width inlet at ceiling with Ar≃40

Half width inlet at ceiling with Ar≃60

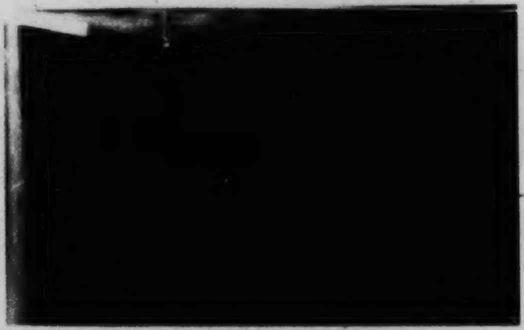

Half width inlet at ceiling with Ar≃35

Full width inlet at lower position with Ar≃100

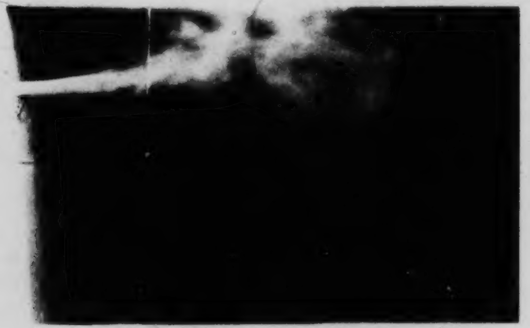

Full width inlet at lower position with Ar≃20

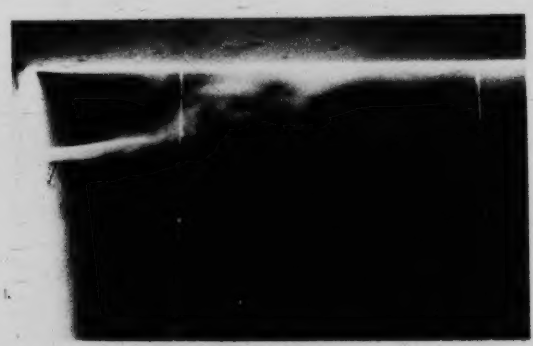

Full width inlet at lower position with Ar≃5

Half width inlet at lower position with Ar≃75

Half width inlet at lower position with Ar≃10

Half width inlet at lower position with Ar≃5